Obesity and type 2 diabetes : cardiovascular and cerebral aspects

Widya, R.L.; Widya R.L.

OBESITY AND TYPE 2 DIABETES

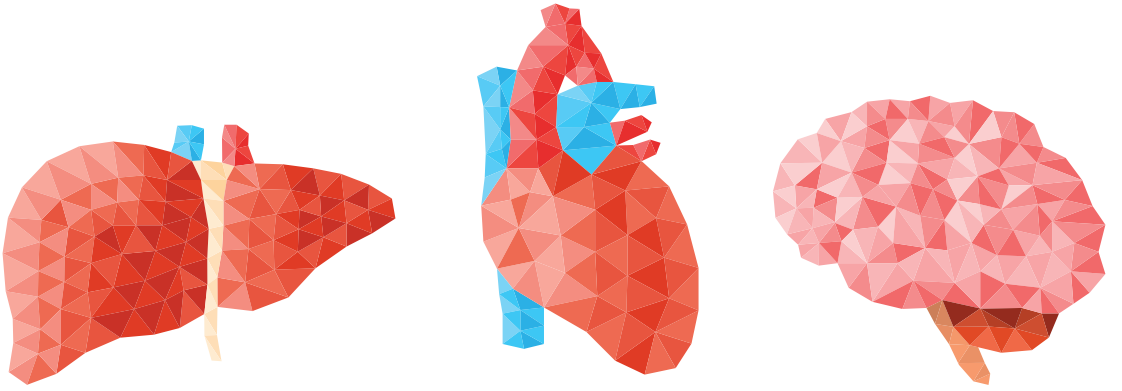

CARDIOVASCULAR AND CEREBRAL ASPECTS

RALPH L. WIDYA

Obesity and Type 2 Diabetes: Cardiovascular and Cerebral Aspects

Ralph Lennart Widya

Obesity and Type 2 Diabetes: Cardiovascular and Cerebral Aspects

ISBN/EAN: 978-94-92683-75-5
Cover illustration: iStock
Cover design: R.L. Widya & Optima Grafische Communicatie, Rotterdam
Layout and printed by: Optima Grafische Communicatie, Rotterdam

Obesity and Type 2 Diabetes: Cardiovascular and Cerebral Aspects

Proefschrift

ter verkrijging van
de graad van Doctor aan de Universiteit Leiden,
op gezag van Rector Magnificus prof. mr. C.J.J.M. Stolker,
volgens besluit van het College voor Promoties
te verdedigen op dinsdag 5 september 2017
klokke 16.15 uur

door

Ralph Lennart Widya
geboren te Delft
in 1984

Promotores	Prof. dr. H.J. Lamb
	Prof. dr. A. de Roos
	Prof. dr. J.W.A. Smit
Promotiecommissie	Prof. dr. A. Webb
	Prof. dr. S. Middeldorp (Academisch Medisch Centrum, Amsterdam)
	Prof. dr. J.E. Wildberger (Maastricht UMC+, Maastricht)
	Prof. dr. H. Pijl
	Dr. J. van der Grond
	Dr. ir. R. de Mutsert

The research described in this thesis was carried out at the departments of Radiology (head: prof. dr. M.A. van Buchem) and Endocrinology (head: prof. dr. A.J. Rabelink) of the Leiden University Medical Center, the Netherlands. Research was partly performed within the framework of the Center for Translational Molecular Medicine (CTMM; www.ctmm.nl), project PREDICCt (grant 01C-104), and was supported by a grant of the Dutch Heart Foundation (DHF2008-T085), Dutch Diabetes Research Foundation, and Dutch Kidney Foundation.

Financial support by the Dutch Heart Foundation for the publication of this thesis is gratefully acknowledged. Additional financial support for the publication of this thesis was kindly provided by Philips Healthcare Nederland, Stichting MiniMAX, Sectra Benelux, Guerbet Nederland BV, Nederlandse Obesitas Kliniek, Tromp Medical BV, Oldelft Benelux, Toshiba Medical Systems Nederland, Alrijne Zorggroep, Medis medical imaging systems BV, Esaote Europe BV, and ChipSoft.

Voor mijn vader

CONTENTS

Chapter 1

General introduction

The prevalence of obesity, defined as a body mass index (BMI) > 30 kg/m^2, is increasing to epidemic proportions. In 2014, 11% of men and 15% of women worldwide were obese. Thus, more than half a billion adults worldwide are classed as obese[1]. The fundamental cause of obesity is an imbalance between energy intake (excessive intake of energy-dense foods) and energy expenditure (reduced physical activity). People with obesity are at risk for a range of chronic conditions including cardiovascular disease (CVD) and nonalcoholic fatty liver disease (NAFLD)[2]. Furthermore, obesity is a major risk factor for the development of type 2 diabetes, which is one of the most common chronic diseases in nearly all countries. According to the World Health Organization, the global prevalence of diabetes in 2014 was estimated to be 9%[1], of which 90% was comprised of type 2 diabetes[3].

Left ventricular (LV) function, central arterial stiffness, and subclinical atherosclerosis are important markers for CVD. NAFLD, or *fatty liver*, is recognized as an amplifier of inflammatory processes which could contribute to the development of CVD. These processes originate in expanded and inflamed visceral adipose tissue (VAT). In addition, increased intrahepatic cytokine expression is suggested to play a key role in the progression of CVD[4]. However, the interrelationships between obesity, markers for CVD, and NAFLD are complex and associations could in part be confounded by the manifestation of multiple metabolic impairments known as the metabolic syndrome.

CVD is one of the major adverse consequences of type 2 diabetes, and chronically elevated plasma nonesterified fatty acid (NEFA) levels in patients with type 2 diabetes are associated with altered myocardial high-energy phosphate metabolism[5]. When evaluating cardiac function most studies focus on the LV, but the right ventricle (RV) is largely overlooked. RV function is an important determinant of outcome in several cardiopulmonary conditions and has proven to be useful for patient risk stratification in heart failure and for prediction of developing atrial fibrillation[6-8]. However, RV anatomy and function have not yet been studied in patients with type 2 diabetes.

The metabolic pathways involved in the pathogenesis of insulin resistance and cardiovascular diseases in patients with type 2 diabetes are complex. Increased lipolysis from adipose tissue causes triglycerides to be stored in different organs outside adipose tissue, known as ectopic fat accumulation. Ectopic fat accumulation in muscle and liver are involved in pathophysiologic insulin resistance[9-11]. Theoretically, limiting organ-specific fat accumulation by exercise training could improve glucose homeostasis and reduce cardiovascular risk.

The brain is another important organ involved in obesity and type 2 diabetes. The hypothalamus plays a key role in the regulation of feeding and the control of glucose metabolism[12]. Moreover, various hypothalamic neuronal circuits are involved in the control of glucose metabolism[13]. It has been shown that the hypothalamic neuronal activity is altered in patients with type 2 diabetes, which may indicate that the hypothalamus inappropriately perceives

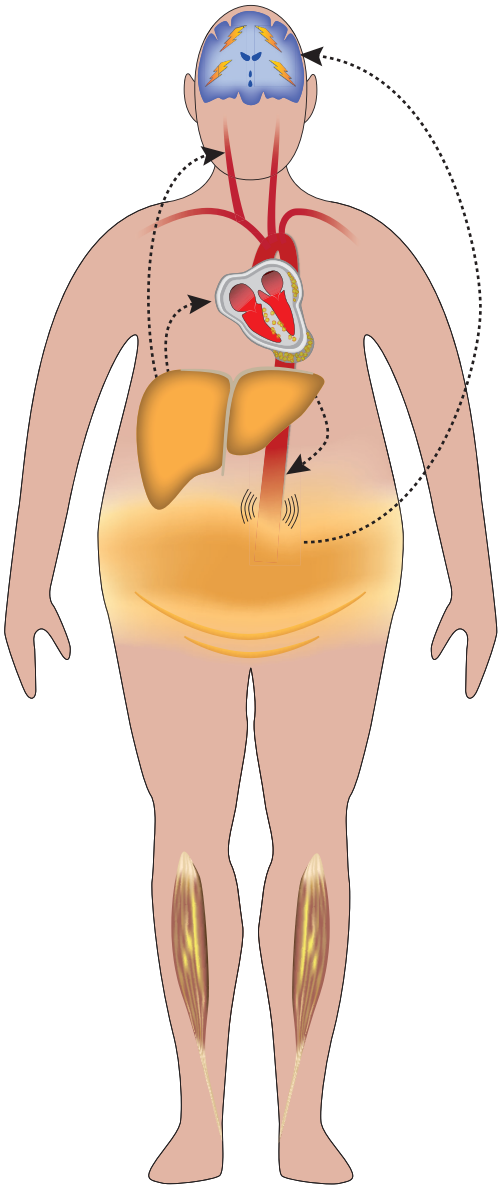

Figure. Schematic overview of the organs and ectopic fat depots studied in this thesis. Expanded visceral adipose tissue is a hallmark of obesity and type 2 diabetes. Several proinflammatory cytokines originate from visceral adipose tissue which may promote aortic stiffness, decreased cardiac function, and microstructural brain damage. The liver is not an innocent bystander, but is recognized as an amplifier of inflammatory processes which could contribute to the development of cardiovascular disease in obesity and type 2 diabetes.

and/or processes signals in response to a nutrient load, reflecting an abnormal perception of the current metabolic status[14]. Caloric restriction is an important therapeutic strategy in type 2 diabetes, but its effect on hypothalamic responsiveness is yet unknown.

Obesity has been associated with structural brain changes, such as brain atrophy[15]. The relationship between obesity and the anatomy of subcortical structures that play a role in human food regulation have not been investigated previously. Such brain structures include the basal ganglia, hippocampus, and thalamus. Furthermore, it can be hypothesized that the inflammatory processes originating from VAT do not only lead to the development of CVD, but could also induce microstructural brain damage.

Magnetic resonance imaging (MRI) is a noninvasive imaging modality that allows for analyzing structural and functional information of the human body. ECG gated cardiac magnetic resonance provides a valuable assessment of cardiac morphology and function[16, 17]. MRI assessment of aortic pulse wave velocity, defined as the velocity of the systolic wave front propagating through the aorta, is a measure for aortic stiffness. It has good agreement with the gold-standard as derived by invasive pressure measurements and can be determined with high reproducibility[18]. Proton (^{1}H) magnetic resonance spectroscopy is the most commonly used magnetic resonance-based method to noninvasively evaluate metabolic changes in the human body. ^{1}H magnetic resonance spectroscopy helps to characterize tissues by assessing biochemistry in vivo. The technique identifies metabolites by observing differences in the resonance frequencies of the ^{1}H signal. Localized ^{1}H magnetic resonance spectroscopy is a sensitive and quantitative method to measure hepatic triglyceride content[19]. Blood oxygen level-dependent (BOLD) functional MRI (fMRI) has been widely applied in spatiotemporal mapping of the human brain function and measuring neuronal activity. The main advantage of BOLD fMRI is its noninvasive nature and local sensitivity combined with a good spatial resolution[20]. Magnetization transfer imaging (MTI) is an MRI technique that is more sensitive to subtle microstructural changes in the brain than conventional techniques[21]. Accordingly, magnetic resonance imaging and spectroscopy are the methods of choice to study the complex interrelationships between visceral obesity, NAFLD, and markers of cardiovascular disease, and to investigate cerebral changes in people with obesity and type 2 diabetes (**Figure**).

OUTLINE OF THIS THESIS

This thesis focuses on cardiovascular and cerebral dimensions and function in people with obesity and type 2 diabetes. State-of-the-art imaging techniques are used to investigate links between the heart, liver, abdominal fat, and brain to elucidate parts of the complex relationships between these organs.

Previous studies have shown a relationship between NAFLD and subclinical cardiovascular measures, but the possible confounding effect of the metabolic syndrome is so far unknown. The association between hepatic triglyceride content and LV diastolic function is evaluated in **Chapter 2** by taking various covariates, including components of the metabolic syndrome, into account. In **Chapter 3** the association between liver fat, the stiffness of the aorta and carotid intima-media thickness is evaluated using a similar approach.

It is known that subclinical LV dysfunction presents in type 2 diabetes, even in the absence of significant coronary artery disease and hypertension. Despite its importance in patient outcome in heart failure, the RV is largely overlooked. **Chapter 4** focuses on the differences of the dimensions and function of the RV between healthy subjects and type 2 diabetes patients. To better understand the changes in RV function, nutritional interventions were applied in a group of healthy subjects to create a physiological and a pathophysiological model of increased plasma NEFA levels. The effects on RV function in these two conditions are evaluated in **Chapter 5**.

Strategies to limit ectopic fat accumulation are rational approaches to improve glucose homeostasis and potentially reduce cardiovascular risk. Most intervention studies have focused on visceral and subcutaneous fat; however, little is known about the effect of exercise alone without diet on ectopic fat accumulation in type 2 diabetes. In **Chapter 6** the effects of an exercise intervention on organ-specific fat accumulation and cardiac function in type 2 diabetes patients is described.

The hypothalamus is critically involved in the regulation of feeding. Type 2 diabetes is a disease of impaired glucose homeostasis and insulin action, with energy imbalance and anomalous fuel flux as metabolic hallmarks. Restoration of the energy balance by reduction of the caloric intake and subsequent weight loss are important therapeutic strategies in type 2 diabetes. The effect of caloric restriction on the hypothalamic neuronal response to glucose ingestion in type 2 diabetic patients is evaluated in **Chapter 7**.

Other brain structures involved in the regulation of human feeding behavior include the basal ganglia, hippocampus, and thalamus. **Chapter 8** focuses on the relationship of the morphometric changes of these structures in obesity. Finally, it has been shown that obesity is associated with brain atrophy, and different fat compartments demonstrate different metabolic and endocrine behaviors. Therefore, **Chapter 9** describes the association of individual associations between abdominal visceral and subcutaneous adipose tissue with microstructural brain tissue damage.

Results of this thesis are summarized in **Chapter 10**.

REFERENCES

1. World Health Organization. Global status report on noncommunicable diseases 2014. http://www.who.int/nmh/publications/ncd-status-report-2014/en. Published 2014.
2. Bray GA. Medical consequences of obesity. *J Clin Endocrinol Metab* 2004;89:2583-2589.
3. World Health Organization. Definition, diagnosis and classification of diabetes mellitus and its complications : report of a WHO consultation. Part 1, Diagnosis and classification of diabetes mellitus. http://apps.who.int/iris/handle/10665/66040. Published 1999.
4. Targher G, Day CP, Bonora E. Risk of cardiovascular disease in patients with nonalcoholic fatty liver disease. *N Engl J Med* 2010;363:1341-1350.
5. Scheuermann-Freestone M, Madsen PL, Manners D, Blamire AM, Buckingham RE, Styles P, Radda GK, Neubauer S, Clarke K. Abnormal cardiac and skeletal muscle energy metabolism in patients with type 2 diabetes. *Circulation* 2003;107:3040-3046.
6. Meyer P, Filippatos GS, Ahmed MI, Iskandrian AE, Bittner V, Perry GJ, White M, Aban IB, Mujib M, Dell'Italia LJ, Ahmed A. Effects of right ventricular ejection fraction on outcomes in chronic systolic heart failure. *Circulation* 2010;121:252-258.
7. Ghio S, Gavazzi A, Campana C, Inserra C, Klersy C, Sebastiani R, Arbustini E, Recusani F, Tavazzi L. Independent and additive prognostic value of right ventricular systolic function and pulmonary artery pressure in patients with chronic heart failure. *J Am Coll Cardiol* 2001;37:183-188.
8. Aziz EF, Kukin M, Javed F, Musat D, Nader A, Pratap B, Shah A, Enciso JS, Chaudhry FA, Herzog E. Right ventricular dysfunction is a strong predictor of developing atrial fibrillation in acutely decompensated heart failure patients, ACAP-HF data analysis. *J Card Fail* 2010;16:827-834.
9. Krssak M, Falk Petersen K, Dresner A, DiPietro L, Vogel SM, Rothman DL, Roden M, Shulman GI. Intramyocellular lipid concentrations are correlated with insulin sensitivity in humans: a 1H NMR spectroscopy study. *Diabetologia* 1999;42:113-116.
10. Perseghin G, Scifo P, De Cobelli F, Pagliato E, Battezzati A, Arcelloni C, Vanzulli A, Testolin G, Pozza G, Del Maschio A, Luzi L. Intramyocellular triglyceride content is a determinant of in vivo insulin resistance in humans: a 1H-13C nuclear magnetic resonance spectroscopy assessment in offspring of type 2 diabetic parents. *Diabetes* 1999;48:1600-1606.
11. Samuel VT, Liu ZX, Qu X, Elder BD, Bilz S, Befroy D, Romanelli AJ, Shulman GI. Mechanism of hepatic insulin resistance in non-alcoholic fatty liver disease. *J Biol Chem* 2004;279:32345-32353.
12. Liu XH, Morris R, Spiller D, White M, Williams G. Orexin a preferentially excites glucose-sensitive neurons in the lateral hypothalamus of the rat in vitro. *Diabetes* 2001;50:2431-2437.
13. van den Hoek AM, van Heijningen C, Schröder-van der Elst JP, Ouwens DM, Havekes LM, Romijn JA, Kalsbeek A, Pijl H. Intracerebroventricular administration of neuropeptide Y induces hepatic insulin resistance via sympathetic innervation. *Diabetes* 2008;57:2304-2310.
14. Vidarsdottir S, Smeets PA, Eichelsheim DL, van Osch MJ, Viergever MA, Romijn JA, van der Grond J, Pijl H. Glucose ingestion fails to inhibit hypothalamic neuronal activity in patients with type 2 diabetes. *Diabetes* 2007;56:2547-2550.
15. Taki Y, Kinomura S, Sato K, Inoue K, Goto R, Okada K, Uchida S, Kawashima R, Fukuda H. Relationship between body mass index and gray matter volume in 1,428 healthy individuals. *Obesity (Silver Spring)* 2008;16:119-124.
16. Pattynama PM, de Roos A, van der Wall EE, van Voorthuisen AE. Evaluation of cardiac function with magnetic resonance imaging. *Am Heart J* 1994;128:595-607.

17. Paelinck BP, Lamb HJ, Bax JJ, van der Wall EE, de Roos A. Assessment of diastolic function by cardiovascular magnetic resonance. *Am Heart J* 2002;144:198-205.
18. Grotenhuis HB, Ottenkamp J, Westenberg JJ, Bax JJ, Kroft LJ, de Roos A. Reduced aortic elasticity and dilatation are associated with aortic regurgitation and left ventricular hypertrophy in nonstenotic bicuspid aortic valve patients. *J Am Coll Cardiol* 2007;49:1660-1665.
19. Szczepaniak LS, Nurenberg P, Leonard D, Browning JD, Reingold JS, Grundy S, Hobbs HH, Dobbins RL. Magnetic resonance spectroscopy to measure hepatic triglyceride content: prevalence of hepatic steatosis in the general population. *Am J Physiol Endocrinol Metab* 2005;288:E462-468.
20. Ogawa S, Lee TM, Kay AR, Tank DW. Brain magnetic resonance imaging with contrast dependent on blood oxygenation. *Proc Natl Acad Sci U S A* 1990;87:9868-9872.
21. van Buchem MA, McGowan JC, Grossman RI. Magnetization transfer histogram methodology: its clinical and neuropsychological correlates. *Neurology* 1999;53:S23-28.

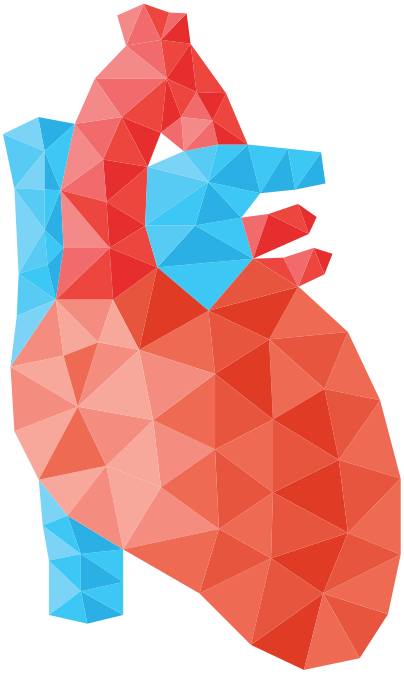

PART 1

CARDIOVASCULAR SYSTEM

Chapter 2

Association between hepatic triglyceride content and left ventricular diastolic function in a population-based cohort: the Netherlands Epidemiology of Obesity study

Ralph L. Widya
Renée de Mutsert
Martin den Heijer
Saskia le Cessie
Frits R. Rosendaal
J. Wouter Jukema
Johannes W.A. Smit
Albert de Roos
Hildo J. Lamb

for the NEO Study Group

Radiology 2016;279(2):443-450

ABSTRACT

Background

Nonalcoholic fatty liver disease is associated with increased prevalence and incidence of cardiovascular disease. The purpose of the study was to investigate the association between hepatic triglyceride content and left ventricular (LV) diastolic function while taking potential confounding factors into account, including the components of the metabolic syndrome.

Methods

The study was approved by the institutional review board, and all participants gave informed consent. In this cross-sectional analysis of baseline data from the Netherlands Epidemiology of Obesity study, a population-based, prospective cohort study, participants (45% men; mean age ± standard deviation, 55.3 years ± 6.2) underwent magnetic resonance (MR) spectroscopy and MR imaging to assess hepatic triglyceride content and LV diastolic heart function (ratio of peak filling rates of the early filling phase and atrial contraction [E/A ratio]). Multivariate linear regression analysis was performed while adjusting for confounding factors, and results were additionally stratified according to body mass index.

Results

Adjustment for age, sex, heart rate, alcohol consumption, pack-years of smoking, all components of the metabolic syndrome, and visceral adiposity attenuated crude observed associations. A 10-fold increase in hepatic triglyceride content was associated with a change in mean E/A ratio of −0.004 (95% confidence interval [CI]: −0.134, 0.125) in the total study population, −0.194 (95% CI: −0.430, 0.042) in the normal-weight subgroup, 0.079 (95% CI: −0.090, 0.248) in the overweight subgroup, and −0.109 (95% CI: −0.186, −0.032) in the obese subgroup.

Conclusions

Fatty liver itself could, at least in obesity, pose a risk of myocardial dysfunction above and beyond known cardiovascular risk factors that are clustered within the metabolic syndrome. The association in the obese subgroup was small, and future studies with larger samples sizes are required to investigate to what extent the association exists and differs in normal-weight, overweight, and obese persons to unravel its clinical relevance.

INTRODUCTION

Obesity has reached epidemic proportions during the past decades and is a well-established risk factor for various diseases, including nonalcoholic fatty liver disease (NAFLD) and cardiovascular disease[1]. NAFLD covers a spectrum of simple steatosis to nonalcoholic steatohepatitis and cirrhosis[2]. It is the most common liver disease, with a prevalence of 20%-30% in the general population, increasing to 70%-90% among persons who are obese or have type 2 diabetes[3]. NAFLD is therefore considered as a hepatic manifestation of the metabolic syndrome. NAFLD, and in particular nonalcoholic steatohepatitis, has been associated with increased prevalence[4, 5] and incidence[3] of cardiovascular disease and with decreased myocardial phosphate metabolism[6]. Cardiac disease is increasingly observed in persons with obesity, including subclinical impairment of left ventricular (LV) diastolic function, a precursor to overt heart failure[7]. Abnormalities of diastolic function have a major role in exercise intolerance in patients with heart failure[8]. Nevertheless, limited data are available concerning the relationship between NAFLD and myocardial function. Individuals with metabolic syndrome have a twofold risk of developing cardiovascular disease[9]. Potential underlying mechanisms, however, remain unclear. Cardiac myocyte contractile function is decreased by macrophages[10]. Although speculative, it can be hypothesized that macrophage recruitment in individuals with NAFLD could be present not only in the liver, but also in the heart, causing diastolic dysfunction. Alternatively, it has been suggested that increased intrahepatic cytokine expression plays a key role in the progression of cardiovascular disease[3].

Furthermore, the individual components that define the metabolic syndrome (three of the following five: high waist circumference, high serum triglyceride level, decreased serum high-density lipoprotein cholesterol level, high blood pressure, high fasting plasma glucose level) are also considered risk factors of both NAFLD and cardiovascular disease. This means that these components, and possibly the metabolic syndrome itself, may be responsible for an observed association between hepatic triglyceride content and diastolic function[3]. In other words, it is yet unclear whether the association between NAFLD and cardiovascular disease is a consequence of shared risk factors within the metabolic syndrome or exists independently of these risk factors.

Localized hydrogen 1 (^{1}H) magnetic resonance (MR) spectroscopy is a sensitive, quantitative, noninvasive method for measuring hepatic triglyceride content[11]. Cardiac MR imaging is a highly accurate and reproducible technique for assessing LV diastolic function[12, 13]. We hypothesized that hepatic triglyceride content is associated with LV diastolic function in a population-based cohort independent of the possible confounding effect of the metabolic syndrome. Therefore, the purpose of this study was to investigate the association between hepatic triglyceride content and LV diastolic function while taking potential confounding factors into account, including the components of the metabolic syndrome.

METHODS

Study population

Men and women aged 45-65 years with a self-reported body mass index (BMI) of 27 kg/m^2 or higher from Leiden and the surrounding area (Midwest of the Netherlands) were eligible to participate in the Netherlands Epidemiology of Obesity (NEO) study. In addition, all inhabitants aged 45-65 years of one municipality (Leiderdorp) were invited irrespective of their BMI, which allowed for a reference distribution of BMI. The study population of the present analysis consists of participants who had undergone MR imaging and ^{1}H MR spectroscopy. Exclusion criteria for this analysis were a history of cardiovascular disease, history of liver disease, alcohol consumption of more than 10 units per day, and use of statins and/or other lipid-lowering drugs. The study was approved by the medical ethics committee of the Leiden University Medical Center, and all participants provided written informed consent.

Study design

The present study is a cross-sectional analysis of baseline data from the NEO study. The NEO study is a population-based, prospective cohort study. Detailed information about the study design and data collection is available in the **Appendix**.

Metabolic syndrome

Characteristics of the metabolic syndrome were based on the updated National Cholesterol Education Program Adult Treatment Panel III definition[14] (see **Appendix**).

MR studies

MR imaging and spectroscopy were performed with a 1.5 Tesla whole-body MR unit (Philips Medical Systems, Best, the Netherlands). More detailed information, including imaging parameters, can be found in the **Appendix**.

MR spectroscopy

Hepatic ^{1}H MR spectra were obtained as described previously[15]. In short, an 8-mL voxel was positioned in the right lobe of the liver. A point-resolved spectroscopy sequence was used to acquire spectroscopic data during continuous breathing with automated shimming. Spectra were obtained with and without water suppression. Spectral data were fitted by using Java-based MR user interface software (jMRUI, version 3.0; developed by A. van den Boogaart, Katholieke Universiteit Leuven, Leuven, Belgium)[16]. Mean line widths of the spectra were calculated. The resonances that were fitted and used for calculation of the triglycerides were methylene (peak at 1.3 ppm, $[CH_2]_n$) and methyl (peak at 0.9 ppm, CH_3). The hepatic triglyceride content relative to water was calculated with the following formula: (signal amplitude of methylene + methyl) / (signal amplitude of water) × 100.

MR imaging

Abdominal visceral adipose tissue (VAT) and subcutaneous adipose tissue areas were quantified with a turbo spin-echo MR imaging protocol. At the level of the fifth lumbar vertebra, three transverse images were acquired during one breath hold. The entire heart was imaged in the short-axis orientation by using electrocardiographically gated breath-hold balanced steady-state free precession imaging to assess LV dimensions and mass. To determine diastolic function, an electrocardiographically gated gradient-echo sequence was performed with velocity encoding to measure blood flow across the mitral valve. Diastolic parameters included peak filling rates of the early filling phase (E) and atrial contraction (A) and their ratio (E/A ratio). Image postprocessing was performed with in-house-developed software packages (MASS and FLOW; Leiden University Medical Center, Leiden, the Netherlands), and decisions were made by consensus between two experienced observers (R.L.W. and H.J.L., with 5 and > 15 years of experience in cardiovascular MR imaging, respectively).

Statistical analyses

Additional information about the statistical analyses is provided in the **Appendix**. Baseline characteristics of participants are summarized as means ± standard deviations, medians and 25th and 75th percentiles, or as percentages according to categories of BMI. To this extent, participants were stratified into subgroups according to World Health Organization criteria (BMI of < 25 kg/m^2, 25-30 kg/m^2, and ≥ 30 kg/m^2). Comparisons among groups were tested with the two-tailed independent samples *t* test or the χ^2 test where appropriate. Multivariate linear regression analyses were used to study the association between hepatic triglyceride content and E/A ratio while adjusting for potential confounders in different models (**Appendix**). Hepatic triglyceride content showed a right-skewed distribution; to use this variable in the regression analysis, a log-transformation was applied (log hepatic triglyceride content). We examined the presence of interaction between hepatic triglyceride content and BMI in their association with E/A ratio by including product terms to the final model. Regression (β) coefficients, 95% confidence intervals (CIs), and *P* and R^2 values were reported. $P < 0.05$ was considered indicative of a statistically significant difference. Statistical analysis was performed with software (SPSS for Windows, version 17.0 [SPSS, Chicago, Ill] and Stata, version 12 [Stata, College Station, Tex]).

RESULTS

Between September 3, 2008, and September 28, 2012, 6673 participants were included in the NEO study, of whom 2580 underwent MR imaging and MR spectroscopy. Of those 2580 subjects, 1207 underwent cardiovascular MR imaging. Cardiovascular MR imaging failed because of technical errors in 35 participants. In another 246 participants, ^{1}H MR

spectroscopy of the liver could not be completed owing to technical errors (*n* = 241) or because the participant felt unwell (*n* = 5), for example because of claustrophobia. In our high-throughput study protocol, only a limited time slot was available per subject, and this

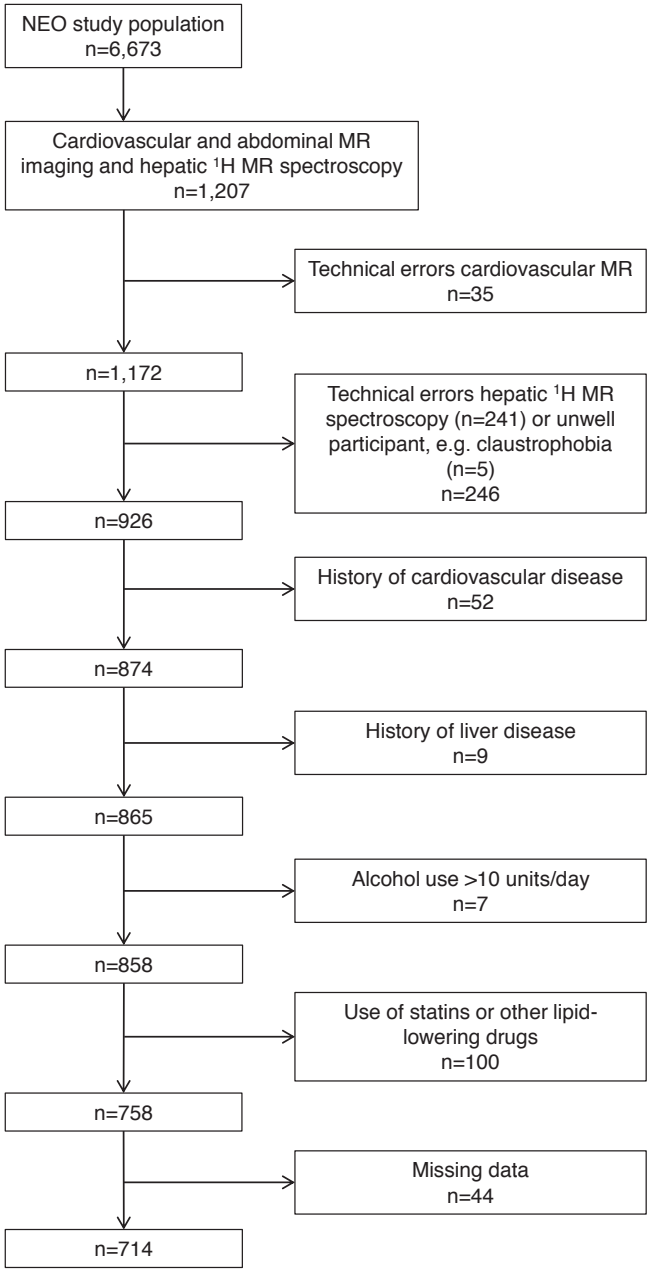

Figure 1. Study flowchart.

did not allow for repeat imaging when technical failures were recognized. The failure rate of MR spectroscopy was not related to age, sex, BMI, waist circumference, VAT, total body fat, or LV E/A ratio. Participants in whom MR spectroscopy was unsuccessful had higher subcutaneous adipose tissue compared with those who successfully underwent MR spectroscopy (mean, 738 cm^3 ± 298 vs. 701 cm^3 ± 290, respectively; $P = 0.04$). Ultimately, 926 participants successfully underwent cardiovascular and abdominal MR imaging and ^{1}H MR spectroscopy of the liver. Participants with a history of cardiovascular disease ($n = 52$), liver disease ($n = 9$), and alcohol consumption of more than 10 units per day ($n = 7$) and those taking statins and other lipid-lowering drugs ($n = 100$) were consecutively excluded. Furthermore, participants with missing data ($n = 44$) were excluded. Finally, 714 participants (45% men, 98% white) were included in the present analysis (**Figure 1**). The subjects had a mean age of 55.3 years ± 6.2 (men, 54.8 years ± 6.6; women, 55.6 years ± 5.8; $P > 0.05$), a median BMI of 25.6 kg/m^2 (25^{th} and 75^{th} percentiles, 22.9 kg/m^2 and 27.9 kg/m^2), and a median hepatic triglyceride content of 2.60% (25^{th} and 75^{th} percentiles, 1.30% and 6.05%). The hepatic triglyceride content ranged from 0.3% to 62.9%. Mean line widths of the spectra were 44.7 Hz ± 14.9 (water, 4.7 ppm), 46.7 Hz ± 18.9 (methylene, 1.3 ppm), and 43.2 Hz ± 18.4 (methyl, 0.9 ppm).

Participant characteristics are shown in **Table 1** and **Figure 2**. The median hepatic triglyceride content was highest in the obese subgroup. Furthermore, the prevalence of the metabolic syndrome was markedly higher in the obese subgroup ($P < 0.05$).

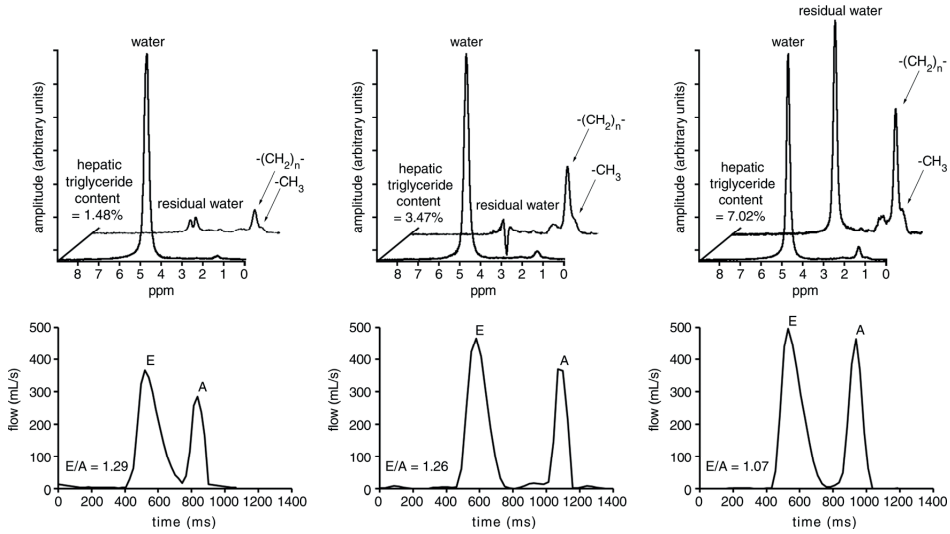

Figure 2. Representative examples of MR spectral data of hepatic triglyceride content (upper row) and MR imaging-derived LV diastolic function (lower row) in normal-weight (left), overweight (middle), and obese (right) participant. Spectra were obtained without (front) and with (back) water suppression. Resonances from protons of methylene (peak at 1.3 ppm, $[CH_2]_n$) and methyl (peak at 0.9 ppm, CH_3) are highlighted. *A* = atrial contraction, *E* = early filling phase.

Table 1. Participant characteristics according to BMI (n = 714)

Parameter	Normal-weight (BMI < 25 kg/m^2)	Overweight (BMI 25-30 kg/m^2)	Obese (BMI ≥ 30 kg/m^2)
Proportion of study population (%)	43	44	13
Men (%)	34	57*	42†
White subjects (%)	99	97	96
Age (y)	55.5 ± 3.5	55.2 ± 6.2	54.8 ± 10.5
Median BMI (kg/m^2)‡	22.4 (21.4, 23.8)	26.9 (25.9, 27.9)*	32.3 (31.0, 34.5)†§
Mean BSA (m^2)	1.8 ± 0.1	2.0 ± 0.2*	2.2 ± 0.3†§
Total body fat (%)	27.7 ± 3.9	31.3 ± 7.8*	40.1 ± 13.0†§
Men	18.9 ± 1.5	25.5 ± 3.3*	32.8 ± 7.8†§
Women	32.2 ± 2.0	39.1 ± 3.7*	45.5 ± 6.2†§
Median HTG content (%)‡	1.49 (0.93, 3.08)	3.44 (1.84, 7.43)*	7.64 (3.47, 15.54)†§
Mean VAT (cm^2)	161 ± 49	302 ± 136*	436 ± 320†§
Mean SAT (cm^2)	527 ± 89	734 ± 204*	1166 ± 554†§
Mean heart rate (beats/min)	66 ± 5	66 ± 11	68 ± 17†§
Mean pack-years of smoking	3.5 ± 3.7	8.4 ± 15.5*	11.1 ± 26.0†§
Mean systolic blood pressure (mmHg)	130 ± 11	131 ± 17	134 ± 30†§
Mean diastolic blood pressure (mmHg)	82 ± 6	85 ± 11*	86 ± 17†§
Metabolic syndrome (%)	6.6	23.9*	60.9†§
Mean waist circumference (cm)$^{\|}$	80.9 ± 4.2	94.9 ± 7.7*	108.2 ± 15.6†§
Men	87.6 ± 2.9	98.4 ± 6.2*	113.0 ± 11.2†§
Women	77.5 ± 3.5	90.4 ± 6.9*	104.7 ± 15.6†§
Median fasting triglyceride level (mmol/L)$^{\ddagger\|}$	0.8 (0.7, 1.1)	1.2 (0.9, 1.5)*	1.4 (1.0, 1.9)†§
Mean fasting HDL cholesterol level (mmol/L)$^{\|}$	1.7 ± 0.3	1.4 ± 0.4*	1.3 ± 0.6†§
Mean fasting total cholesterol level (mmol/L)	5.7 ± 0.5	5.9 ± 1.0	5.8 ± 1.8
Mean fasting glucose level (mmol/L)$^{\|}$	5.1 ± 0.2	5.5 ± 0.9*	5.7 ± 1.6†§
Hypertension (%)$^{\|}$	53.8	59.8	75.1†§
Diabetes (%)	0.0	3.8*	8.2†§

Results are based on weighted analyses. BSA = body surface area, HDL = high-density lipoprotein, HTG = hepatic triglyceride, SAT = subcutaneous adipose tissue.

* P < 0.05 normal-weight versus overweight subjects.

† P < 0.05 overweight versus obese subjects.

‡ Numbers in parentheses are the 25th and 75th percentiles.

§ P < 0.05 normal-weight versus obese subjects.

$^{\|}$ Component of the metabolic syndrome.

LV end-diastolic volume and LV mass indexed to body surface area were higher in the obese subgroup (P < 0.05) (**Table 2**). Although cardiac output was higher in the overweight and obese subgroups compared with the normal-weight subgroup, the cardiac index was similar among groups. Ejection fraction was similar between the normal-weight participants and overweight participants but was slightly higher in normal-weight compared with

Table 2. Left ventricular dimensions and function according to BMI ($n = 714$)

Parameter	Normal-weight (BMI < 25 kg/m^2)	Overweight (BMI 25-30 kg/m^2)	Obese (BMI ≥ 30 kg/m^2)
Dimensions			
End-diastolic volume (mL)	137.1 ± 16.1	153.7 ± 33.8*	161.1 ± 63.7†‡
End-diastolic volume index (mL/m^2)	76.9 ± 7.7	76.5 ± 13.3	73.9 ± 22.9‡
End-systolic volume (mL)	49.2 ± 7.1	56.8 ± 18.0*	60.9 ± 33.3†‡
End-systolic volume index (mL/m^2)	27.6 ± 3.7	28.2 ± 7.9	27.9 ± 13.6
Mass (g)	92.6 ± 11.8	107.4 ± 28.4*	111.4 ± 58.1†
Mass index (g/m^2)	51.7 ± 5.2	53.3 ± 11.6	50.8 ± 21.7‡
Systolic function			
Stroke volume (mL)	87.9 ± 10.6	96.9 ± 21.4*	100.2 ± 39.0†
Cardiac output (L/min)	5.8 ± 0.7	6.3 ± 1.4*	6.8 ± 2.7†‡
Cardiac index (L/min/m^2)	3.2 ± 0.3	3.2 ± 0.6	3.1 ± 1.0
Ejection fraction (%)	64.2 ± 2.7	63.4 ± 6.4	62.5 ± 10.9†
Diastolic function			
Peak flow rate of early filling phase (mL/s)	432.9 ± 53.4	452.6 ± 114.7	467.4 ± 209.9†
Peak flow rate of atrial contraction (mL/s)	330.1 ± 43.0	366.6 ± 104.0*	404.5 ± 159.4†‡
E/A ratio	1.36 ± 0.19	1.32 ± 0.49	1.20 ± 0.61†‡

Data are means ± standard deviations. Results are based on weighted analyses.

* $P < 0.05$ normal-weight versus overweight subjects.

† $P < 0.05$ normal-weight versus obese subjects.

‡ $P < 0.05$ overweight versus obese subjects.

obese participants. Diastolic function was lower in the obese subgroup, as demonstrated by a lower E/A ratio compared with the normal-weight and overweight subgroups ($P < 0.05$).

There was no statistically significant interaction between log hepatic triglyceride content and the three World Health Organization categories or with BMI as a continuous variable in their association with LV E/A ratio. However, there was a significant interaction between log hepatic triglyceride content and the binary variable BMI less than and greater than 27 kg/m^2 ($P = 0.012$), meaning that the association between log hepatic triglyceride content and LV E/A ratio is different below and above a BMI of 27 kg/m^2. Because of this arbitrary cutoff, we show the results stratified according to the World Health Organization categories of normal weight, overweight, and obesity.

Table 3 shows the association between hepatic triglyceride content and LV diastolic function in the entire study population and according to BMI. A significant crude inverse association was observed in the total study population (β: −0.170; 95% CI: −0.273, −0.068), normal-weight participants (β: −0.336; 95% CI: −0.509, −0.163), and obese participants (β: −0.209; 95% CI: −0.298, −0.121) (model 1). These associations diminished after adjusting for confounding factors in model 2. The addition of all components of the metabolic syndrome (model 3) or the metabolic syndrome as a single variable (model 3a) to the multivariate linear regression

model did not alter the results. After additional adjustment for VAT and total body fat in the final model (model 4), the inverse association between hepatic triglyceride content and E/A ratio was significant only in the obese subgroup (β:–0.109; 95% CI: –0.186, –0.032), which represents a decrease in mean E/A ratio of 0.109 for a 10-fold increase in hepatic triglyceride content. In other words, in two otherwise-identical obese individuals with hepatic triglyceride contents of 1.5% and 15%, the difference in E/A ratio is estimated to be 0.109. This applies on any 10-fold difference in hepatic triglyceride content. Additional adjustment for the presence of the metabolic syndrome above the five individual components did not alter the results.

Table 3. Association between hepatic triglyceride content and LV diastolic function in total study population and in normal-weight, overweight, and obese individuals

Model and subject group	β logHTGC*	95% CI	*P* value	R^2
Model 1 (crude)				
Total study population	-0.170	-0.273, -0.068	0.001	0.036
Normal-weight	-0.336	-0.509, -0.163	0.000	0.134
Overweight	-0.002	-0.180, 0.177	0.986	0.000
Obese	-0.209	-0.298, -0.121	0.000	0.067
Model 2 (model 1 + age, sex, heart rate, alcohol use, and pack-years)				
Total study population	-0.068	-0.160, 0.025	0.150	0.345
Normal-weight	-0.159	-0.319, 0.002	0.053	0.448
Overweight	0.059	-0.112, 0.230	0.501	0.323
Obese	-0.112	-0.185, -0.039	0.003	0.386
Model 3 (model 2 + all components metabolic syndrome)				
Total study population	0.001	-0.130, 0.131	0.994	0.379
Normal-weight	-0.180	-0.417, 0.057	0.134	0.474
Overweight	0.095	-0.077, 0.268	0.279	0.398
Obese	-0.118	-0.197, -0.040	0.003	0.408
Model 3a (model 2 + metabolic syndrome)				
Total study population	-0.028	-0.136, 0.081	0.618	0.354
Normal-weight	-0.120	-0.319, 0.078	0.232	0.453
Overweight	0.084	-0.094, 0.262	0.353	0.333
Obese	-0.118	-0.191, -0.045	0.002	0.387
Model 4 (model 3 + VAT + total body fat)				
Total study population	-0.004	-0.134, 0.125	0.946	0.381
Normal-weight	-0.194	-0.430, 0.042	0.106	0.476
Overweight	0.079	-0.090, 0.248	0.357	0.409
Obese	-0.109	-0.186, -0.032	0.006	0.411

Reported differences represent differences in E/A ratio associated with a 10-fold increase in hepatic triglyceride content. Corresponding 95% CIs and *P* values are shown. R^2 indicates the explained variance of E/A ratio according to the applied model. Results are based on weighted analyses.

* LogHTGC is the log-transformation of hepatic triglyceride content.

DISCUSSION

After stratification in BMI categories according to the World Health Organization, hepatic triglyceride content was significantly associated with diastolic function independent of confounding factors including the metabolic syndrome, VAT, and total body fat in obese adults aged 45-65 years. This association was not statistically significant in normal-weight and overweight subgroups. Future studies with larger sample sizes should reveal to what extent associations between hepatic triglyceride content and diastolic function exist and differ in normal-weight, overweight, and obese persons.

A large Korean epidemiologic study recently reported that NAFLD was associated with subclinical diastolic dysfunction independent of the metabolic syndrome[17]. Furthermore, LV diastolic function was impaired in normotensive nondiabetic patients with NAFLD compared with control subjects[18], and NAFLD was associated with the early diastolic velocity of the mitral annulus at tissue Doppler imaging in a multivariate stepwise regression analysis including metabolic and multiple echocardiographic variables[19]. In addition, patients with hypertension and NAFLD had a higher prevalence of diastolic dysfunction (E/A ratio, < 1) compared with hypertensive patients without NAFLD, and NAFLD was associated with diastolic function[20]. NAFLD was also associated with early diastolic dysfunction in patients with well-controlled type 2 diabetes mellitus after adjustment for age, sex, triglyceride level, hemoglobin A_{1c} level, and hypertension[21]. Most studies assessed NAFLD by using criteria for abdominal ultrasonography. Quantification of hepatic steatosis could therefore often not be assessed. Furthermore, most studies were limited by small sample sizes, whereas the current study aimed to investigate the relationship between hepatic triglyceride content and diastolic function in a large sample of the general population. The association between hepatic triglyceride content and LV E/A ratio in the normal-weight subgroup could not be detected with statistical significance, probably because of the small number of individuals in the normal-weight subgroup (n = 91). Therefore, future studies with larger sample sizes should reveal to what extent associations between hepatic triglyceride content and diastolic function exist and differ in normal-weight, overweight, and obese persons.

The complex interrelationships among NAFLD, the metabolic syndrome, visceral obesity, and cardiovascular complications make it difficult to distinguish the causal links underlying the increased risk of cardiovascular disease among patients with NAFLD and/or the metabolic syndrome[3]. For example, subjects who meet the diagnostic criteria for the metabolic syndrome have multiple risk factors for cardiovascular disease[22]. The findings from our study suggest that hepatic triglyceride content contributes to subclinical impairment of LV diastolic function independently of the components of the metabolic syndrome, at least in obese persons. Further study is required to unravel the clinical relevance of the observed small association.

Causal pathways between fatty liver and diastolic function are speculative, but inflammatory cytokines, lipids, and advanced glycation end-products may play an important role[23]. An important link between hepatic steatosis and cardiac disease has been described by Rijzewijk et al[6], who reported an association between hepatic steatosis and decreased myocardial perfusion, glucose uptake, and high-energy phosphate metabolism, but not with LV function, in type 2 diabetes. In addition, interstitial myocardial fibrosis has been associated with myocardial systolic and diastolic function in patients with diabetes[24]. These findings may indicate an early alteration in myocardial tissue and/or vascular properties. Perseghin et al[25] reported that fatty liver was associated with changes in LV energy metabolism in healthy obese individuals. An animal study provided evidence that decreased adenosine triphosphate synthesis may be responsible for LV dysfunction in obesity[26]. It may be hypothesized that NAFLD causes myocardial tissue alterations that lead to diastolic dysfunction. Diastolic dysfunction reflects increased LV diastolic stiffness, which is recognized as the earliest manifestation of LV dysfunction in diabetes mellitus, and is caused by fibrosis, deposition of advanced glycation end-products, and increased cardiomyocyte resting tension[27]. Structural myocardial changes have been found in this study and are reflected by decreased LV end-diastolic volume index and increased LV mass in obesity.

Our study adds to the present knowledge that fatty liver was inversely associated with LV diastolic function independent of the metabolic syndrome and abdominal visceral adiposity, which may suggest subclinical impaired LV relaxation. The importance of subclinical effects is the potential reversibility of the pathophysiologic process, and the possibility to detect and follow up before overt cardiovascular failure is apparent. Increased intrahepatic cytokine expression is likely to play a key role in the progression of NAFLD[3, 23, 28] and cardiovascular disease[29, 30].

Strengths of this study are the large study population and the availability of ^{1}H MR spectroscopy to quantify hepatic steatosis in combination with cardiac MR imaging. To the best of our knowledge, the current study is the first to report associations between hepatic triglyceride content and diastolic dysfunction in a general Western population. Further strengths are the availability of information about the components of the metabolic syndrome and other potential confounding variables, including total body fat and VAT.

A few limitations of this study should be addressed. No imaging modality is currently able to depict subtle histologic changes of inflammation and thus help differentiate simple steatosis from nonalcoholic steatohepatitis. Therefore, liver biopsy is the standard of reference for differentiating these two stages of NAFLD[31]. For ethical reasons, we could not perform liver biopsies in this study and therefore could not classify nonalcoholic steatohepatitis. To assess NAFLD, we measured hepatic triglyceride content by using localized ^{1}H MR spectroscopy. Because of limited MR protocol time per participant in this large population-based cohort study, we did not correct for individual T2 relaxation times and we could not perform repeat imaging when technical failures were recognized. Proton-density fat fraction measurement

with MR imaging recently showed good diagnostic accuracy for quantifying steatosis[32, 33]. Unfortunately, this technique was not yet validated at the time our study started in 2008. Optimally, such an advanced MR imaging technique would be better than MR spectroscopy, not least because MR spectroscopy is technically demanding. Participants in whom MR spectroscopy was unsuccessful had slightly higher amounts of subcutaneous adipose tissue, which potentially could have introduced selection bias. Finally, the observational, cross-sectional nature of our study precludes a causal interpretation of our results.

In conclusion, we showed that hepatic triglyceride content was associated with decreased diastolic function; however, adjustments for confounding factors attenuated this association. Only in persons with obesity could an association independent of the metabolic syndrome and abdominal visceral adiposity be demonstrated significantly. Therefore, confounding factors seem to largely explain the relationship between hepatic triglyceride content and diastolic function, but fatty liver itself could, at least in obesity, pose a risk of myocardial dysfunction above and beyond known cardiovascular risk factors that are clustered within the metabolic syndrome. Prospective follow-up research is required to study the effect of hepatic steatosis on incident cardiovascular events.

REFERENCES

1. Bray GA. Medical consequences of obesity. *J Clin Endocrinol Metab* 2004;89:2583-2589.
2. Mulhall BP, Ong JP, Younossi ZM. Non-alcoholic fatty liver disease: an overview. *J Gastroenterol Hepatol* 2002;17:1136-1143.
3. Targher G, Day CP, Bonora E. Risk of cardiovascular disease in patients with nonalcoholic fatty liver disease. *N Engl J Med* 2010;363:1341-1350.
4. Targher G, Bertolini L, Padovani R, Rodella S, Zoppini G, Zenari L, Cigolini M, Falezza G, Arcaro G. Relations between carotid artery wall thickness and liver histology in subjects with nonalcoholic fatty liver disease. *Diabetes Care* 2006;29:1325-1330.
5. Lin YC, Lo HM, Chen JD. Sonographic fatty liver, overweight and ischemic heart disease. *World J Gastroenterol* 2005;11:4838-4842.
6. Rijzewijk LJ, Jonker JT, van der Meer RW, Lubberink M, de Jong HW, Romijn JA, Bax JJ, de Roos A, Heine RJ, Twisk JW, Windhorst AD, Lammertsma AA, Smit JW, Diamant M, Lamb HJ. Effects of hepatic triglyceride content on myocardial metabolism in type 2 diabetes. *J Am Coll Cardiol* 2010;56:225-233.
7. Abel ED, Litwin SE, Sweeney G. Cardiac remodeling in obesity. *Physiol Rev* 2008;88:389-419.
8. Nishimura RA, Tajik AJ. Evaluation of diastolic filling of left ventricle in health and disease: Doppler echocardiography is the clinician's Rosetta Stone. *J Am Coll Cardiol* 1997;30:8-18.
9. Mottillo S, Filion KB, Genest J, Joseph L, Pilote L, Poirier P, Rinfret S, Schiffrin EL, Eisenberg MJ. The metabolic syndrome and cardiovascular risk a systematic review and meta-analysis. *J Am Coll Cardiol* 2010;56:1113-1132.
10. Simms MG, Walley KR. Activated macrophages decrease rat cardiac myocyte contractility: importance of ICAM-1-dependent adhesion. *Am J Physiol* 1999;277:H253-260.
11. Szczepaniak LS, Nurenberg P, Leonard D, Browning JD, Reingold JS, Grundy S, Hobbs HH, Dobbins RL. Magnetic resonance spectroscopy to measure hepatic triglyceride content: prevalence of hepatic steatosis in the general population. *Am J Physiol Endocrinol Metab* 2005;288:E462-468.
12. Pattynama PM, de Roos A, van der Wall EE, van Voorthuisen AE. Evaluation of cardiac function with magnetic resonance imaging. *Am Heart J* 1994;128:595-607.
13. Paelinck BP, Lamb HJ, Bax JJ, van der Wall EE, de Roos A. Assessment of diastolic function by cardiovascular magnetic resonance. *Am Heart J* 2002;144:198-205.
14. Grundy SM, Cleeman JI, Daniels SR, Donato KA, Eckel RH, Franklin BA, Gordon DJ, Krauss RM, Savage PJ, Smith SC, Jr., Spertus JA, Costa F. Diagnosis and management of the metabolic syndrome: an American Heart Association/National Heart, Lung, and Blood Institute Scientific Statement. *Circulation* 2005;112:2735-2752.
15. van der Meer RW, Hammer S, Lamb HJ, Frölich M, Diamant M, Rijzewijk LJ, de Roos A, Romijn JA, Smit JW. Effects of short-term high-fat, high-energy diet on hepatic and myocardial triglyceride content in healthy men. *J Clin Endocrinol Metab* 2008;93:2702-2708.
16. Naressi A, Couturier C, Devos JM, Janssen M, Mangeat C, de Beer R, Graveron-Demilly D. Java-based graphical user interface for the MRUI quantitation package. *MAGMA* 2001;12:141-152.
17. Kim NH, Park J, Kim SH, Kim YH, Kim DH, Cho GY, Baik I, Lim HE, Kim EJ, Na JO, Lee JB, Lee SK, Shin C. Non-alcoholic fatty liver disease, metabolic syndrome and subclinical cardiovascular changes in the general population. *Heart* 2014;100:938-943.
18. Fotbolcu H, Yakar T, Duman D, Karaahmet T, Tigen K, Cevik C, Kurtoglu U, Dindar I. Impairment of the left ventricular systolic and diastolic function in patients with non-alcoholic fatty liver disease. *Cardiol J* 2010;17:457-463.
19. Goland S, Shimoni S, Zornitzki T, Knobler H, Azoulai O, Lutaty G, Melzer E, Orr A, Caspi A,

Malnick S. Cardiac abnormalities as a new manifestation of nonalcoholic fatty liver disease: echocardiographic and tissue Doppler imaging assessment. *J Clin Gastroenterol* 2006;40:949-955.

20. Fallo F, Dalla PA, Sonino N, Lupia M, Tona F, Federspil G, Ermani M, Catena C, Soardo G, Di Piazza L, Bernardi S, Bertolotto M, Pinamonti B, Fabris B, Sechi LA. Non-alcoholic fatty liver disease is associated with left ventricular diastolic dysfunction in essential hypertension. *Nutr Metab Cardiovasc Dis* 2009;19:646-653.
21. Bonapace S, Perseghin G, Molon G, Canali G, Bertolini L, Zoppini G, Barbieri E, Targher G. Nonalcoholic fatty liver disease is associated with left ventricular diastolic dysfunction in patients with type 2 diabetes. *Diabetes Care* 2012;35:389-395.
22. Bonora E. The metabolic syndrome and cardiovascular disease. *Ann Med* 2006;38:64-80.
23. Shoelson SE, Herrero L, Naaz A. Obesity, inflammation, and insulin resistance. *Gastroenterology* 2007;132:2169-2180.
24. Ng AC, Auger D, Delgado V, van Elderen SG, Bertini M, Siebelink HM, van der Geest RJ, Bonetti C, van der Velde ET, de Roos A, Smit JW, Leung DY, Bax JJ, Lamb HJ. Association between diffuse myocardial fibrosis by cardiac magnetic resonance contrast-enhanced T(1) mapping and subclinical myocardial dysfunction in diabetic patients: a pilot study. *Circ Cardiovasc Imaging* 2012;5:51-59.
25. Perseghin G, Lattuada G, De Cobelli F, Esposito A, Belloni E, Ntali G, Ragogna F, Canu T, Scifo P, Del Maschio A, Luzi L. Increased mediastinal fat and impaired left ventricular energy metabolism in young men with newly found fatty liver. *Hepatology* 2008;47:51-58.
26. Ge F, Hu C, Hyodo E, Arai K, Zhou S, Lobdell H 4th, Walewski JL, Homma S, Berk PD. Cardiomyocyte triglyceride accumulation and reduced ventricular function in mice with obesity reflect increased long chain Fatty Acid uptake and de novo Fatty Acid synthesis. *J Obes* 2012;2012:205648.
27. van Heerebeek L, Hamdani N, Handoko ML, Falcao-Pires I, Musters RJ, Kupreishvili K, IJsselmuiden AJ, Schalkwijk CG, Bronzwaer JG, Diamant M, Borbely A, van der Velden J, Stienen GJ, Laarman GJ, Niessen HW, Paulus WJ. Diastolic stiffness of the failing diabetic heart: importance of fibrosis, advanced glycation end products, and myocyte resting tension. *Circulation* 2008;117:43-51.
28. Stefan N, Kantartzis K, Haring HU. Causes and metabolic consequences of Fatty liver. *Endocr Rev* 2008;29:939-960.
29. Targher G, Marra F, Marchesini G. Increased risk of cardiovascular disease in non-alcoholic fatty liver disease: causal effect or epiphenomenon? *Diabetologia* 2008;51:1947-1953.
30. de Alwis NM, Day CP. Non-alcoholic fatty liver disease: the mist gradually clears. *J Hepatol* 2008;48 Suppl 1:S104-112.
31. Adams LA, Feldstein AE. Non-invasive diagnosis of nonalcoholic fatty liver and nonalcoholic steatohepatitis. *J Dig Dis* 2011;12:10-16.
32. Idilman IS, Aniktar H, Idilman R, Kabacam G, Savas B, Elhan A, Celik A, Bahar K, Karcaaltincaba M. Hepatic steatosis: quantification by proton density fat fraction with MR imaging versus liver biopsy. *Radiology* 2013;267:767-775.
33. Yokoo T, Bydder M, Hamilton G, Middleton MS, Gamst AC, Wolfson T, Hassanein T, Patton HM, Lavine JE, Schwimmer JB, Sirlin CB. Nonalcoholic fatty liver disease: diagnostic and fat-grading accuracy of low-flip-angle multiecho gradient-recalled-echo MR imaging at 1.5 T. *Radiology* 2009;251:67-76.

APPENDIX

METHODS

Study design

Detailed information about the study design of the NEO study and data collection has been described elsewhere[34]. In short, enrolled participants completed a questionnaire about demographic and clinical information and came to the NEO study site for one morning after an overnight fast for several baseline measurements, including anthropometric measurements and blood sampling. In a random subset of approximately 30% of the study population without contraindications to MR imaging (metallic devices, claustrophobia, or a body circumference > 170 cm), MR imaging of the abdomen and ^{1}H MR spectroscopy of the liver were performed. The MR imaging data of abdominal visceral and subcutaneous adipose tissue of our study population have been described in previously published articles[35-37]; however, this is the first article reporting results of ^{1}H MR spectroscopy of the liver and cardiovascular MR imaging.

Data collection

Information about alcohol consumption, smoking behavior, history of cardiovascular disease, and liver disease was collected with a baseline questionnaire. Alcohol consumption was classified in six categories (0 units per day, ≤ 1 unit per week, 2-6 units per week, 1 unit per day, 2-4 units per day, and 5-9 units per day). Smoking data were converted to pack-years, defined as mean packs per day times years of smoking. History of cardiovascular disease was defined as myocardial infarction, angina, congestive heart failure, stroke, or peripheral vascular disease. History of liver disease included cirrhosis and hepatitis. Medication use in the month preceding the study visit was recorded at the study site. Body weight and total body fat (in percentage) were measured by using the Tanita bioimpedance balance (TBF-310; Tanita International Division, Yiewsley, United Kingdom) without shoes; 1 kilogram was subtracted to correct for the weight of clothing. BMI was calculated by dividing weight in kilograms by the height in meters squared. Body surface area was calculated according to the Mosteller formula[38,39], as follows: (weight [in kilograms] × height [in centimeters]/3600)$^{0.5}$. Waist circumference was measured between the border of the lower costal margin and the iliac crest, and measurements were rounded to the nearest millimeter. Blood samples were taken after an overnight fast of at least 10 hours. Serum concentrations of total cholesterol and high-density lipoprotein (HDL) were determined by using standard enzymatic methods (Roche Modular Analytics P800; Roche Diagnostics, Mannheim, Germany). Serum alanine aminotransferase and aspartate aminotransferase were measured by using ultraviolet tests

(Cobas Integra 800 Analyzer, Roche Diagnostics). All analyses were performed in the central clinical chemistry laboratory of Leiden University Medical Center[34].

Metabolic syndrome

According to the National Cholesterol Education Program Adult Treatment Panel III definition, the metabolic syndrome is defined as having any three of the following five measures: (a) waist circumference of at least 102 cm in men or 88 cm in women, (b) triglyceride level of at least 1.7 mmol/L or receiving drug treatment for elevated triglyceride level, (c) HDL level less than 1.03 mmol/L in men or less than 1.3 mmol/L in women or receiving drug treatment for reduced HDL, (d) systolic blood pressure of at least 130 mmHg and/or diastolic blood pressure of at least 85 mmHg or on antihypertensive drug treatment, and (e) elevated fasting glucose level of at least 5.6 mmol/L or on drug treatment for elevated glucose.

MR spectroscopy

Gross vascular structures and adipose tissue depots were avoided when positioning the 8-mL voxel in the right lobe of the liver. Sixty-four signals were acquired with water suppression (repetition time = 2900 ms; echo time = 23 ms [2900/23]). Data points (1024) were collected by using a 1000-Hz spectral line. Without changing any parameters, spectra without water suppression (repetition time = 10 seconds; four signals acquired) were obtained as an internal reference. Spectra were not corrected for frequency drift. Spectral data were analyzed while blinded to all study parameters, including age, sex, LV function and dimensions, BMI, waist circumference, visceral adipose tissue, and total body fat. Spectra were initially included when automatic fitting was successful. When line shapes were distorted by eddy currents or as a result of poor shimming, spectral data were rejected.

MR imaging

Imaging parameters of the turbo spin-echo protocol to assess abdominal VAT and subcutaneous adipose tissue were as follows: 300/20; flip angle, 90˚; section thickness, 10 mm, section gap, 2 mm. VAT and subcutaneous adipose tissue areas were quantified by converting the number of pixels to square centimeters and totaling the areas of the three sections, using in-house-developed software (MASS; Leiden University Medical Center, Leiden, the Netherlands)[40]. In the cardiovascular imaging protocol, the parameters of the balanced steady-state free precession imaging for measuring LV dimensions were as follows: 3.4/1.7; flip angle, 35˚; section thickness, 10 mm, section gap, 0 mm; field of view, 400 × 400 mm; and reconstructed matrix size, 256 × 256. LV dimensions (end-diastolic volume and end-systolic volume), mass, and cardiac output were indexed to body surface area. Imaging parameters of the gradient-echo sequence for measuring blood flow across the mitral valve were as follows: 6.5/1; flip angle, 20˚; section thickness, 8 mm; field of view, 350 × 350 mm; matrix size, 256 × 256; velocity encoding gradient, 150 cm/s; and imaging percentage, 80%.

Statistical analyses

In the NEO study, individuals with a BMI of 27 kg/m^2 and greater were oversampled. To correctly represent associations in the general population[41], adjustments for the oversampling of individuals with a BMI of at least 27 kg/m^2 were made. This was done by weighting individuals toward the BMI distribution of participants from the Leiderdorp municipality[42], whose BMI distribution was similar to the BMI distribution in the general Dutch population[43]. All results were based on weighted analyses. Consequently, results apply to a population-based study without an oversampling of BMI of at least 27 kg/m^2. Participants were stratified into subgroups according to the World Health Organization criteria (< 25 kg/m^2, 25-30 kg/m^2, ≥ 30 kg/m^2). Because there was only one participant with a BMI of less than 18.5 kg/m^2, this category could not be studied separately. The following multivariate linear regression analyses were used to study the association between hepatic triglyceride content and E/A ratio: We adjusted the crude (model 1) association between hepatic triglyceride content and E/A ratio for age, sex, heart rate, alcohol consumption, pack-years of smoking (model 2), and, additionally for all components of the metabolic syndrome, waist circumference, serum triglycerides, high-density lipoprotein cholesterol, systolic and diastolic blood pressure, and fasting plasma glucose level (model 3). It may be possible that the metabolic syndrome represents more than the sum of its parts. Therefore, we also adjusted for the metabolic syndrome as a dichotomous variable instead of the individual components (model 3a). Subsequently, VAT and total body fat were added to the regression model (model 4). Finally, the metabolic syndrome as a single variable was added to the regression model.

REFERENCES

34. de Mutsert R, den Heijer M, Rabelink TJ, Smit JW, Romijn JA, Jukema JW, de Roos A, Cobbaert CM, Kloppenburg M, le Cessie S, Middeldorp S, Rosendaal FR. The Netherlands Epidemiology of Obesity (NEO) study: study design and data collection. *Eur J Epidemiol* 2013;28:513-523.
35. Visser AW, Ioan-Facsinay A, de Mutsert R, Widya RL, Loef M, de Roos A, le Cessie S, den Heijer M, Rosendaal FR, Kloppenburg M, for the NEO study group. Adiposity and hand osteoarthritis: the Netherlands Epidemiology of Obesity study. *Arthritis Res Ther* 2014;16:R19.
36. Hillebrand S, de Mutsert R, Christen T, Maan AC, Jukema JW, Lamb HJ, de Roos A, Rosendaal FR, den Heijer M, Swenne CA. Body fat, especially visceral fat, is associated with electrocardiographic measures of sympathetic activation. *Obesity (Silver Spring)* 2014;22:1553-1559.
37. Gast KB, den Heijer M, Smit JW, Widya RL, Lamb HJ, de Roos A, Jukema JW, Rosendaal FR, de Mutsert R, for the NEO study group. Individual contributions of visceral fat and total body fat to subclinical atherosclerosis: The NEO study. *Atherosclerosis* 2015;241:547-554.
38. Mosteller RD. Simplified calculation of body-surface area. *N Engl J Med* 1987;317:1098.
39. Verbraecken J, van de Heyning P, de Backer W, van Gaal L. Body surface area in normal-weight, overweight, and obese adults. A comparison study. *Metabolism* 2006;55:515-524.
40. Hammer S, van der Meer RW, Lamb HJ, de Boer HH, Bax JJ, de Roos A, Romijn JA, Smit JW. Short-term flexibility of myocardial triglycerides and diastolic function in patients with type 2 diabetes mellitus. *Am J Physiol Endocrinol Metab* 2008;295:E714-718.
41. Korn EL, Graubard BI. Epidemiologic studies utilizing surveys: accounting for the sampling design. *Am J Public Health* 1991;81:1166-1173.
42. Lumley T. Analysis of complex survey samples. Journal of Statistical Software. 2004;9. http://www.jstatsoft.org/v09/i08/paper. Published April 15, 2004.
43. Nederland de Maat Genomen. Ministerie van Volksgezondheid, Welzijn en Sport. http://www.rivm.nl/dsresource?objectid=rivmp:76024&type=org&disposition=inline&ns_nc=1. Published January 26, 2012.

Chapter 3

Is hepatic triglyceride content associated with aortic pulse wave velocity and carotid intima-media thickness? The Netherlands Epidemiology of Obesity study

Ralph L. Widya
Renée de Mutsert
Jos J.M. Westenberg
Karin B. Gast
Martin den Heijer
Saskia le Cessie
Johannes W.A. Smit
J. Wouter Jukema
Frits R. Rosendaal
Albert de Roos
Hildo J. Lamb

for the NEO Study Group

Accepted for publication in Radiology 2017

ABSTRACT

Background

Nonalcoholic fatty liver disease is associated with an increased risk of cardiovascular disease. The purpose of this study was to test the hypothesis that hepatic triglyceride content is associated with subclinical vascular impairment and is not confounded by various cardiometabolic risk factors.

Methods

This study was approved by the institutional review board, and all participants gave written informed consent. In this cross-sectional analysis of baseline measurements of the Netherlands Epidemiology of Obesity study, a population-based cohort study, 1899 participants (52% men; mean age, 55 years ± 6 [standard deviation]) underwent magnetic resonance (MR) spectroscopy and MR imaging to assess hepatic triglyceride content, aortic pulse wave velocity (PWV), and visceral fat. Carotid intima-media thickness (IMT) was acquired and measured by trained research nurses according to standard procedures. Multivariate regression analyses were used to study associations of hepatic triglyceride content with total and regional aortic PWV and carotid IMT while adjusting for several possible confounding factors, including the metabolic syndrome.

Results

Total aortic PWV (mean difference, 0.5 m/s; 95% confidence interval [CI]: 0.3, 0.7) and carotid IMT (mean difference, 37 μm; 95% CI: 25, 49) were higher in participants with hepatic steatosis. After adjusting for various covariates, a 10-fold increase in hepatic triglyceride content was associated with an increased mean aortic PWV of 0.19 m/s (95% CI: 0.03, 0.36) in total and an increased mean aortic PWV of 0.42 m/s (95% CI: 0.03, 0.81) in the abdominal segment. A 10-fold increase in hepatic triglyceride content was also associated with an increased mean carotid IMT of 15 μm (95% CI: 0, 29) but not after additional adjustments for visceral and total body fat.

Conclusions

In this relatively large population-based cohort study, hepatic triglyceride content was associated with aortic pulse wave velocity and carotid IMT. These associations were only partly explained by the metabolic syndrome and visceral adiposity, suggesting a possible specific contribution of hepatic steatosis to subclinical vascular impairment.

INTRODUCTION

Nonalcoholic fatty liver disease (NAFLD) is being diagnosed with increasing frequency and is considered to be the most common chronic liver disease in Western countries, with a prevalence of 20%-30% in the general population[1, 2] and a prevalence of 90% in patients with severe obesity[3]. The recent literature shows an ongoing worldwide trend of increasing body mass index (BMI), with a global prevalence of severe obesity (BMI ≥ 35 kg/m^2) of 2.3% in men and 5.0% in women in 2014[4].

NAFLD has been associated with increased brachial-ankle pulse wave velocity (PWV)[5, 6] and increased carotid intima-media thickness (IMT)[7]. PWV of the aorta is a marker for central arterial stiffness, and it is a prognostic marker for cardiovascular disease[8-10]. Aortic PWV assessed with magnetic resonance (MR) imaging has an advantage over brachial-ankle PWV, in that the true path length of the pulse wave along the aorta can be directly assessed, even in the presence of a tortuous course of the aorta, and regional elastic properties of the aorta can be studied depending on the number of aortic segments examined[11]. Increased carotid IMT is an early indicator of generalized atherosclerosis and is a risk factor for myocardial infarction and stroke[12].

Obesity is recognized as an important contributor to NAFLD[13], increased arterial stiffness[14, 15], and subclinical atherosclerosis[16]. Additionally, NAFLD and cardiovascular disease share common risk factors, which are clustered in the metabolic syndrome[17]. These risk factors may confound observed associations between NAFLD and surrogate markers of cardiovascular disease. We have previously shown that hepatic triglyceride content is associated with decreased diastolic function after adjustment for the individual components of the metabolic syndrome and visceral adiposity[18]. However, it is unclear whether hepatic triglyceride content is truly associated with aortic PWV and carotid IMT or if hepatic steatosis and subclinical vascular impairment are merely common consequences of the obese state. We hypothesized that hepatic triglyceride content is associated with subclinical vascular changes. Thus, the purpose of our study was to investigate the relationships between hepatic triglyceride content and aortic PWV and carotid IMT and to what extent these relationships were explained by the metabolic syndrome and measurements of overall and abdominal obesity in a relatively large number of individuals.

METHODS

Study design and study population

This is a cross-sectional analysis of baseline measurements of the Netherlands Epidemiology of Obesity (NEO) study. The NEO study is a population-based prospective cohort study, with an oversampling of individuals with a BMI of 27 kg/m^2 or higher. A detailed description

of the study design and data collection has been published elsewhere[19]. In short, men and women aged 45-65 years with a self-reported BMI of 27 kg/m^2 or higher from Leiden, the Netherlands, and the surrounding area were included between September 2008 and October 2012. In addition, all inhabitants aged 45-65 years in one municipality (Leiderdorp, the Netherlands) were invited irrespective of their BMI, allowing for a reference distribution of BMI. For pragmatic reasons (time), only three participants could undergo MR imaging and MR spectroscopy each day. Thus, we randomly selected the first three participants without contraindications for MR imaging and MR spectroscopy. This resulted in a subset of approximately 30% of all NEO study participants who underwent MR imaging of the aorta and abdomen in addition to proton (^{1}H) MR spectroscopy of the liver. In our current study, we included participants with MR imaging of the aorta and abdomen, ^{1}H MR spectroscopy of the liver, and a carotid IMT measurement. Exclusion criteria for this analysis were missing data of any of the aforementioned measurements, missing data of any parameter used in the multivariate regression analyses, a history of liver disease, alcohol consumption of more than 10 units per day, or any combination thereof. The relationship between hepatic steatosis and left ventricular diastolic function was previously described in a subset ($n = 714$) of the current study population[18]. Our study was approved by the medical ethics committee of Leiden University Medical Center, and all participants provided written informed consent.

Data collection

A history of cardiovascular disease was defined as myocardial infarction, angina, congestive heart failure, stroke, or peripheral vascular disease. History of liver disease included cirrhosis and hepatitis. Total body fat was estimated with a bioimpedance device (TBF-310; Tanita International Division, Yiewsley, England). Blood was sampled after an overnight fast of at least 10 hours. Metabolic syndrome was defined by the updated National Cholesterol Education Program Adult Treatment Panel III report[20] (**Appendix**).

MR studies

All MR studies were performed with a 1.5 Tesla whole-body MR imager (Philips Medical Systems, Best, the Netherlands). Detailed information, including imaging parameters, can be found in the **Appendix**.

Hepatic triglyceride content

Hepatic spectral data were acquired with a point-resolved spectroscopy sequence with free breathing. All spectral data were analyzed with the reader blinded to all study parameters and patient information. Spectra were initially included when automatic fitting was successful. When line shapes were distorted by eddy currents or as a result of poor shimming, spectral data were rejected. In addition, mean line widths of the spectra were calculated. Hepatic triglyceride content relative to water was calculated as the sum of signal amplitudes

of methyl and methylene divided by the signal amplitude of water and then multiplied by 100.

Aortic PWV

Through-plane flow measurements of the ascending, proximal descending, mid-descending, and distal descending aorta were acquired. Aortic PWV was calculated by dividing the aortic path length between the measurement sites by the transit time between the arrival of the systolic wave front at these sites, and it is expressed in meters per second.

Visceral adipose tissue

Visceral adipose tissue was assessed with a fast spin-echo MR imaging protocol. At the level of the fifth lumbar vertebra, three transverse images were acquired during one breath hold. Visceral adipose tissue was quantified by converting the number of pixels to square centimeters and adding the areas of the individual sections by using in-house software (MASS; Leiden University Medical Center, Leiden, the Netherlands)[21].

Carotid IMT

Ultrasonography (US) was used to measure carotid IMT in the left and right common carotid arteries. Additional information is provided in the **Appendix**.

Statistical analyses

In the NEO study, individuals with a BMI of 27 kg/m^2 or higher were oversampled. To correctly represent associations in the general population[22], adjustments for the oversampling of individuals with a BMI of 27 kg/m^2 or higher were made by weighting individuals toward the BMI distribution of participants from the Leiderdorp municipality[23], whose BMI distribution was similar to the BMI distribution of the Dutch general population[24]. All results were based on weighted analyses; consequently, the results apply to a population-based study without oversampling of participants with a BMI of 27 kg/m^2 or higher. Participants were stratified into a group with hepatic steatosis and a group without hepatic steatosis according to a hepatic triglyceride content cut-off value for hepatic steatosis of 5.56%[2]. Baseline characteristics of participants were expressed as mean ± standard deviation, as median and interquartile range, or as a percentage. Comparisons between groups were tested with the two-tailed independent samples *t* test. Hepatic triglyceride content showed a right skewed distribution at visual inspection of the data; therefore, log transformation was applied. Linear regression analyses were performed to study the association of the log of hepatic triglyceride content with aortic PWV and carotid IMT: First, we estimated the crude associations of hepatic triglyceride content with aortic PWV and carotid IMT (model 1). Second, we adjusted for age, sex, heart rate, systolic and diastolic blood pressure, alcohol consumption, pack years of smoking, and use of antihypertensive and lipid-lowering drugs

(model 2). In model 3, the remaining components of the metabolic syndrome besides blood pressure (waist circumference, serum triglycerides, high-density lipoprotein cholesterol level, and fasting plasma glucose level) were added. To adjust more precisely for the effects of abdominal and total body fat, we additionally adjusted for these parameters in model 4. In additional analyses, we excluded participants who used lipid-lowering drugs because of their known hepatic lipid-lowering effects[25]. Because serum triglyceride, high-density lipoprotein cholesterol, and fasting plasma glucose levels could be possible mediators in the relationship between hepatic triglyceride content and vascular stiffness, we repeated analyses without correction for these factors. We calculated variance inflation factors to check for multicollinearity in our regression models. Variance inflation factor values were less than 10 in all models and were considered appropriate. Regression coefficients, 95% confidence intervals (CIs), and *P* values were reported. Regression coefficients can be interpreted as the difference in outcome associated with a 10-fold increase in hepatic triglyceride content. $P < 0.05$ was considered indicative of a significant difference. Statistical analysis was performed with IBM SPSS Statistics for Windows (version 20.0; IBM, Armonk, NY) and Stata (version 12; Stata, College Station, Tex) software.

RESULTS

From the total of 6673 participants in the NEO study, 2581 underwent MR imaging and spectroscopy. Because of our high-throughput study protocol, only a limited time slot was available per subject, and this did not allow time for a repeat examination when technical failures were recognized. For this reason, the technical failure rate of MR spectroscopy in the liver was approximately 20%. There was no difference in BMI ($P = 0.186$) or waist circumference ($P = 0.130$) between participants with successful MR spectroscopy and those with unsuccessful MR spectroscopy. After consecutive exclusion of participants with missing data of hepatic triglyceride content ($n = 498$), aortic PWV ($n = 60$), carotid IMT ($n = 15$), pack years of smoking ($n = 37$), plasma glucose level ($n = 12$), liver disease ($n = 8$), visceral fat ($n = 6$), use of alcohol ($n = 5$), total body fat ($n = 3$), heart rate ($n = 1$), and diastolic blood pressure ($n = 1$) and after exclusion of participants with a history of liver disease ($n = 23$) and alcohol consumption of more than 10 units per day ($n = 13$), 1899 participants (52% men, 96% white) were included in the present analysis (**Figure 1**).

PWV of the descending aorta could not be assessed in 177 participants (9%) due to technical errors. Separate analyses of the thoracic and abdominal segments of the descending aorta were performed in a subgroup of 1490 participants (78%).

Maximum detection limits were exceeded in 77 participants (4%) for the aortic arch PWV, in 81 participants (5%) for the thoracic descending aortic PWV, and in 25 participants (2%)

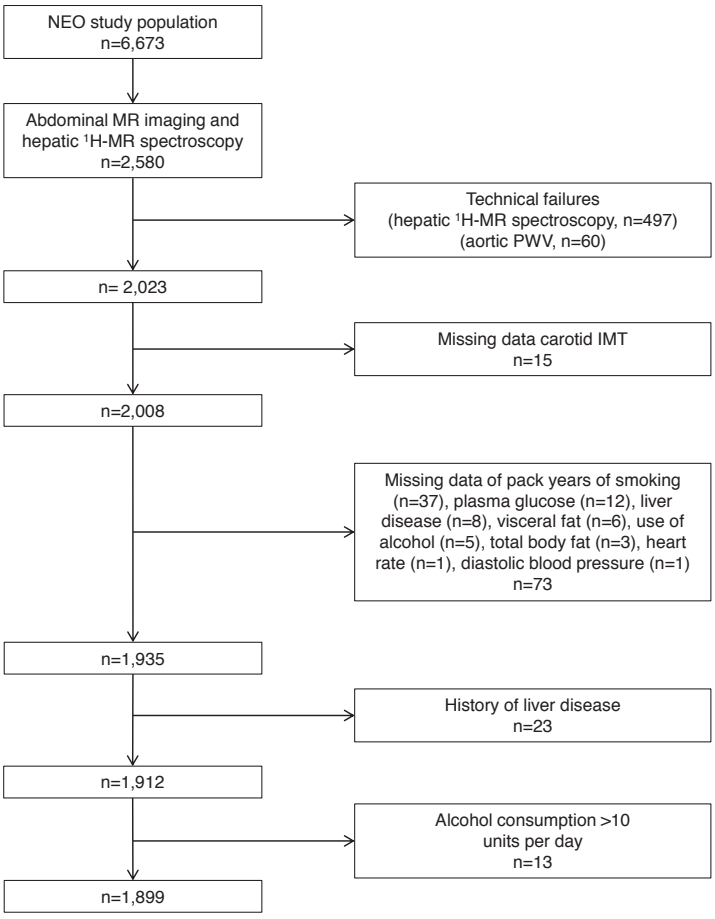

Figure 1. Flowchart shows details of the study design.

for the abdominal descending aortic PWV. The maximum PWV values, as calculated for each individual, were assigned to these participants.

Weighted participant characteristics of the total study population (*n* = 1899) are described in **Table 1**. Participants had a mean age of 55 years ± 6, and a median BMI of 25.5 kg/m2 (interquartile range, 23.1-27.9 kg/m^2). Median hepatic triglyceride content was 2.64% (interquartile range, 1.33%-6.18%), and 29% of the study population had hepatic steatosis. Mean line widths of the spectra were 45.7 Hz ± 15.5 (water, 4.7 ppm), 46.8 Hz ± 19.1 (methylene, 1.3 ppm), and 43.2 Hz ± 17.9 (methyl, 0.9 ppm). Mean PWV values were 6.6 m/s ± 1.3 (total aorta), 6.6 m/s ± 1.8 (aortic arch), 6.7 m/s ± 1.9 (total descending aorta), 7.3 m/s ± 2.4 (thoracic segment of descending aorta), and 6.4 m/s ± 2.1 (abdominal segment of descending aorta). Mean carotid IMT was 615 μm ± 92. All aortic PWV and carotid IMT values were higher in participants with hepatic steatosis. Examples of hepatic triglyceride content quantification and aortic PWV measurements are shown in **Figure 2**.

Table 1. Characteristics of participants aged 45-65 years in the Netherlands Epidemiology of Obesity study stratified by hepatic triglyceride content (n = 1899)

Characteristic	Without hepatic steatosis (hepatic triglyceride content ≤ 5.56%)	With hepatic steatosis (hepatic triglyceride content > 5.56%)	Mean difference*	*P* value
Percentage of study population (%)	71	29	NA	NA
Male sex (%)	40	61	NA	< 0.001
Age (y)	55 ± 5	57 ± 7	1.7 (0.9, 2.4)	< 0.001
BMI (kg/m^2)	24.7 (22.2-26.7)	27.7 (25.4-30.6)	3.5 (3.0, 4.0)	< 0.001
Total body fat (%)				
Men	23 ± 4	27 ± 7	4.5 (3.6, 5.4)	< 0.001
Women	35 ± 5	41 ± 7	6.4 (5.3, 7.5)	< 0.001
VAT (cm^2)				
Men	282 ± 127	426 ± 222	143.4 (117.2, 169.7)	< 0.001
Women	164 ± 81	324 ± 184	160.6 (138.6, 182.6)	< 0.001
Hepatic triglyceride content (%)	1.78 (1.08-2.95)	10.89 (7.06-17.72)	12.16 (11.21, 13.11)	< 0.001
Total aortic PWV (m/s)	6.4 ± 1.1	6.9 ± 1.7	0.5 (0.3, 0.7)	< 0.001
Aortic arch PWV (m/s)	6.5 ± 1.5	6.7 ± 2.3	0.2 (0.0, 0.4)	0.053
Descending aortic PWV (m/s)	6.6 ± 1.5	7.1 ± 2.7	0.6 (0.3, 0.9)	< 0.001
Thoracic descending aortic PWV (m/s)	7.1 ± 2.0	7.8 ± 3.2	0.7 (0.4, 1.1)	< 0.001
Abdominal descending aortic PWV (m/s)	6.3 ± 1.7	6.9 ± 3.1	0.6 (0.2, 1.0)	< 0.001
Carotid IMT (μm)	604 ± 80	641 ± 11	37 (25, 49)	< 0.001
Heart rate (beats/min)	67 ± 8	70 ± 14	2.9 (1.5, 4.3)	< 0.001
Smoking history (no. of pack years)	6.9 ± 10.2	10.6 ± 19.2	3.8 (2.3, 5.3)	< 0.001
Systolic blood pressure (mmHg)	128 ± 15	135 ± 21	7.3 (5.0, 9.6)	< 0.001
Diastolic blood pressure (mmHg)	82 ± 9	87 ± 12	4.9 (3.6, 6.2)	< 0.001
Metabolic syndrome (%)	15	55	NA	< 0.001
Waist circumference (cm)†				
Men	94.3 ± 8.1	102.1 ± 12.8	7.9 (6.2, 9.6)	< 0.001
Women	82.7 ± 8.9	95.5 ± 14.7	12.8 (10.7, 14.9)	< 0.001
Fasting serum triglyceride level (mmol/L)†	0.9 (0.7-1.3)	1.5 (1.0-2.1)	0.7 (0.6, 0.8)	< 0.001
Fasting serum HDL cholesterol level (mmol/L)†	1.7 ± 0.4	1.4 ± 0.5	-0.3 (-0.4, -0.2)	< 0.001
Hypertension (%)†	54	75	NA	< 0.001
Fasting plasma glucose level (mmol/L)†	5.2 ± 0.6	5.9 ± 1.8	0.6 (0.4, 0.8)	< 0.001
Diabetes (%)	2	11	NA	< 0.001
History of cardiovascular disease (%)	5	6	NA	0.286
AST level (units/L)	23.6 ± 5.4	26.9 ± 10.1	3.3 (2.5, 4.1)	< 0.001
ALT level (units/L)	22.1 ± 6.8	31.6 ± 18.2	9.5 (8.2, 10.8)	< 0.001
Use of antihypertensive drugs (%)	13	30	NA	< 0.001
Use of RAS antagonists	8	18	NA	< 0.001

Table 1. Characteristics of participants aged 45-65 years in the Netherlands Epidemiology of Obesity study stratified by hepatic triglyceride content (n = 1899) (continued)

Characteristic	Without hepatic steatosis (hepatic triglyceride content ≤ 5.56%)	With hepatic steatosis (hepatic triglyceride content > 5.56%)	Mean difference*	*P* value
Use of lipid-lowering drugs	7	15	NA	< 0.001

Unless otherwise indicated, data are mean ± SD, median and interquartile range, or percentage. Results are based on analyses weighted toward the BMI distribution in the general population (n = 1899). The number of participants with a measurement of aortic PWV in the descending aorta was 1722, and the number of participants with aortic PWV in the thoracic and abdominal segments of the descending aorta was 1490. ALT = alanine aminotransferase, AST = aspartate aminotransferase, HDL = high-density lipoprotein, NA = not applicable, RAS = renin-angiotensin system, VAT = visceral adipose tissue.

* Data in parentheses are the 95% CI.

† Component of the metabolic syndrome (National Cholesterol Education Program Adult Treatment Panel III).

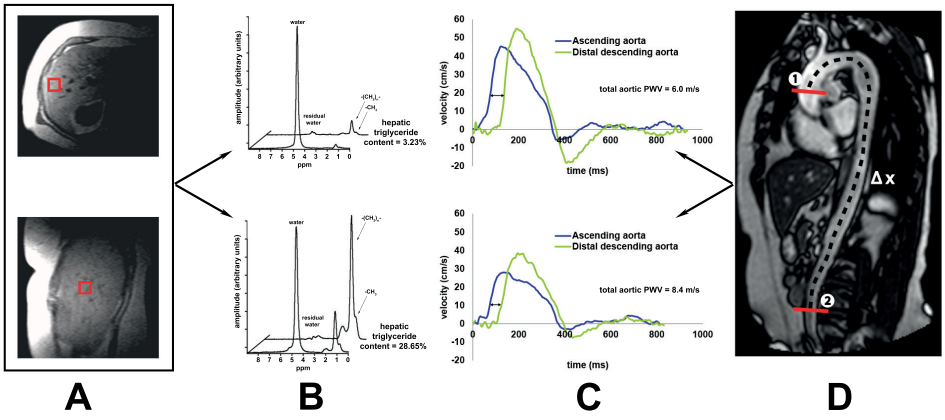

Figure 2. Assessment of hepatic triglyceride content and aortic PWV in a participant without (BMI, 26.0 kg/m^2) and in a participant with (BMI, 30.6 kg/m^2) hepatic steatosis. A, ^{1}H MR spectroscopy of the liver was used to measure hepatic triglyceride content. An 8-mL voxel was positioned in the right liver lobe, avoiding major vascular structures and extrahepatic visceral fat. Transverse (upper) and sagittal (lower) scout images are shown. B, Representative examples of MR spectral data in a participant without (upper graph; hepatic triglyceride content, 3.23%) and in a participant with (lower graph; hepatic triglyceride content, 28.65%) hepatic steatosis. Spectra were obtained without (front) and with (back) water suppression. Resonances from protons of methylene (peak at 1.3 ppm, $[CH_2]_n$) and methyl (peak at 0.9 ppm, CH_3) are highlighted. C, Systolic wave propagation of aortic flow was evaluated from maximal velocity-time curves that were obtained at each measurement site. Upper: PWV of the total aorta of the participant without hepatic steatosis was 6.0 m/s. Lower: PWV of the total aorta of the participant with hepatic steatosis was 8.4 m/s. D, PWV assessment with through-plane velocity-encoded MR imaging. The two measurement sites used to calculate total aortic PWV are shown. Aortic PWV (in meters per second) was calculated by dividing the aortic path length between the ascending aorta (1) and the distal descending aorta (2) by the transit time between the arrival of the systolic wave front at these sites.

Table 2. Differences in aortic PWV associated with a 10-fold increase in hepatic triglyceride content

Model	Difference	95% CI	*P* value
Total aorta (*n* = 1899)			
Model 1	0.56	0.40, 0.73	< 0.001
Model 2	0.15	0.00, 0.29	0.046
Model 3	0.15	-0.01, 0.31	0.072
Model 4	0.19	0.03, 0.36	0.022
Aortic arch (*n* = 1899)			
Model 1	0.36	0.14, 0.58	< 0.001
Model 2	0.02	-0.22, 0.25	0.882
Model 3	-0.02	-0.30, 0.26	0.886
Model 4	0.00	-0.28, 0.28	0.999
Descending aorta (*n* = 1722)			
Model 1	0.60	0.34, 0.87	< 0.001
Model 2	0.19	-0.05, 0.44	0.126
Model 3	0.23	-0.03, 0.49	0.078
Model 4	0.28	0.02, 0.54	0.038
Thoracic descending aorta (*n* = 1490)			
Model 1	0.93	0.60, 1.26	< 0.001
Model 2	0.29	-0.07, 0.65	0.111
Model 3	0.21	-0.20, 0.62	0.309
Model 4	0.28	-0.13, 0.70	0.179
Abdominal descending aorta (*n* = 1490)			
Model 1	0.58	0.25, 0.90	< 0.001
Model 2	0.17	-0.17, 0.51	0.327
Model 3	0.33	-0.06, 0.72	0.100
Model 4	0.42	0.03, 0.81	0.037

Reported differences represent differences in aortic PWV associated with a 10-fold increase in hepatic triglyceride content. Corresponding 95% CIs and *P* values are shown. Model 1 = crude association. Model 2 = model 1 + age, sex, heart rate, systolic and diastolic blood pressure, alcohol use, smoking history (in number of pack years), and use of antihypertensive and lipid-lowering drugs. Model 3 = model 2 + all components of metabolic syndrome. Model 4 = model 3 + visceral adipose tissue + total body fat. Results are based on analyses weighted toward the BMI distribution of the general population.

Table 2 shows the associations between hepatic triglyceride content and total and regional aortic PWV in the whole study population. The association with total aortic PWV attenuated after adjustments for several covariates. After adjustments for all covariates, the regression coefficient was 0.19 m/s (95% CI: 0.03, 0.36), representing an increase in mean total aortic PWV of 0.19 m/s per 10-fold increase in hepatic triglyceride content. After adjustments for all covariates, a 10-fold increase in hepatic triglyceride content was associated with a PWV increase of 0.28 m/s (95% CI: 0.02, 0.54) in the total descending aorta and a PWV

increase of 0.42 m/s (95% CI: 0.03, 0.81) in the abdominal segment of the descending aorta. No associations were observed between hepatic triglyceride content and PWV of the aortic arch (0.00 m/s; 95% CI: −0.28, 0.28 per 10-fold increase in hepatic triglyceride content) or the thoracic segment of the descending aorta (0.28 m/s; 95% CI: −0.13, 0.70 per 10-fold increase in hepatic triglyceride content).

Table 3 shows the association between hepatic triglyceride content and mean carotid IMT. In model 3, the regression coefficient was 15 µm (95% CI: 0, 29), representing an increase in mean carotid IMT of 15 µm for every 10-fold increase in hepatic triglyceride content. After additional adjustments for visceral and total body fat, this attenuated to 14 µm (95% CI: −1, 29).

The additional analyses in which we excluded participants who used lipid-lowering drugs showed similar results. For example, in model 4, the increase in mean total aortic PWV was 0.21 m/s (95% CI: 0.03, 0.38; $P = 0.020$), and the increase in mean carotid IMT was 16 µm (95% CI: 0, 32; $P = 0.049$) per 10-fold increase in hepatic triglyceride content. The additional analyses in which we did not adjust for triglycerides, high-density lipoprotein cholesterol level, and fasting plasma glucose level yielded slightly higher regression coefficients. For example, in model 4, the increase in mean total aortic PWV was 0.24 m/s (95% CI: 0.08, 0.40; $P = 0.004$), and the increase in mean carotid IMT was 18 µm (95% CI: 3, 32; $P = 0.015$) per 10-fold increase in hepatic triglyceride content.

Table 3. Differences in carotid IMT associated with a 10-fold increase in hepatic triglyceride content

Model	Difference	95% CI	*P* value
1	50	39, 61	< 0.001
2	32	19, 44	< 0.001
3	15	0, 29	0.044
4	14	-1, 29	0.060

Reported differences indicate differences in carotid IMT for every 10-fold increase in hepatic triglyceride content. Corresponding 95% CIs and *P* values are shown. Model 1 = crude association. Model 2 = model 1 + age, sex, heart rate, systolic and diastolic blood pressure, alcohol use, smoking history (in number of pack years), and use of antihypertensive and lipid-lowering drugs. Model 3 = model 2 + all components of metabolic syndrome. Model 4 = model 3 + visceral adipose tissue + total body fat. Results are based on analyses weighted toward the BMI distribution of the general population.

DISCUSSION

The main findings in our cohort study are that hepatic triglyceride content was associated with aortic pulse wave velocity (in particular, with regional abdominal aortic pulse wave velocity) and carotid IMT. These associations were only partly confounded by the individual components of the metabolic syndrome, and they remained after adjustments for these confounding factors. The association with aortic pulse wave velocity also remained after adjustment for visceral adipose tissue.

Aortic PWV is a measure of aortic stiffness and is recognized as an important surrogate marker of cardiovascular disease. Aortic stiffness can be assessed with different noninvasive methods. Most studies investigating the relationship between hepatic steatosis and arterial stiffness used oscillometry or tonometry devices to assess brachial-ankle or carotid-femoral PWV[5, 26-28]. These techniques are relatively inexpensive, but they are limited by the absence of vascular imaging; thus, the vascular length traveled by the pulse wave must be estimated[8]. To our knowledge, studies on whether the relationship between hepatic steatosis and vascular stiffness is attributed to concomitant risk factors have yielded conflicting results. In a large community-based cohort of mostly white subjects studied by Long et al[29], several vascular function measures, including carotid-femoral PWV, were associated with NAFLD, and these associations were largely attributed to coexisting cardiometabolic risk factors. In contrast, a large Korean epidemiologic study by Kim et al[6] and a large population-based Chinese study by Huang et al[30] reported that NAFLD was associated with brachial-ankle PWV, independent of the metabolic syndrome. Both studies also investigated carotid IMT, but only Huang et al[30] found a relationship between NAFLD and carotid IMT independent of conventional cardiovascular risk factors, including components of the metabolic syndrome. Our results in a relatively large predominantly white population enable us to confirm that an association exists between hepatic steatosis and vascular stiffness and subclinical atherosclerosis, which is not confounded by various cardiometabolic risk factors. Moreover, our study adds to the current knowledge that there are regional differences in the association of hepatic steatosis with aortic PWV.

Strengths of our cohort study were its relatively large size, the combined use of MR techniques to directly assess hepatic steatosis and aortic PWV in addition to the carotid IMT measurements, and detailed phenotyping of all participants that enables us to control for important confounding factors. Hepatic MR spectroscopy has shown better diagnostic accuracy in the identification and quantification of hepatic steatosis than has CT or US[31]. Furthermore, by using MR imaging, we were able to assess the true aortic path length, thereby enabling us to estimate central arterial PWV more precisely than we could with brachial-ankle PWV. Moreover, this technique enabled us to investigate the PWV of multiple aortic regions. Further strengths of our study were the availability of detailed information about the components of the metabolic syndrome and other potential confounding variables, including visceral adipose tissue and total body fat.

Currently, alternative noninvasive methods other than MR spectroscopy are available to measure hepatic steatosis. Quantitative imaging approaches to fat quantification are generally preferable to MR spectroscopy, as they provide spatial coverage of the liver[32]. Proton density fat fraction measurement with MR imaging showed good diagnostic accuracy in the quantification of steatosis[33]. Because our study started in 2008, this technique was unfortunately not yet validated at the time. Future trials monitoring change in hepatic steatosis are

needed to evaluate the extent to which hepatic fat measurements with MR techniques may serve as a biomarker for treatment response in patients with vascular disease.

To our knowledge, we are the first to observe a specific association of hepatic steatosis with stiffness of the abdominal aorta. It is known that the high elastin-to-collagen ratio in the aortic wall progressively declines toward the periphery[34, 35]. Elastin degradation of the media layer is a major reason for vascular stiffening in the large arteries during aging. Vascular inflammation and proliferation of smooth muscle cells in the subendothelial space cause an accumulation of collagen, resulting in an increased PWV[36]. Furthermore, cytokines are involved in low-grade inflammation and are associated with greater arterial stiffness in healthy adults[37] and men with type 1 diabetes[38]. Hence, circulating inflammatory cytokines in the state of hepatic steatosis could have a greater effect on distal regions of the aorta. This pattern of a predominantly distal decrease in aortic elastic function is supported by previous studies on obesity[39, 40].

We also observed an association between hepatic triglyceride content and subclinical atherosclerosis after taking individual components of the metabolic syndrome into account, whereas visceral fat abolished this relationship. This is consistent with findings described by Targher et al[41]. In conditions of insulin resistance, increased lipolysis in visceral adipose tissue generates an increased flux of free fatty acids. This increased flux promotes hepatic triglyceride accumulation, which is associated with enhanced oxidative stress, abnormal lipoprotein metabolism, and secretion of proinflammatory markers, such as interleukin-6, tumor necrosis factor α, and C-reactive protein[17, 42, 43]. These abnormalities may play an important role in the proatherogenic effect of NAFLD[7, 44-47]. Our data show that visceral fat is a confounder in the relationship between hepatic steatosis and subclinical atherosclerosis, but not in the relationship with aortic stiffness. It is conceivable that the pathophysiologic pathways of atherosclerosis and central arterial stiffness are not identical and that the role of visceral fat in the development of atherosclerosis is possibly more significant. Nonetheless, weight loss not only has been shown to decrease visceral adipose tissue[48] and carotid IMT and to improve inflammatory profile[49], but has also been shown to decrease arterial stiffness in overweight and obese people[39, 50].

There were several limitations to our study. First, hepatic steatosis was not proven by biopsy. Liver biopsy is the reference standard used to assess NAFLD and its necroinflammatory form, nonalcoholic steatohepatitis[51]. However, for ethical reasons, it was not possible to perform liver biopsies in such a relatively large study population. Alternatively, localized ^{1}H MR spectroscopy provides a sensitive quantitative noninvasive method with which to estimate hepatic triglyceride content[2]. Second, we aimed to study the relationship between hepatic steatosis and subclinical vascular impairment in the general population. Some participants who were more likely to have hepatic steatosis were excluded from MR imaging because their body circumference was larger than 170 cm. As a result, our findings only pertain to people with a body circumference less than 170 cm. Third, by adjusting for the components

of the metabolic syndrome, we may have overadjusted the associations being studied because from certain components, such as glucose, cholesterol, and triglyceride concentrations, it is not clear to what extent they are truly confounding factors or may be part of the causal pathway between NAFLD and cardiovascular disease. Such overadjustment for these components may have led to an underestimation of the regression coefficients. A fourth limitation of our study was the relatively high rate of technical failure for MR spectroscopy of the liver and, to a lesser extent, for MR imaging of the aorta. We were challenged by a high-throughput study protocol with only a limited time slot available per study participant. Nevertheless, technical failure of MR spectroscopy occurred randomly throughout the MR subgroup, and we do not believe it influenced our results. In addition, hepatic triglyceride content did not differ between participants with and those without PWV measurement. Furthermore, the same high-throughput study protocol with detailed phenotyping of the NEO study participants enabled us to answer our research question and to perform the present analyses with adjustment for many confounding factors. A fifth limitation is the use of a point-resolved spectroscopy sequence, which may systematically overestimate hepatic steatosis[52]. We chose to use point-resolved spectroscopy as the ^{1}H MR spectroscopy sequence because of the double signal-to-noise ratio when compared with stimulated echo acquisition mode and to keep our methods in line with those used in the population study by Szczepaniak et al[2]. Because our primary analyses were based on hepatic triglyceride content as a continuous variable, a systematic overestimation of hepatic triglyceride content would not affect the strength (i.e., the regression coefficient calculated from the multivariate regression analysis) or precision (95% CIs) of the associations between hepatic triglyceride content and aortic PWV and carotid IMT, nor would it affect our conclusions. A sixth limitation of our study is its observational cross-sectional design, which precludes a causal interpretation. Prospective studies are required to investigate the effect of hepatic steatosis on incident cardiovascular events. Finally, our study population primarily consists of white people, and our findings need to be confirmed in other ethnic groups.

In conclusion, our study showed that hepatic triglyceride content is associated with aortic stiffness, particularly stiffness of the abdominal aorta, and subclinical atherosclerosis. These associations were only partly explained by the metabolic syndrome and visceral adiposity, suggesting a possible specific contribution of hepatic steatosis to subclinical vascular impairment.

REFERENCES

1. Bedogni G, Miglioli L, Masutti F, Tiribelli C, Marchesini G, Bellentani S. Prevalence of and risk factors for nonalcoholic fatty liver disease: the Dionysos nutrition and liver study. *Hepatology* 2005;42:44-52.
2. Szczepaniak LS, Nurenberg P, Leonard D, Browning JD, Reingold JS, Grundy S, Hobbs HH, Dobbins RL. Magnetic resonance spectroscopy to measure hepatic triglyceride content: prevalence of hepatic steatosis in the general population. *Am J Physiol Endocrinol Metab* 2005;288:E462-468.
3. Machado M, Marques-Vidal P, Cortez-Pinto H. Hepatic histology in obese patients undergoing bariatric surgery. *J Hepatol* 2006;45:600-606.
4. NCD Risk Factor Collaboration. Trends in adult body-mass index in 200 countries from 1975 to 2014: a pooled analysis of 1698 population-based measurement studies with 19.2 million participants. *The Lancet* 2016;387:1377-1396.
5. Kim BJ, Kim NH, Kim BS, Kang JH. The association between nonalcoholic fatty liver disease, metabolic syndrome and arterial stiffness in nondiabetic, nonhypertensive individuals. *Cardiology* 2012;123:54-61.
6. Kim NH, Park J, Kim SH, Kim YH, Kim DH, Cho GY, Baik I, Lim HE, Kim EJ, Na JO, Lee JB, Lee SK, Shin C. Non-alcoholic fatty liver disease, metabolic syndrome and subclinical cardiovascular changes in the general population. *Heart* 2014;100:938-943.
7. Targher G, Bertolini L, Padovani R, Rodella S, Zoppini G, Zenari L, Cigolini M, Falezza G, Arcaro G. Relations between carotid artery wall thickness and liver histology in subjects with nonalcoholic fatty liver disease. *Diabetes Care* 2006;29:1325-1330.
8. Cavalcante JL, Lima JA, Redheuil A, Al-Mallah MH. Aortic stiffness: current understanding and future directions. *J Am Coll Cardiol* 2011;57:1511-1522.
9. Mitchell GF, Hwang SJ, Vasan RS, Larson MG, Pencina MJ, Hamburg NM, Vita JA, Levy D, Benjamin EJ. Arterial stiffness and cardiovascular events: the Framingham Heart Study. *Circulation* 2010;121:505-511.
10. Vlachopoulos C, Aznaouridis K, Stefanadis C. Prediction of cardiovascular events and all-cause mortality with arterial stiffness: a systematic review and meta-analysis. *J Am Coll Cardiol* 2010;55:1318-1327.
11. Grotenhuis HB, Westenberg JJ, Steendijk P, van der Geest RJ, Ottenkamp J, Bax JJ, Jukema JW, de Roos A. Validation and reproducibility of aortic pulse wave velocity as assessed with velocity-encoded MRI. *J Magn Reson Imaging* 2009;30:521-526.
12. O'Leary DH, Polak JF, Kronmal RA, Manolio TA, Burke GL, Wolfson SK, Jr. Carotid-artery intima and media thickness as a risk factor for myocardial infarction and stroke in older adults. Cardiovascular Health Study Collaborative Research Group. *N Engl J Med* 1999;340:14-22.
13. de Alwis NM, Day CP. Non-alcoholic fatty liver disease: the mist gradually clears. *J Hepatol* 2008;48 Suppl 1:S104-112.
14. Robinson MR, Scheuermann-Freestone M, Leeson P, Channon KM, Clarke K, Neubauer S, Wiesmann F. Uncomplicated obesity is associated with abnormal aortic function assessed by cardiovascular magnetic resonance. *J Cardiovasc Magn Reson* 2008;10:10.
15. Safar ME, Czernichow S, Blacher J. Obesity, arterial stiffness, and cardiovascular risk. *J Am Soc Nephrol* 2006;17:S109-111.
16. Yan RT, Yan AT, Anderson TJ, Buithieu J, Charbonneau F, Title L, Verma S, Lonn EM. The differential association between various anthropometric indices of obesity and subclinical atherosclerosis. *Atherosclerosis* 2009;207:232-238.
17. Targher G, Day CP, Bonora E. Risk of cardiovascular disease in patients with nonalcoholic fatty liver disease. *N Engl J Med* 2010;363:1341-1350.
18. Widya RL, de Mutsert R, den Heijer M, le Cessie S, Rosendaal FR, Jukema JW, Smit JW, de Roos A, Lamb HJ. Association between hepatic tri-

glyceride content and left ventricular diastolic function in a population-based cohort: the Netherlands Epidemiology of Obesity Study. *Radiology* 2016;279:443-450.

19. de Mutsert R, den Heijer M, Rabelink TJ, Smit JW, Romijn JA, Jukema JW, de Roos A, Cobbaert CM, Kloppenburg M, le Cessie S, Middeldorp S, Rosendaal FR. The Netherlands Epidemiology of Obesity (NEO) study: study design and data collection. *Eur J Epidemiol* 2013;28:513-523.
20. Grundy SM, Cleeman JI, Daniels SR, Donato KA, Eckel RH, Franklin BA, Gordon DJ, Krauss RM, Savage PJ, Smith SC, Jr., Spertus JA, Costa F. Diagnosis and management of the metabolic syndrome: an American Heart Association/National Heart, Lung, and Blood Institute Scientific Statement. *Circulation* 2005;112:2735-2752.
21. Hammer S, van der Meer RW, Lamb HJ, de Boer HH, Bax JJ, de Roos A, Romijn JA, Smit JW. Short-term flexibility of myocardial triglycerides and diastolic function in patients with type 2 diabetes mellitus. *Am J Physiol Endocrinol Metab* 2008;295:E714-718.
22. Korn EL, Graubard BI. Epidemiologic studies utilizing surveys: accounting for the sampling design. *Am J Public Health* 1991;81:1166-1173.
23. Lumley T. Analysis of complex survey samples. *J Stat Softw* 2004;9.
24. Nederland de Maat Genomen. Body mass index en gewichtsklasse, naar leeftijd en geslacht. Rijksinstituut voor Volksgezondheid en Milieu. http://www.rivm.nl/nldemaat. Published January 26, 2012.
25. de Haan W, van der Hoogt CC, Westerterp M, Hoekstra M, Dallinga-Thie GM, Princen HM, Romijn JA, Jukema JW, Havekes LM, Rensen PC. Atorvastatin increases HDL cholesterol by reducing CETP expression in cholesterol-fed APOE*3-Leiden.CETP mice. *Atherosclerosis* 2008;197:57-63.
26. Lee YJ, Shim JY, Moon BS, Shin YH, Jung DH, Lee JH, Lee HR. The relationship between arterial stiffness and nonalcoholic fatty liver disease. *Dig Dis Sci* 2012;57:196-203.
27. Salvi P, Ruffini R, Agnoletti D, Magnani E, Pagliarani G, Comandini G, Pratico A, Borghi C, Benetos A, Pazzi P. Increased arterial stiffness in nonalcoholic fatty liver disease: the Cardio-GOOSE study. *J Hypertens* 2010;28:1699-1707.
28. Vlachopoulos C, Manesis E, Baou K, Papatheodoridis G, Koskinas J, Tiniakos D, Aznaouridis K, Archimandritis A, Stefanadis C. Increased arterial stiffness and impaired endothelial function in nonalcoholic fatty liver disease: a pilot study. *Am J Hypertens* 2010;23:1183-1189.
29. Long MT, Wang N, Larson MG, Mitchell GF, Palmisano J, Vasan RS, Hoffmann U, Speliotes EK, Vita JA, Benjamin EJ, Fox CS, Hamburg NM. Nonalcoholic fatty liver disease and vascular function: cross-sectional analysis in the Framingham heart study. *Arterioscler Thromb Vasc Biol* 2015;35:1284-1291.
30. Huang Y, Bi Y, Xu M, Ma Z, Xu Y, Wang T, Li M, Liu Y, Lu J, Chen Y, Huang F, Xu B, Zhang J, Wang W, Li X, Ning G. Nonalcoholic fatty liver disease is associated with atherosclerosis in middle-aged and elderly Chinese. *Arterioscler Thromb Vasc Biol* 2012;32:2321-2326.
31. van Werven JR, Marsman HA, Nederveen AJ, Smits NJ, ten Kate FJ, van Gulik TM, Stoker J. Assessment of hepatic steatosis in patients undergoing liver resection: comparison of US, CT, T1-weighted dual-echo MR imaging, and point-resolved 1H MR spectroscopy. *Radiology* 2010;256:159-168.
32. Reeder SB, Cruite I, Hamilton G, Sirlin CB. Quantitative assessment of liver fat with magnetic resonance imaging and spectroscopy. *J Magn Reson Imaging* 2011;34:729-749.
33. Idilman IS, Aniktar H, Idilman R, Kabacam G, Savas B, Elhan A, Celik A, Bahar K, Karcaaltincaba M. Hepatic steatosis: quantification by proton density fat fraction with MR imaging versus liver biopsy. *Radiology* 2013;267:767-775.
34. Oliver JJ, Webb DJ. Noninvasive assessment of arterial stiffness and risk of atherosclerotic events. *Arterioscler Thromb Vasc Biol* 2003;23:554-566.

35. Safar ME, Levy BI, Struijker-Boudier H. Current perspectives on arterial stiffness and pulse pressure in hypertension and cardiovascular diseases. *Circulation* 2003;107:2864-2869.
36. Lee SJ, Park SH. Arterial ageing. *Korean Circ J* 2013;43:73-79.
37. van Bussel BC, Schouten F, Henry RM, Schalkwijk CG, de Boer MR, Ferreira I, Smulders YM, Twisk JW, Stehouwer CD. Endothelial dysfunction and low-grade inflammation are associated with greater arterial stiffness over a 6-year period. *Hypertension* 2011;58:588-595.
38. Llauradó G, Ceperuelo-Mallafré V, Vilardell C, Simó R, Freixenet N, Vendrell J, González-Clemente JM. Arterial stiffness is increased in patients with type 1 diabetes without cardiovascular disease: a potential role of low-grade inflammation. *Diabetes Care* 2012;35:1083-1089.
39. Rider OJ, Tayal U, Francis JM, Ali MK, Robinson MR, Byrne JP, Clarke K, Neubauer S. The effect of obesity and weight loss on aortic pulse wave velocity as assessed by magnetic resonance imaging. *Obesity (Silver Spring)* 2010;18:2311-2316.
40. Danias PG, Tritos NA, Stuber M, Botnar RM, Kissinger KV, Manning WJ. Comparison of aortic elasticity determined by cardiovascular magnetic resonance imaging in obese versus lean adults. *Am J Cardiol* 2003;91:195-199.
41. Targher G, Bertolini L, Padovani R, Zenari L, Zoppini G, Falezza G. Relation of nonalcoholic hepatic steatosis to early carotid atherosclerosis in healthy men: role of visceral fat accumulation. *Diabetes Care* 2004;27:2498-2500.
42. Stefan N, Kantartzis K, Haring HU. Causes and metabolic consequences of Fatty liver. *Endocr Rev* 2008;29:939-960.
43. Gaggini M, Morelli M, Buzzigoli E, DeFronzo RA, Bugianesi E, Gastaldelli A. Non-alcoholic fatty liver disease (NAFLD) and its connection with insulin resistance, dyslipidemia, atherosclerosis and coronary heart disease. *Nutrients* 2013;5:1544-1560.
44. Valenti L, Fracanzani AL, Dongiovanni P, Santorelli G, Branchi A, Taioli E, Fiorelli G, Fargion S. Tumor necrosis factor alpha promoter polymorphisms and insulin resistance in nonalcoholic fatty liver disease. *Gastroenterology* 2002;122:274-280.
45. Fracanzani AL, Burdick L, Raselli S, Pedotti P, Grigore L, Santorelli G, Valenti L, Maraschi A, Catapano A, Fargion S. Carotid artery intima-media thickness in nonalcoholic fatty liver disease. *Am J Med* 2008;121:72-78.
46. Volzke H, Robinson DM, Kleine V, Deutscher R, Hoffmann W, Ludemann J, Schminke U, Kessler C, John U. Hepatic steatosis is associated with an increased risk of carotid atherosclerosis. *World J Gastroenterol* 2005;11:1848-1853.
47. Targher G, Bertolini L, Scala L, Zoppini G, Zenari L, Falezza G. Non-alcoholic hepatic steatosis and its relation to increased plasma biomarkers of inflammation and endothelial dysfunction in non-diabetic men. Role of visceral adipose tissue. *Diabet Med* 2005;22:1354-1358.
48. Wajchenberg BL. Subcutaneous and visceral adipose tissue: their relation to the metabolic syndrome. *Endocr Rev* 2000;21:697-738.
49. Masquio DC, de Piano A, Sanches PL, Corgosinho FC, Campos RM, Carnier J, da Silva PL, Caranti DA, Tock L, Oyama LM, Oller do Nascimento CM, de Mello MT, Tufik S, Damaso AR. The effect of weight loss magnitude on pro-/anti-inflammatory adipokines and carotid intima-media thickness in obese adolescents engaged in interdisciplinary weight loss therapy. *Clin Endocrinol (Oxf)* 2013;79:55-64.
50. Cooper JN, Buchanich JM, Youk A, Brooks MM, Barinas-Mitchell E, Conroy MB, Sutton-Tyrrell K. Reductions in arterial stiffness with weight loss in overweight and obese young adults: potential mechanisms. *Atherosclerosis* 2012;223:485-490.
51. Adams LA, Feldstein AE. Non-invasive diagnosis of nonalcoholic fatty liver and nonalcoholic steatohepatitis. *J Dig Dis* 2011;12:10-16.
52. Hamilton G, Middleton MS, Bydder M, Yokoo T, Schwimmer JB, Kono Y, Patton HM, Lavine JE, Sirlin CB. Effect of PRESS and STEAM sequences on magnetic resonance spectroscopic liver fat quantification. *J Magn Reson Imaging* 2009;30:145-152.

APPENDIX

METABOLIC SYNDROME

According to the updated National Cholesterol Education Program Adult Treatment Panel III report[20], patients with the metabolic syndrome have any three of the following five characteristics: (a) waist circumference of at least 102 cm in men or at least 88 cm in women, (b) a serum triglyceride level of at least 1.7 mmol/L or currently taking medication for an elevated triglyceride level, (c) a high-density lipoprotein cholesterol level less than 1.03 mmol/L in men or less than 1.3 mmol/L in women or currently taking medication to reduce high-density lipoprotein cholesterol level, (d) systolic blood pressure of 130 mm Hg or higher and/or diastolic blood pressure of 85 mm Hg or higher or currently taking antihypertensive drugs; and (e) elevated fasting glucose level of 5.6 mmol/L or higher or currently taking medication for an elevated glucose level.

HEPATIC TRIGLYCERIDE CONTENT

Hepatic ^{1}H magnetic resonance (MR) spectra were acquired, as previously described[18, 53]. A body coil for radiofrequency transmission and a surface coil (diameter of 17 cm) for signal receiving were used. Furthermore, automated three-dimensional volume first-order iterative shimming was performed. In short, an 8-mL voxel was positioned in the right liver lobe while avoiding major vascular structures and abdominal subcutaneous and visceral adipose tissue depots. Sixty-four signals were acquired with water suppression (repetition time ms/echo time ms, 2900/23). Data points (n = 1024) were collected by using a 1000-Hz spectral line. Without changing any parameters, four signal averages without water suppression (repetition time, 10 s) were obtained as an internal reference. Areas of resonances from protons of water (4.7 ppm), methyl (0.9 ppm), and methylene (1.3 ppm) groups in fatty acid chains of the hepatic triglyceride were evaluated by using Java-based MR-user interface software (jMRUI, version 3.0; A. van den Boogaart, Katholieke Universiteit Leuven, Leuven, Belgium)[54].

AORTIC PULSE WAVE VELOCITY

Aortic pulse wave velocity (PWV) was determined by using a previously described protocol[55]. In short, a scout view of the aorta was obtained. Next, retrospectively electrocardiographically gated gradient-echo sequences with velocity encoding were performed during free breathing to assess flow at the following levels: perpendicular to the ascending aorta at the level of the pulmonary trunk, perpendicular to the descending aorta just below the diaphragm, and just above the aortic bifurcation. This resulted in through-plane flow measurements of the ascending, proximal descending, mid-descending, and distal descending aorta. A maximum number of phases was reconstructed to ensure high temporal resolution. Maximum velocity encoding was set to 200 m/s. Wave propagation was evaluated from maximal velocity-time curves that were obtained at each sampling site. Aortic PWV was calculated by dividing the aortic path length between the measurement sites by the transit time between the arrival of the systolic wave front at these sites. The foot of the systolic velocity wave front was detected by assessing the intersection point of the horizontal line modeling the constant diastolic flow and a line along the upslope of the systolic wave front, modeled by linear regression along 20%-80% of the range of the flow velocity values along this upslope. Aortic path length measurements and manual contour drawing in the aortic velocity maps was performed by using in-house software packages (MASS and FLOW; Leiden University Medical Center, Leiden, the Netherlands). The maximum detectable PWV was calculated by multiplying the repetition time (5 ms) by two and then multiplying by the distance between each measurement site.

CAROTID INTIMA-MEDIA THICKNESS

Ultrasonography was used to measure carotid intima-media thickness (IMT) in the far wall of the left and right common carotid arteries along a 15-mm long section, 10-mm proximal to the bifurcation, and in the supine position. A 7.5-10.0-MHz linear array transducer (Art Laboratory, version 2.1; Esaote, Maastricht, the Netherlands) in the B-mode setting was used to depict the distal common carotid artery, and an online wall track system was used to detect the lumen-intima and media-adventitia boundaries. Carotid IMT was measured in three predefined angles per side (180˚, 135˚, and 90˚ for the right common carotid artery; 180˚, 225˚, and 270˚ for the left common carotid artery) during six heartbeats. We calculated the mean carotid IMT for each participant by averaging all 36 carotid IMT measurements within each individual.

REFERENCES

53. van der Meer RW, Hammer S, Lamb HJ, Frölich M, Diamant M, Rijzewijk LJ, de Roos A, Romijn JA, Smit JW. Effects of short-term high-fat, high-energy diet on hepatic and myocardial triglyceride content in healthy men. *J Clin Endocrinol Metab* 2008;93:2702-2708.
54. Naressi A, Couturier C, Devos JM, Janssen M, Mangeat C, de Beer R, Graveron-Demilly D. Java-based graphical user interface for the MRUI quantitation package. *MAGMA* 2001;12:141-152.
55. van der Meer RW, Diamant M, Westenberg JJ, Doornbos J, Bax JJ, de Roos A, Lamb HJ. Magnetic resonance assessment of aortic pulse wave velocity, aortic distensibility, and cardiac function in uncomplicated type 2 diabetes mellitus. *J Cardiovasc Magn Reson* 2007;9:645-651.

Chapter 4

Right ventricular involvement in diabetic cardiomyopathy

Ralph L. Widya
Rutger W. van der Meer
Johannes W.A. Smit
Luuk J. Rijzewijk
Michaela Diamant
Jeroen J. Bax
Albert de Roos
Hildo J. Lamb

Diabetes Care 2013;36(2);457-462

ABSTRACT

Background

Right ventricular (RV) function has proven to be of importance for patient risk stratification in heart failure and is associated with sudden death and exercise limitation. RV dysfunction might play an important role in diabetic cardiomyopathy. The objective of this study was to compare magnetic resonance imaging-derived RV dimensions and function between men with type 2 diabetes and healthy subjects, and to relate these parameters to left ventricular (LV) dimensions and function.

Methods

RV and LV volumes and functions were assessed in 78 men with uncomplicated type 2 diabetes and 28 healthy men within the same range of age using magnetic resonance imaging. Steady-state free precession sequences were used to assess ventricular dimensions. Flow velocity mapping across the pulmonary valve and tricuspid valve was used to assess RV outflow and diastolic filling patterns, respectively. Univariate general linear models were used for statistical analyses.

Results

RV end-diastolic volume was significantly decreased in patients compared with healthy subjects after adjustment for BMI and pulse pressure (177 ± 28 mL vs. 197 ± 47 mL, $P < 0.01$). RV systolic function was impaired: peak ejection rate across the pulmonary valve was decreased (433 ± 54 mL/s vs. 463 ± 71 mL/s, $P < 0.01$) and pulmonary flow acceleration time was longer (124 ± 17 ms vs. 115 ± 25 ms, $P < 0.05$). Indexes of RV diastolic function were impaired: peak filling rate and peak deceleration gradient of the early filling phase were 315 ± 63 mL/s vs. 356 ± 90 mL/s ($P < 0.01$) and 2.3 ± 0.8 mL/s^2 × 10^{-3} vs. 2.8 ± 0.8 mL/s^2 × 10^{-3} ($P < 0.01$), respectively. All RV parameters were strongly associated with its corresponding LV parameter ($P < 0.001$).

Conclusions

Diabetic cardiomyopathy affects the right ventricle, as demonstrated by RV remodeling and impaired systolic and diastolic functions in men with type 2 diabetes, in a similar manner as changes in LV dimensions and functions. These observations suggest that RV impairment might be a component of the diabetic cardiomyopathy phenotype.

INTRODUCTION

Cardiovascular disease is one of the major adverse consequences of type 2 diabetes. Patients with type 2 diabetes have an increased cardiovascular mortality rate[1]. Even in the absence of significant coronary artery disease and hypertension, subclinical left ventricular (LV) dysfunction presents in type 2 diabetes[2]. This so-called diabetic cardiomyopathy has a complex and multifactorial pathogenesis. Atherosclerosis, subclinical microinfarctions, mitochondrial dysfunction, and lipotoxicity all have been proposed as contributors to diabetic cardiomyopathy. Furthermore, it has been recognized that deposition of advanced glycation end products, caused by long-standing hyperglycemia, affects ventricular stiffness[3]. The formation of advanced glycation end products yields fibrosis by cross-linking collagen[4], thus increasing myocardial stiffness. This may lead to a decreased LV end-diastolic volume and impaired subclinical LV function[5-7].

All proposed mechanisms leading to LV impairment in type 2 diabetes are systemic changes and therefore also might hamper right ventricular (RV) function. RV involvement in diabetic cardiomyopathy might be of importance because the right ventricle has a substantial contribution to overall myocardial contractility. RV function has proven to be of importance for patient risk stratification in heart failure[8] and for prediction of development of atrial fibrillation[9]. In general, RV dysfunction and fibrosis are associated with lethal ventricular arrhythmias, sudden death, exercise limitation, and impaired RV cardiac output[10]. In addition, the prevalence of cardiac conduction abnormalities is increased in diabetic patients[11].

However, only limited data exist on RV involvement in type 2 diabetes. Whereas animal studies have shown that dysfunction of the right ventricle might play a role in diabetic cardiomyopathy[12], the right ventricle is largely overlooked in human studies. Only a few echocardiographic studies discuss the right ventricle in diabetes[13-17]. These studies were limited by inclusion of patients with cardiovascular diabetes-related complications[13-15, 17], and study populations consisted partially[13, 14] or entirely of type 1 diabetic patients[16]. Moreover, none of these studies reported RV volumes.

The right ventricle is a difficult structure from which to obtain reproducible echocardiographic signals because of the irregular geometrical shape and the anterior position within the thorax. Without mathematical modeling, conventional two-dimensional echo techniques commonly underestimate or overestimate the true size of the adult right ventricle[18]. Cardiovascular magnetic resonance imaging (MRI) has become the reference standard for the assessment of RV function and volumes because good reproducibility has been shown[19, 20].

To our knowledge, no studies to date have evaluated volumetric as well as systolic and diastolic functional involvement of the right ventricle in uncomplicated type 2 diabetes compared with healthy subjects assessed by MRI. Accordingly, the purpose of the current

study was to compare MRI-derived RV dimensions and systolic and diastolic function between well-controlled uncomplicated type 2 diabetic patients and healthy subjects, in relation to LV dimensions and function.

METHODS

Subjects

Data were derived from the PIRAMID trial (Pioglitazone Influence on tRiglyceride Accumulation in the Myocardium In Diabetes), in which participants were randomized to pioglitazone or metformin after baseline measurements to study the effects of these agents on cardiac function and metabolism[21]. This prospective trial included a total of 78 men with uncomplicated, well-controlled type 2 diabetes of short duration and with verified absence of cardiac ischemia. In the PIRAMID trial, only men were included because in women hormonal status and use of contraceptives have been shown to influence metabolism. Inclusion and exclusion criteria have been reported previously[21]. In summary, the inclusion criteria were age 45-65 years; type 2 diabetes diagnosed according to the World Health Organization criteria[22] and treated with sulfonylurea derivates and/or metformin in stable doses; glycated hemoglobin 6.5-8.5%; and sitting blood pressure < 150/85 mmHg, with or without use of antihypertensive medication. Exclusion criteria included known cardiovascular disease or diabetes-related complications, and contraindications for MRI. In addition, to exclude inducible myocardial ischemia or silent infarction caused by coronary artery disease, high-dose dobutamine stress echocardiography was performed.

When patients were eligible for inclusion in the PIRAMID trial, they entered a 10-week run-in period during which their previous blood glucose-lowering agents (metformin monotherapy, 39.8%; sulfonylurea monotherapy, 25.6%; and metformin and sulfonylurea combination therapy, 34.6%) were washed out. They were transferred to glimepiride monotherapy, which was titrated until a stable dose was reached. MRI assessments were made after this run-in period.

Thirty healthy male control subjects were recruited. Control subjects were included if they met the following criteria: age 45-65 years and no known acute or chronic disease based on medical history, physical examination, and standard laboratory tests (blood counts, fasting blood glucose, lipids, serum creatinine, liver enzymes, and electrocardiogram). Exclusion criteria included hypertension, chronic use of any drug, substance abuse, and impaired glucose tolerance, as excluded by a 75-g oral glucose test[23]. Written informed consent was obtained from all participants. This study was conducted in accordance with the ethics principles of the Declaration of Helsinki and was consistent with Good Clinical Practice guidelines and applicable local regulatory requirements.

Cardiovascular MRI protocol

All participants underwent blood sampling and MRI scanning for assessment of heart function after an overnight fast. All MRI studies were performed with a 1.5 Tesla whole-body MRI scanner (Gyroscan ACS/NT15; Philips, Best, the Netherlands), with subjects in the supine position at rest. Image postprocessing was performed with software packages developed in-house (MASS and FLOW; Medis, Leiden, the Netherlands).

To assess dimensions and systolic function of the right ventricle and left ventricle, the entire heart was imaged in short-axis orientation using electrocardiographically gated breath-hold balanced steady-state free precession imaging. Endocardial contours of the right ventricle and left ventricle were manually drawn in end-diastolic phase and end-systolic phase. The papillary muscles, trabeculae carnae, trabecula septomarginalis (moderator band), and RV outflow tract were included in the RV volume (**Figures 1A and B**). Imaging parameters were as follows: repetition time = 3.4 ms; echo time = 1.7 ms; flip angle = 35°; slice thickness = 10 mm; slice gap = 0 mm; field of view = 400 × 400 mm; and reconstructed matrix size = 256 × 256. Dimensions were end-diastolic volume (EDV) and end-systolic volume (ESV) for the right ventricle and left ventricle. Functional parameters were derived as follows for each ventricle: stroke volume (SV) was calculated by subtracting the ESV from the EDV, cardiac output was calculated by multiplying the SV by the heart rate, and ejection fraction was calculated by dividing the SV by the EDV and multiplying by 100. Because RV afterload may affect RV function, we assessed the peak ejection rate and pulmonary flow acceleration time. We therefore performed an electrocardiographically gated gradient echo sequence with velocity encoding to measure blood flow across the pulmonary valve for determination of RV outflow. The peak ejection rate was defined as the highest velocity. The pulmonary flow acceleration time was defined as the time from the onset of flow to the peak ejection rate (**Figure 1C**). The following imaging parameters were used: repetition time = 6.5 ms; echo time = 1 ms; flip angle = 20°; slice thickness = 8 mm; field of view = 350 × 350 mm; matrix size = 256 × 256; echo planar imaging-factor = 3; velocity encoding gradient = 150 cm/s; and scan percentage = 80%.

To determine RV and LV diastolic functions, an electrocardiographically gated gradient echo sequence with velocity encoding was performed to measure blood flow across the tricuspid valve and mitral valve, respectively. Similar imaging parameters as described for the pulmonary valve were used, with the exception of the velocity encoding gradient (100 cm/s). For the left ventricle, no echo planar imaging-factor was used. Diastolic parameters included peak filling rates of the early filling phase (E) and atrial contraction (A), and their ratio (E/A). Also, the peak deceleration gradient of the E (hereafter referred to as E deceleration peak) was calculated (**Figure 1D**).

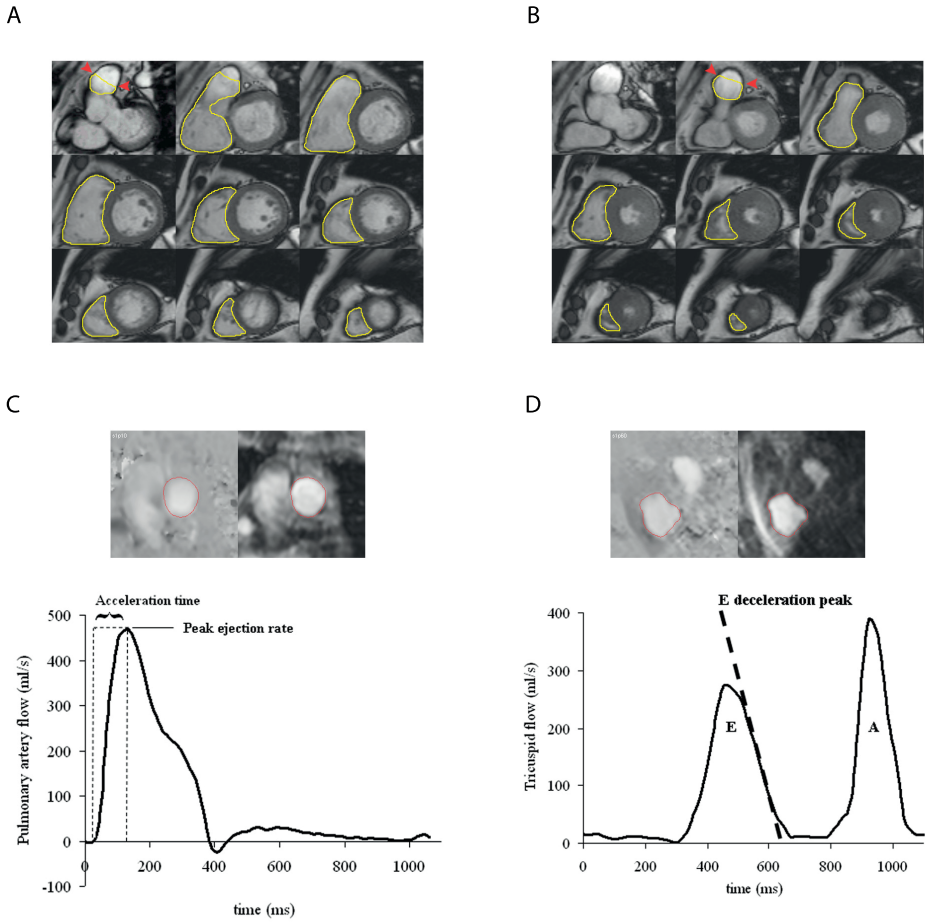

Figure 1. Example of MRI analyses of the right ventricle. Endocardial contour drawing of the right ventricle in end-diastolic (*A*) and end-systolic phases (*B*). The RV outflow tract ends at the pulmonary valves (arrowheads). *C*: Phase contrast velocity map (*left*) and modulus image (*right*) across the pulmonary valve in one cardiac phase to assess pulmonary flow pattern. *D*: Phase contrast velocity map (*left*) and modulus image (*right*) across the tricuspid valve in one cardiac phase to assess diastolic filling pattern.

Statistical analysis

Statistical analysis was performed using SPSS for Windows version 17.0 (SPSS, Chicago, Ill). Data are expressed as mean ± SD when normally distributed; data not normally distributed are expressed as median (interquartile range). Non-normally distributed data were log-transformed, and unpaired *t* tests (or, when appropriate, nonparametric tests) were used for comparisons. A univariate general linear model was used to compare RV dimensions and function. The RV parameters were adjusted for BMI and pulse pressure. Diabetic state was entered as fixed factor and BMI and pulse pressure were entered as covariates. Associations between RV parameters and the corresponding LV parameters were tested using univariate general linear models, adjusted for diabetic state. $P < 0.05$ was considered statistically significant.

RESULTS

Parts of these data were previously used for publication in subgroups[6, 7, 24]. One healthy subject was excluded for the current study because of poor scan quality. Another healthy subject was excluded because of a coincidental finding, namely an aneurysmatic focal abnormality of the left ventricle. Patient characteristics are shown in **Table 1**.

Table 1. Clinical and biochemical characteristics

Characteristics	Healthy subjects $n = 28$	Type 2 diabetic patients $n = 78$
Clinical		
Age (y)	54.5 ± 7.7	56.5 ± 5.6
BMI (kg/m^2)	26.8 ± 2.6	28.7 ± 3.5*
Waist circumference (cm)	100 ± 9	104 ± 10*
Systolic blood pressure (mm/Hg)	116 ± 10	128 ± 12*
Diastolic blood pressure (mm/Hg)	73 ± 8	76 ± 7
Pulse pressure (mm/Hg)	46 ± 9	52 ± 10*
Heart rate (bpm)	59 (53-63)	64 (60-70)*
Time since diagnosis diabetes (y)	NA	4 (2-6)
Alcoholic consumers (*n*)†	20 (80%)	58 (74%)
Smokers (*n*)†	4 (16%)	17 (22%)
Physically active (*n*)†	24 (96%)	50 (64%)*
Biochemical		
Glycated hemoglobin (%)	5.4 ± 0.2	7.1 ± 1.0*
Plasma glucose (mmol/L)	5.3 (5.0-5.5)	8.3 (7.4-9.8)*
Plasma insulin (pmol/L)	36 (24-51)	66 (37-100)*
Total cholesterol (mmol/L)	5.3 ± 0.7	4.7 ± 1.0*
HDL cholesterol (mmol/L)	1.4 (1.2-1.6)	1.1 (0.9-1.3)*
LDL cholesterol (mmol/L)	3.4 ± 0.64	2.7 ± 0.78*
Plasma triglycerides (mmol/L)	0.9 (0.7-1.2)	1.5 (1.0-2.2)*
Nonesterified fatty acids (mmol/L)	0.4 ± 0.2	0.5 ± 0.2

Data are mean ± SD, median (interquartile range) or *n* (%).
* $P < 0.05$.
† Data are missing for three healthy subjects.

Mean BMI was higher in patients compared with controls (28.7 ± 3.5 kg/m^2 vs. 26.8 ± 2.6 kg/m^2, $P < 0.01$). Mean systolic blood pressure was within normal range, although it was higher in patients compared with controls (128 ± 12 mmHg vs. 116 ± 10 mmHg, $P < 0.001$). Pulse pressure (systolic blood pressure-diastolic blood pressure) was higher in patients (52 ± 10 mmHg vs. 46 ± 9 mmHg, $P < 0.01$). Smoking habits and alcohol use did not differ between the two groups. Alcohol abuse was an exclusion criterion. Healthy subjects performed

physical exercise more regularly. In 73 patients, microalbuminuria was assessed at screening (before the glimepiride run-in period) either by 24-h urine collection or by assessing the albumin/creatinine ratio in a spot sample. Thirteen of these patients had microalbuminuria (> 30 mg in 24-h urine collection or albumin/creatinine ratio > 2.5 in a spot sample).

RV MRI parameters

RV dimensions and function data are shown in **Table 2**. Because BMI differed between the groups, parameters were adjusted for BMI. In addition, adjustments were made for pulse pressure. RV EDV was decreased in patients compared with controls (177 ± 28 mL vs. 197 ± 47 mL, $P < 0.01$) (**Figure 2A**). A similar difference was observed for the RV ESV (83 ± 18 mL vs. 93 ± 28 mL, $P < 0.05$). All differences remained significant after adjustment for BMI and pulse pressure.

Table 2. MRI study parameters

Parameters	Healthy subjects $n = 28$	Type 2 diabetic patients $n = 78$
RV dimensions		
End-diastolic volume (mL)	197 ± 47	177 ± 28*†
End-systolic volume (mL)	93 ± 28	83 ± 18*†
RV systolic function		
Stroke volume (mL)	104 ± 21	95 ± 15*†
Cardiac output (mL/min)	6060 (5432-6661)	6227 (5524-7091)
Ejection fraction (%)	53 ± 4	54 ± 5
Peak ejection rate (mL/s)	463 ± 71	433 ± 54*†
Pulmonary flow acceleration time (ms)	115 ± 25	124 ± 17†
RV diastolic function		
E peak filling rate (mL/s)	356 ± 90	315 ± 63*†
E deceleration peak ($mL/s^2 \times 10^{-3}$)	2.8 ± 0.8	2.3 ± 0.8*†
A peak filling rate (mL/s)	349 ± 60	353 ± 68
E/A	0.95 (0.82-1.28)	0.85 (0.73-1.06)*

Data are mean ± SD or median (interquartile range).
* $P < 0.05$ unadjusted for pulse pressure and BMI.
† $P < 0.05$ after adjustment for pulse pressure and BMI.

Several parameters of systolic function were impaired in patients. Although RV ejection fraction was preserved, RV SV (95 ± 15 vs. 104 ± 21 mL, $P < 0.05$) and peak ejection rate across the pulmonary valve (433 ± 54 vs. 463 ± 71 mL/s, $P < 0.05$) were decreased, and pulmonary flow acceleration time was longer (124 ± 17 vs. 115 ± 25 ms, $P < 0.05$) in patients as compared with healthy subjects after adjustment for BMI and pulse pressure.

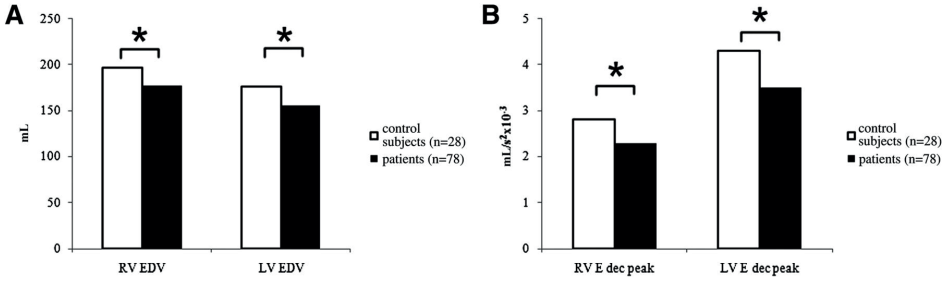

Figure 2. End-diastolic volume and E deceleration peak of the right ventricle and left ventricle. RV end-diastolic volume was decreased in type 2 diabetic patients compared with healthy controls, similar to the left ventricle (*A*). Likewise, the E deceleration peak was impaired in both ventricles (*B*). E dec peak = E deceleration peak. * $P < 0.05$.

Moreover, RV diastolic function was impaired in patients as compared with healthy subjects. RV E peak filling rate, RV E deceleration peak, and RV E/A were 315 ± 63 mL/s vs. 356 ± 90 mL/s ($P < 0.05$), 2.3 ± 0.8 mL/s^2 × 10^{-3} vs. 2.8 ± 0.8 mL/s^2 x 10^{-3} ($P < 0.05$), and 0.85 (0.73-1.06) vs. 0.95 (0.82-1.28) ($P < 0.05$), respectively (**Figure 2B**). The RV E peak filling rate and RV E deceleration peak remained significantly lower in patients after adjustment for BMI and pulse pressure. The E/A peak remained lower in patients after adjustment for pulse pressure ($P = 0.041$) but tended to be significant after adjusting for BMI ($P = 0.073$).

Comparison of RV parameters between patients and healthy subjects could not be adjusted reliably for physical exercise because only one healthy subject did not exercise. When RV parameters were compared between physically active and inactive patients, no statistically significant differences were encountered. In addition, when RV parameters were compared between patients with and without microalbuminuria, no statistically significant differences were encountered. Therefore, we think that physical exercise and microalbuminuria cannot explain the RV impairment in our diabetic population.

LV MRI parameters

LV EDV and LV ESV were lower in patients compared with controls (respectively, 156 ± 25 mL vs. 176 ± 36 mL, $P < 0.01$; and 59 [52-71] mL vs. 72 [61-81] mL, $P < 0.01$) (**Figure 2A**). LV diastolic function was impaired in a similar manner as for the right ventricle. LV E peak filling rate, LV E deceleration peak, and LV E/A were lower compared with healthy subjects (respectively, 417 ± 84 mL/s vs. 484 ± 112 mL/s, $P < 0.01$; 3.4 [2.9-4.0] mL/s^2 × 10^{-3} vs. 4.6 (2.8-5.2) mL/s^2 × 10^{-3}, $P < 0.01$; and 1.04 ± 0.25 vs. 1.23 ± 0.35; $P < 0.01$) (**Figure 2B**). All differences remained statistically significant after adjustment for BMI and pulse pressure.

All RV parameters were strongly associated with their corresponding LV parameters, unconfounded by diabetic state. Corresponding unstandardized β values were: EDV = 0.753; ESV = 0.508; SV = 1.034; cardiac output = 0.994; ejection fraction = 0.618; E peak filling rate = 0.847; E deceleration peak = 0.602; A peak filling rate = 0.353; and E/A peak = 0.497 (all $P <$ 0.001). Moreover, there were no significant interactions with diabetic state.

DISCUSSION

The main finding in the current study is that RV dimensions and function are impaired in men with uncomplicated type 2 diabetes, similar to the left ventricle. This suggests that both ventricles are influenced by the metabolic abnormalities characterizing diabetes. Although RV function has been evaluated in several diseases, including sepsis[25], pulmonary embolism[26], rheumatoid arthritis[27], and idiopathic dilated cardiomyopathy[28], most studies discussing diabetic cardiomyopathy have focused on the left ventricle only.

Impairment of RV systolic function, measured by tricuspid annular plane systolic excursion, has been reported in Zucker diabetic fatty rats[12]. In our diabetic population, RV systolic function as measured by the peak ejection rate and the acceleration time of the pulmonary artery flow was impaired, whereas RV ejection fraction was preserved and did not differ between groups. This pattern of pulmonary artery flow is characteristic for pulmonary hypertension[29] and may reflect an increase in RV afterload. In diabetes, microangiopathy of the alveolar-capillary network in the lung[30] may cause increased RV afterload and, consequently, RV systolic dysfunction may occur.

In the current study, parameters of RV diastolic function were impaired in patients compared with healthy subjects. RV E deceleration peak and RV E peak filling rate were lower in patients, indicating impaired myocardial relaxation and/or increased myocardial stiffness, which are the hallmarks of diastolic dysfunction[31]. Furthermore, RV EDV was decreased in patients.

In the left ventricle, diffuse interstitial fibrosis and collagen deposition within the myocardium are the primary structural changes observed in diabetic cardiomyopathy and eventually lead to impaired ventricular relaxation[32, 33]. In addition, deposition of advanced glycation end products and increased cardiomyocyte resting tension are important mechanisms in diabetic cardiomyopathy causing diastolic stiffness[33]. Because we observed reduced parameters of diastolic function and reduced EDV of the right ventricle in addition to the left ventricle, it may be hypothesized that the mechanisms responsible for LV stiffness also affect the right ventricle. Alternatively, the present changes could be the consequence of left ventricle changes.

A possible explanation for the coexistence of RV and LV abnormalities in diabetic patients may be that subendocardial fibers are interwoven between the right ventricle and the left ventricle in the interventricular septum[34]. Therefore, it may be suggested that the diffuse fibrotic processes that take place in diabetes could affect the function of both ventricles. Dibble et al[35] reported an independent association between septal function and RV systolic function. However, they did not investigate the association between septal function and RV diastolic function.

Effects on the right ventricle in diabetic cardiomyopathy have not been investigated extensively, and the few human studies focusing explicitly on this subject have used

various techniques. Previous studies reporting on impaired RV diastolic function in diabetic patients[13-17] were limited by the inclusion of patients with diabetes-related cardiovascular complications and/or inclusion of type 1 diabetic patients. None of these studies has evaluated RV volumes to study geometrical changes of the right ventricle in diabetes. Therefore, besides inclusion of well-controlled uncomplicated type 2 diabetic patients, a strength of this study is the combination of RV volumetric and functional assessment by MRI to investigate RV involvement in diabetic cardiomyopathy.

Some limitations of this study need to be addressed. First, only men were included. Exclusion of women limits the generalizability of the current study and, therefore, further studies are needed to extend our findings to the female population. Second, the rather small number of patients and healthy subjects might cause underpowering of the study. Our findings possibly are hampered by the relatively small study population and therefore need to be interpreted with caution.

In conclusion, diabetic cardiomyopathy affects the right ventricle, as demonstrated by RV remodeling and impaired systolic and diastolic function in men with type 2 diabetes, similar to changes in LV dimensions and function. These observations suggest that RV impairment might be a component of the diabetic cardiomyopathy phenotype.

REFERENCES

1. Francis GS. Diabetic cardiomyopathy: fact or fiction? *Heart* 2001;85:247-248.
2. Boudina S, Abel ED. Diabetic cardiomyopathy revisited. *Circulation* 2007;115:3213-3223.
3. Kass DA, Bronzwaer JG, Paulus WJ. What mechanisms underlie diastolic dysfunction in heart failure? *Circ Res* 2004;94:1533-1542.
4. Aronson D. Cross-linking of glycated collagen in the pathogenesis of arterial and myocardial stiffening of aging and diabetes. *J Hypertens* 2003;21:3-12.
5. Devereux RB, Roman MJ, Paranicas M, O'Grady MJ, Lee ET, Welty TK, Fabsitz RR, Robbins D, Rhoades ER, Howard BV. Impact of diabetes on cardiac structure and function: the strong heart study. *Circulation* 2000;101:2271-2276.
6. Rijzewijk LJ, van der Meer RW, Smit JW, Diamant M, Bax JJ, Hammer S, Romijn JA, de Roos A, Lamb HJ. Myocardial steatosis is an independent predictor of diastolic dysfunction in type 2 diabetes mellitus. *J Am Coll Cardiol* 2008;52:1793-1799.
7. Rijzewijk LJ, van der Meer RW, Lamb HJ, de Jong HW, Lubberink M, Romijn JA, Bax JJ, de Roos A, Twisk JW, Heine RJ, Lammertsma AA, Smit JW, Diamant M. Altered myocardial substrate metabolism and decreased diastolic function in nonischemic human diabetic cardiomyopathy: studies with cardiac positron emission tomography and magnetic resonance imaging. *J Am Coll Cardiol* 2009;54:1524-1532.
8. Ghio S, Gavazzi A, Campana C, Inserra C, Klersy C, Sebastiani R, Arbustini E, Recusani F, Tavazzi L. Independent and additive prognostic value of right ventricular systolic function and pulmonary artery pressure in patients with chronic heart failure. *J Am Coll Cardiol* 2001;37:183-188.
9. Aziz EF, Kukin M, Javed F, Musat D, Nader A, Pratap B, Shah A, Enciso JS, Chaudhry FA, Herzog E. Right ventricular dysfunction is a strong predictor of developing atrial fibrillation in acutely decompensated heart failure patients, ACAP-HF data analysis. *J Card Fail* 2010;16:827-834.
10. Warnes CA. Adult congenital heart disease importance of the right ventricle. *J Am Coll Cardiol* 2009;54:1903-1910.
11. Movahed MR. Diabetes as a risk factor for cardiac conduction defects: a review. *Diabetes Obes Metab* 2007;9:276-281.
12. van den Brom CE, Bosmans JW, Vlasblom R, Handoko LM, Huisman MC, Lubberink M, Molthoff CF, Lammertsma AA, Ouwens MD, Diamant M, Boer C. Diabetic cardiomyopathy in Zucker diabetic fatty rats: the forgotten right ventricle. *Cardiovasc Diabetol* 2010;9:25.
13. Kosmala W, Colonna P, Przewlocka-Kosmala M, Mazurek W. Right ventricular dysfunction in asymptomatic diabetic patients. *Diabetes Care* 2004;27:2736-2738.
14. Kosmala W, Przewlocka-Kosmala M, Mazurek W. Subclinical right ventricular dysfunction in diabetes mellitus--an ultrasonic strain/strain rate study. *Diabet Med* 2007;24:656-663.
15. Movahed MR, Milne N. Presence of biventricular dysfunction in patients with type II diabetes mellitus. *Congest Heart Fail* 2007;13:78-80.
16. Karamitsos TD, Karvounis HI, Dalamanga EG, Papadopoulos CE, Didangellos TP, Karamitsos DT, Parharidis GE, Louridas GE. Early diastolic impairment of diabetic heart: the significance of right ventricle. *Int J Cardiol* 2007;114:218-223.
17. Tayyareci Y, Yurdakul S, Tayyareci G, Nisanci Y, Umman B, Bugra Z. Impact of myocardial acceleration during isovolumic contraction in evaluating subclinical right ventricular systolic dysfunction in type 2 diabetes mellitus patients. *Echocardiography* 2010;27:1211-1218.
18. Crean AM, Maredia N, Ballard G, Menezes R, Wharton G, Forster J, Greenwood JP, Thomson JD. 3D Echo systematically underestimates right ventricular volumes compared to cardiovascular magnetic resonance in adult congenital heart disease patients with

moderate or severe RV dilatation. *J Cardiovasc Magn Reson* 2011;13:78.

19. Pattynama PM, Lamb HJ, van der Velde EA, van der Geest RJ, van der Wall EE, de Roos A. Reproducibility of MRI-derived measurements of right ventricular volumes and myocardial mass. *Magn Reson Imaging* 1995;13:53-63.
20. Grothues F, Moon JC, Bellenger NG, Smith GS, Klein HU, Pennell DJ. Interstudy reproducibility of right ventricular volumes, function, and mass with cardiovascular magnetic resonance. *Am Heart J* 2004;147:218-223.
21. van der Meer RW, Rijzewijk LJ, de Jong HW, Lamb HJ, Lubberink M, Romijn JA, Bax JJ, de Roos A, Kamp O, Paulus WJ, Heine RJ, Lammertsma AA, Smit JW, Diamant M. Pioglitazone improves cardiac function and alters myocardial substrate metabolism without affecting cardiac triglyceride accumulation and high-energy phosphate metabolism in patients with well-controlled type 2 diabetes mellitus. *Circulation* 2009;119:2069-2077.
22. Alberti KG, Zimmet PZ. Definition, diagnosis and classification of diabetes mellitus and its complications. Part 1: diagnosis and classification of diabetes mellitus provisional report of a WHO consultation. *Diabet Med* 1998;15:539-553.
23. Expert Committee on the Diagnosis and Classification of Diabetes Mellitus. Report of the expert committee on the diagnosis and classification of diabetes mellitus. *Diabetes Care* 2003;26(Suppl 1):S5-20.
24. Ng AC, Delgado V, Bertini M, van der Meer RW, Rijzewijk LJ, Hooi ES, Siebelink HM, Smit JW, Diamant M, Romijn JA, de Roos A, Leung DY, Lamb HJ, Bax JJ. Myocardial steatosis and biventricular strain and strain rate imaging in patients with type 2 diabetes mellitus. *Circulation* 2010;122:2538-2544.
25. Lambermont B, Ghuysen A, Kolh P, Tchana-Sato V, Segers P, Gerard P, Morimont P, Magis D, Dogne JM, Masereel B, D'Orio V. Effects of endotoxic shock on right ventricular systolic function and mechanical efficiency. *Cardiovasc Res* 2003;59:412-418.
26. Hirsh J, Hoak J. Management of deep vein thrombosis and pulmonary embolism. A statement for healthcare professionals. Council on Thrombosis (in consultation with the Council on Cardiovascular Radiology), American Heart Association. *Circulation* 1996;93:2212-2245.
27. Seyfeli E, Guler H, Akoglu S, Karazincir S, Akgul F, Saglam H, Seydaliyeva T, Yalcin F. Right ventricular diastolic abnormalities in rheumatoid arthritis and its relationship with left ventricular and pulmonary involvement. A tissue Doppler echocardiographic study. *Int J Cardiovasc Imaging* 2006;22:745-754.
28. La Vecchia L, Zanolla L, Varotto L, Bonanno C, Spadaro GL, Ometto R, Fontanelli A. Reduced right ventricular ejection fraction as a marker for idiopathic dilated cardiomyopathy compared with ischemic left ventricular dysfunction. *Am Heart J* 2001;142:181-189.
29. Kovacs G, Reiter G, Reiter U, Rienmuller R, Peacock A, Olschewski H. The emerging role of magnetic resonance imaging in the diagnosis and management of pulmonary hypertension. *Respiration* 2008;76:458-470.
30. Klein OL, Krishnan JA, Glick S, Smith LJ. Systematic review of the association between lung function and Type 2 diabetes mellitus. *Diabet Med* 2010;27:977-987.
31. Borlaug BA, Paulus WJ. Heart failure with preserved ejection fraction: pathophysiology, diagnosis, and treatment. *Eur Heart J* 2011;32:670-679.
32. Aneja A, Tang WH, Bansilal S, Garcia MJ, Farkouh ME. Diabetic cardiomyopathy: insights into pathogenesis, diagnostic challenges, and therapeutic options. *Am J Med* 2008;121:748-757.
33. van Heerebeek L, Hamdani N, Handoko ML, Falcao-Pires I, Musters RJ, Kupreishvili K, IJsselmuiden AJ, Schalkwijk CG, Bronzwaer JG, Diamant M, Borbely A, van der Velden J, Stienen GJ, Laarman GJ, Niessen HW, Paulus WJ. Diastolic stiffness of the failing diabetic heart: importance of fibrosis, advanced gly-

cation end products, and myocyte resting tension. *Circulation* 2008;117:43-51.

34. Morris DA, Gailani M, Vaz PA, Blaschke F, Dietz R, Haverkamp W, Ozcelik C. Right ventricular myocardial systolic and diastolic dysfunction in heart failure with normal left ventricular ejection fraction. *J Am Soc Echocardiogr* 2011;24:886-897.
35. Dibble CT, Lima JA, Bluemke DA, Chirinos JA, Chahal H, Bristow MR, Kronmal RA, Barr RG, Ferrari VA, Propert KJ, Kawut SM. Regional left ventricular systolic function and the right ventricle: the multi-ethnic study of atherosclerosis right ventricle study. *Chest* 2011;140:310-316.

Chapter 5

Effects of short-term nutritional interventions on right ventricular function in healthy men

Ralph L. Widya
Sebastiaan Hammer
Mariëtte R. Boon
Rutger W. van der Meer
Johannes W.A. Smit
Albert de Roos
Patrick C.N. Rensen
Hildo J. Lamb

PLOS ONE 2013;8(9):e76406

ABSTRACT

Background

A physiological model of increased plasma nonesterified fatty acid (NEFA) levels result in myocardial triglyceride (TG) accumulation, which is related to cardiac dysfunction. A pathophysiological model of increased plasma NEFA levels result in hepatic steatosis, which has been linked to abnormal myocardial energy metabolism. Hepatic steatosis is accompanied by hepatic inflammation, reflected by plasma cholesteryl ester transfer protein (CETP) levels. The current study aimed to investigate effects of these models via different nutritional interventions on right ventricular (RV) function.

Methods

Fifteen men (age 25.0 ± 6.6 years) were included and underwent magnetic resonance imaging and spectroscopy in this prospective crossover intervention study. RV function, myocardial and hepatic TG content, and CETP levels were assessed on three occasions: after normal diet, very low-calorie diet (VLCD, physiological model) and high-fat high-energy (HFHE, pathophysiological model) diet (all 3-days diets, randomly ordered, washout phase at least 14 days).

Results

VLCD induced a decrease in mean E deceleration by 27%. Myocardial TG content increased by 55%, whereas hepatic TG content decreased by 32%. Plasma CETP levels decreased by 14% (all $P < 0.05$). HFHE diet induced a decrease in E/A by 19% ($P < 0.05$). Myocardial TG content did not change, whereas hepatic TG content increased by 112% ($P < 0.01$). Plasma CETP levels increased by 14% ($P < 0.05$).

Conclusions

These findings show that RV diastolic function is impaired after short-term VLCD and HFHE diet in healthy men, respectively a physiological and a pathophysiological model of increased plasma NEFA levels. After short-term VLCD, myocardial lipotoxicity may be of importance in decreased RV diastolic function. RV diastolic dysfunction is accompanied by increased hepatic TG content and plasma CETP levels after short-term HFHE diet, suggesting that systemic inflammation reflecting local macrophage infiltration in the heart may be involved in RV dysfunction.

INTRODUCTION

Nutritional interventions have shown to be useful for studying plasma nonesterified fatty acid (NEFA) levels and plasma triglyceride (TG) levels, and the flexibility of myocardial TG content and its relation to myocardial function[1-4]. Prior dietary intervention studies have focused on LV function. The effects of nutritional interventions on right ventricular (RV) function have not yet been studied. RV function is important in patient risk stratification in heart failure[5,6] and prediction of developing atrial fibrillation[7]. Advanced RV dysfunction and fibrosis are associated with exercise limitation, lethal ventricular arrhythmias, sudden death, and reduced RV cardiac output[8,9]. Moreover, it has been shown that RV dimensions and function are impaired in type 2 diabetes[10,11], a disease with abnormal fuel flux and energy imbalance as metabolic hallmarks.

It has been reported that short-term exposure to a very low-calorie diet (VLCD) increases plasma NEFA levels[12]. Excessive plasma NEFA levels result in myocardial TG accumulation in animal models of obesity and type 2 diabetes[13,14]. In such models, TG accumulation in cardiomyocytes is related to cardiac dysfunction[15-17] and an increased susceptibility for cardiac ischemia[18]. Complex mechanisms, most likely involving intermediates of NEFA metabolism and oxidative stress[13,17,19], are responsible for this phenomenon called "myocardial lipotoxicity". It has previously been shown that a VLCD induces an increase in myocardial TG content and a concomitant decrease in left ventricular (LV) diastolic function in lean healthy men[2]. These observations suggest that when NEFAs are taken up in excess of fatty acid oxidation, myocardial TG content increases. We therefore hypothesized that such a physiological model, induced by short-term exposure to a VLCD, would also impair RV function in lean healthy men.

Increased NEFA levels induced by a short-term high-fat high-energy (HFHE) diet caused increased hepatic TG content, but did not influence myocardial TG content or LV function in the same healthy population[3]. Hepatic steatosis has been linked to abnormal myocardial energy metabolism[20,21]. In addition, hepatic steatosis may be accompanied by hepatic inflammation. The liver macrophage is suggested to be a primary contributor to plasma cholesteryl ester transfer protein (CETP) mass[22]. Plasma CETP may therefore serve as a biomarker for the hepatic macrophage content and, thus, hepatic inflammation. Interestingly, short-term (5 days) exposure to HFHE diet increases plasma CETP along with an increase in macrophage expression markers in muscle biopsies, indicating that HFHE diet causes macrophage recruitment to tissues, including liver and muscle but possibly also the heart (MR Boon, MSc, and PCN Rensen, PhD, unpublished data, 2012). Activated macrophages in the myocardium contribute to cardiac myocyte contractile dysfunction[23]. We, therefore, hypothesized that in a pathophysiological model created by a short-term HFHE diet systemic macrophage recruitment (as reflected by increased plasma CETP levels) is linked to both hepatic tissue changes and RV dysfunction in lean healthy men.

Therefore, the aim of this study was to investigate the effects on right ventricular function in lean healthy men in two different conditions: the first was a physiological model created by a short-term caloric restriction; the second was a pathophysiological model created by a short-term high-fat diet.

METHODS

Subjects

Fifteen healthy men were included in this prospective crossover intervention study. Inclusion criteria were: 1. age > 18 years; 2. no known acute or chronic disease based on history, physical examination, or standard laboratory tests (blood counts, serum creatinine, alanine aminotransferase, aspartate aminotransferase, and electrocardiogram). Exclusion criteria were drug treatment, smoking, substance abuse, hypertension, or impaired glucose tolerance (as confirmed by a 75-g oral glucose intolerance test). All subjects performed exercise (walking, running, biking) regularly (3-5 hours weekly), but none engaged in high-performance sports. Part of these data was previously published in reports describing hepatic and myocardial TG accumulation[2, 3]. To study effects of a HFHE diet on RV function similar volunteers were used[3]. To study the effects of a VLCD, one volunteer was added[2]. This study was approved by the Medical Ethical Committee of the Leiden University Medical Center and was conducted in accordance with the Declaration of Helsinki. Written informed consent was obtained from all participants.

Study design

All subjects underwent venous blood sampling and magnetic resonance (MR) scanning in the afternoon at three different occasions. Before every visit, subjects were instructed to follow different dietary regimes. First, baseline data were collected after a 3-day normal diet, which consisted of approximately 2100 kcal/day. Next, subjects underwent a 3-day VLCD and a 3-day HFHE diet. The sequence of the nutritional interventions was randomly assigned to minimize influences caused by the sequence of the interventions. Both interventions were separated by a washout phase of at least 14 days (**Figure 1**). The VLCD consisted of 471 kcal, 50.2 g carbohydrates, and 6.9 g fat, of which 0.94 g saturated fat (Modifast Intensive, Nutrition & Santé Benelux, Breda, the Netherlands) per day. The intake of the HFHE diet was similar to the reference diet, complemented with 800 mL cream every day. The cream added 2632 kcal/day, totaling approximately 4732 kcal/day. Subjects were instructed to maintain a sufficient fluid intake (at least 1.5 L daily). Alcohol use was not allowed during the diets. Every meal was consumed 4 h prior to data collection.

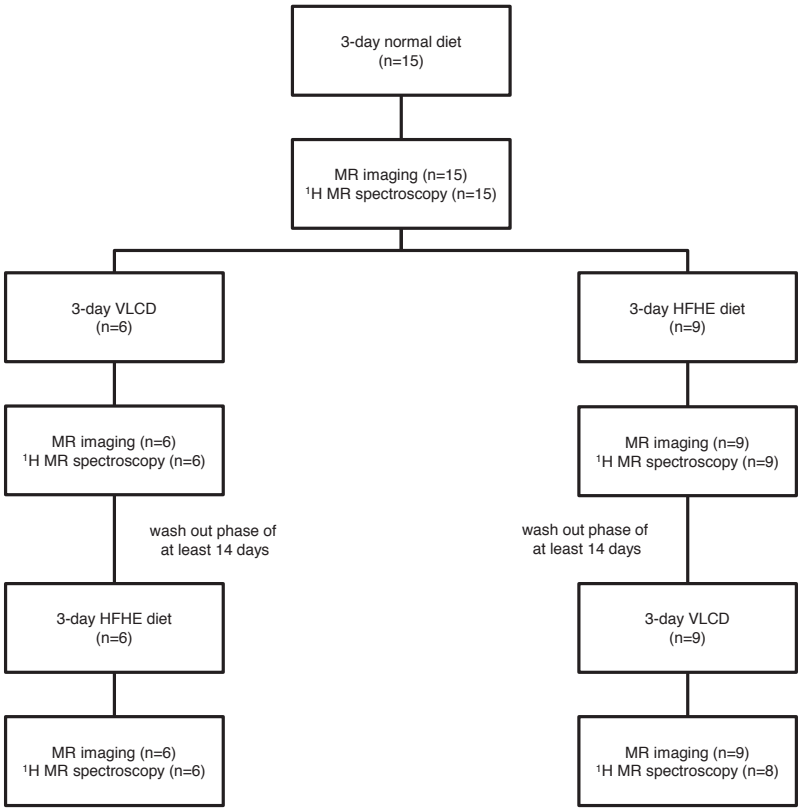

Figure 1. Workflow of the study. Baseline data were collected after a 3-day normal diet. Next, subjects underwent a 3-day very low-calorie diet (VLCD) and a 3-day high-fat high-energy (HFHE) diet. The sequence of the nutritional interventions was randomly assigned to minimize influences caused by the sequence of the interventions. Both interventions were separated by a washout phase of at least 14 days.

Proton MR spectroscopy

Myocardial and hepatic TG content were assessed by proton MR spectroscopy as described previously[2, 3, 24]. In short, MR spectroscopy studies were performed using a 1.5 Tesla whole-body MR scanner (Gyroscan ACS/NT15; Philips, Best, the Netherlands) with subjects in the supine position at rest. Cardiac proton MR spectra were obtained from the interventricular septum using a point-resolved spectroscopy sequence to acquire single voxel MR spectroscopic data from an 8-mL voxel. Spectra were acquired at end systole, with an echo time (TE) of 26 ms and a repetition time (TR) of at least 3000 ms. A total of 1024 data points was collected using a 1000-Hz spectral width and averaged over 128 acquisitions. The spectroscopic data acquisition was ECG triggered, and respiratory gating based on navigator echoes was applied to minimize breathing influences[24]. Without changing any parameter, spectra without water suppression with a TR of 10 s and four averages were obtained, to be used as an internal standard.

Proton MR spectroscopy of the liver was performed with an 8-mL voxel positioned in the liver, avoiding gross vascular structures and adipose tissue depots. The 12th thoracic vertebra was used as a landmark to ensure the same position of the voxel during both visits. Spectra were obtained without respiratory motion compensation using similar parameters as described previously. Only 64 averages were collected with water suppression.

All spectroscopic data were fitted using Java-based MR user interface software (jMRUI version 2.2; developed by A. van den Boogaart, Katholieke Universiteit Leuven, Leuven, Belgium)[25] as described before[24]. The percentage of myocardial and hepatic TG signals relative to the water signal was calculated as: (signal amplitude of TGs) / (signal amplitude of water) × 100.

MR imaging

Velocity-encoded MR imaging is a noninvasive imaging modality extensively used for blood flow assessment[26]. Moreover, cardiovascular MR imaging has become the reference standard for the assessment of RV function and volumes, yielding high accuracy and good reproducibility[27, 28]. MR scanning was performed on a 1.5 Tesla whole body MRI scanner (Gyroscan ACS/NT15; Philips, Best, the Netherlands), with subjects in the supine position at rest as previously described[2, 3]. In short, RV dimensions and systolic function were assessed by imaging the entire heart in short-axis orientation using electrocardiographically gated breath-hold balanced steady-state free precession imaging. Endocardial contours of the RV were manually drawn in end-diastolic phase and end-systolic phase as previously described[11]. Imaging parameters were as follows: repetition time (TR) = 3.3 ms, echo time (TE) = 1.67 ms, flip angle = 35°, slice thickness = 10 mm, slice gap = 0 mm, field of view = 400 x 400 mm, reconstructed matrix size = 256 x 256. Dimensions were indexed to body surface area, resulting in end diastolic volume index (EDVI) and end systolic volume index (ESVI).

Body surface area was calculated according to the Mosteller formula: (weight (kg) × height (cm)/3600)$^{0.529}$.

RV diastolic function was determined by measuring blood flow across the tricuspid valve. Diastolic parameters included peak filling rates of the early filling phase (E) and atrial contraction (A), and their ratio (E/A). Also, the peak and mean deceleration gradient of E was calculated. Electrocardiographically gated gradient echo sequences with velocity encoding were performed. The following imaging parameters were used: TR = 6.5 ms, TE = 1 ms, flip angle = 20°, slice thickness = 8 mm, field of view = 350 x 350 mm, matrix size = 256 x 256, EPI-factor = 3, velocity encoding gradient = 100 cm/s. Image postprocessing was performed with in-house-developed software packages (MASS and FLOW, Medis, Leiden, the Netherlands).

CETP

Plasma samples were obtained at all three occasions, stored in aliquots at −80°C, and analyzed after thawing once in a single laboratory (Dept. Endocrinology, Leiden, the Neth-

erlands). Plasma CETP concentration was quantified using kit CETP ELISA Daiichi (Daiichi Pure Chemicals, Tokyo, Japan).

Statistical analysis

Statistical analyses were performed using SPSS Statistics version 20 (IBM, Armonk, NY). Data are expressed as means ± SD. The study conditions were compared by a two-tailed paired *t* test. Because a change in heart rate influences the interpretation of RV functional measures, a linear mixed model was performed to correct for heart rate when altered after a diet. Finally, multivariate linear regression models were used to study correlations of differences of myocardial TG content with differences of RV diastolic function after VLCD, and differences of hepatic TG content and CETP with differences of RV diastolic function after HFHE diet. Because E/A decreases with age, we adjusted for age in the multivariate linear regression models[30]. Furthermore, we also adjusted for the difference in heart rate in the condition after HFHE diet. A P value < 0.05 was considered statistically significant.

RESULTS

Part of these data, including MR spectroscopy data, was previously published[2, 3]. Mean age of the studied subjects was 25.0 ± 6.6 years.

Very low-calorie diet

Participant characteristics at baseline and after the VLCD are shown in **Table 1**. BMI range at baseline was 19.4-28.2 kg/m^2 and after VLCD 19.2-27.4 kg/m^2. BMI decreased from 23.4 ± 2.5 to 23.1 ± 2.4 kg/m^2 and body surface area decreased from 2.10 ± 0.21 to 2.08 ± 0.21 m^2 (both P < 0.01). Plasma glucose levels decreased from 4.9 ± 0.3 to 4.3 ± 0.4 mmol/L, and plasma NEFA levels increased from 0.54 ± 0.29 to 1.12 ± 0.38 mmol/L (both P < 0.001).

MR imaging results are depicted in **Table 2**. RV dimensions changed, as shown by a decreased EDV and ESV (251 ± 39 to 238 ± 39 mL and 131 ± 22 to 123 ± 23 mL, respectively). After indexing for body surface area, RV EDVI decreased from 119.5 ± 12.6 to 114.4 ± 14.0 mL/m^2 (P < 0.05), while a decrease in RV ESVI did not reach significance (P = 0.056). Systolic function did not change. The mean deceleration of the early diastolic flow across the tricuspid valve decreased from 1.81 ± 0.49 to 1.33 ± 0.32 mL/s^2 x 10^{-3} (P < 0.01).

MR spectroscopy failed in one subject for unknown reasons leading to insufficient spectral resolution. As a result 14 men were included in the myocardial and hepatic fat analyses. Myocardial TG content increased by 55% from 0.38 ± 0.19 to 0.59 ± 0.24% (P < 0.01) (**Figure 2A**), whereas hepatic TG content decreased by 32% from 2.19 ± 1.94 to 1.50 ± 1.36% (P < 0.05) (**Figure 2B**). Plasma CETP levels decreased by 14% from 2.87 ± 0.51 to 2.48 ± 0.49 µg/mL (P < 0.01) (**Figure 2C**), while HDL-cholesterol was not changed (**Table 1**).

No correlations were found between the difference in myocardial TG content and the difference in any of the RV diastolic function parameters.

Table 1. Participant characteristics at baseline and after short-term caloric restriction and short-term high-fat diet

	Baseline	VLCD	HFHE
Body mass index (kg/m^2)	23.4 ± 2.5	23.1 ± 2.4*	23.6 ± 2.5
Body surface area (m^2)	2.10 ± 0.21	2.08 ± 0.21*	2.11 ± 0.21
Systolic blood pressure (mmHg)	123 ± 13	118 ± 10	125 ± 13
Diastolic blood pressure (mmHg)	67 ± 8	62 ± 8*	64 ± 8
Heart rate (bpm)	60 ± 9	61 ± 10	69 ± 11*
Plasma glucose (mmol/L)	4.9 ± 0.3	4.3 ± 0.4*	5.0 ± 0.4
Plasma insulin (mU/L)	9.1 ± 4.6	7.7 ± 4.3	21.4 ± 8.8*
Plasma triglycerides (mmol/L)	1.3 ± 0.4	0.9 ± 0.3*	2.9 ± 1.1*
Plasma NEFA (mmol/L)	0.54 ± 0.29	1.12 ± 0.38*	0.92 ± 0.33*
Total cholesterol (mmol/L)	4.7 ± 1.2	4.7 ± 1.3	5.0 ± 1.3
HDL cholesterol (mmol/L)	1.5 ± 0.4	1.5 ± 0.4	1.6 ± 0.4*

Values are means ± SD. HDL = high-density lipoprotein. HFHE = high-fat high-energy. NEFA = nonesterified fatty acids. VLCD = very low-calorie diet.
* $P < 0.05$ compared to baseline.
These data are partly based on previous reports (2,3) (see Methods section).

Table 2. RV parameters at baseline and after short-term caloric restriction and short-term high-fat diet

	Baseline	VLCD	HFHE
Dimensions			
End diastolic volume index (mL/m^2)	119.5 ± 12.6	114.4 ± 14.0*	118.1 ± 13.2
End systolic volume index (mL/m^2)	62.1 ± 6.9	58.7 ± 8.7	59.9 ± 9.4
Systolic function			
Stroke volume (mL)	121 ± 21	116 ± 18	123 ± 19
Cardiac output (L/min)	7.5 ± 1.7	7.2 ± 1.1	8.5 ± 1.1
Ejection fraction (%)	48.0 ± 3.1	48.7 ± 2.8	49.4 ± 4.0
Diastolic function			
E peak flow rate (mL/s)	422 ± 92	391 ± 79	400 ± 70
Peak E deceleration (mL/s^2 x 10^{-3})	3.17 ± 1.01	2.63 ± 0.78	2.60 ± 0.97
Mean E deceleration (mL/s^2 x 10^{-3})	1.81 ± 0.49	1.33 ± 0.32*	1.40 ± 0.49
A peak flow rate (mL/s)	301 ± 84	310 ± 76	355 ± 99
E/A	1.47 ± 0.43	1.30 ± 0.27	1.19 ± 0.29*

Values are means ± SD. A = atrial contraction. E = early filling phase. HFHE = high-fat high-energy. VLCD = very low-calorie diet.
* $P < 0.05$ compared to baseline.

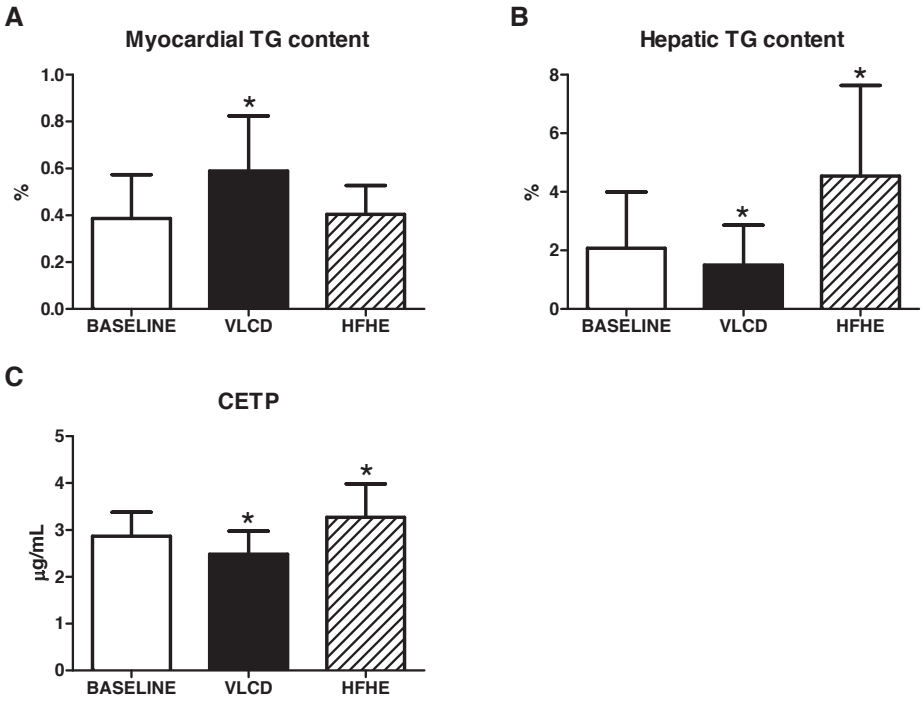

Figure 2. Myocardial and hepatic TG content and plasma CETP levels after short-term caloric restriction and short-term high-fat diet. Myocardial (A) and hepatic (B) triglyceride content and plasma CETP levels (C) at baseline (white bars), after short-term caloric restriction (black bars), and after short-term high-energy diet (hatched bars). CETP = cholesteryl ester transfer protein. HFHE = high-fat high-energy. TG = triglyceride. VLCD = very low-calorie diet. * $P < 0.05$. These data are partly based on previous reports (2,3) (see Methods section).

High-fat high-energy diet

Participant characteristics at baseline and after the HFHE diet are depicted in **Table 1**. BMI range after the HFHE was 19.9-27.9 kg/m^2. BMI and body surface area remained similar, as well as plasma glucose levels. Plasma NEFA levels increased from 0.54 ± 0.29 to 0.92 ± 0.33 mmol/L ($P < 0.01$). The 3-day HFHE diet (hereafter, high-fat diet) increased heart rate from 60 ± 9 to 69 ± 11 bpm ($P < 0.01$). For this reason changes in RV dimensions and function were corrected for heart rate, corrected data are shown.

RV dimensions remained similar. Systolic function did not change. E/A was decreased from 1.47 ± 0.43 to 1.19 ± 0.29 ($P < 0.05$) (**Table 2**).

Myocardial TG content did not change (**Figure 2A**), whereas hepatic TG content increased by 112% from 2.01 ± 1.79 to 4.26 ± 2.78% ($P < 0.01$) (**Figure 2B**). Plasma CETP levels increased by 14% from 2.87 ± 0.51 to 3.27 ± 0.72 µg/mL ($P < 0.05$) (**Figure 2C**). HDL-cholesterol increased from 1.5 ± 0.4 to 1.6 ± 0.4 mmol/L ($P < 0.05$) (**Table 1**).

A correlation was found between the increase in hepatic TG content and decrease in E/A (β −0.099, R^2 0.364, $P = 0.05$). The increase of plasma CETP levels did not correlate with the difference in any of the RV diastolic function parameters.

DISCUSSION

The main finding of the current study is that in the physiological as well as in the patho-physiological model of increased NEFA levels, induced by respectively short-term caloric restriction and short-term high fat diet, RV function is decreased in healthy men. Furthermore, plasma CETP levels decrease after short-term caloric restriction and increase after short-term high-fat diet.

Effects after very low-calorie diet

It has been recognized that short-term caloric restriction causes tissue-specific partitioning of plasma TG and/or fatty acids among non-adipose organs in healthy subjects, with respect to the liver and the heart. In a prior study, short-term caloric restriction induced an increase of myocardial TG, whereas hepatic TG content decreased. Furthermore, LV diastolic function was decreased[2]. We hypothesized that such a physiological model would also impair RV function. To the best of our knowledge, this is the first study to show decreased RV diastolic function after VLCD in lean healthy men. Possible causes include impaired relaxation through the activation of phospholipases after a short-term caloric restriction causing changes in calcium homeostasis[31-33]. Another explanation for decreased diastolic function might be a relatively higher reliability of the heart on NEFA, since plasma NEFA levels were found to be increased and plasma glucose levels decreased after short-term caloric restriction. Therefore, the myocardium may not benefit from potential favorable effects of carbohydrate oxidation on myocardial function and efficiency[2, 34, 35].

The mean deceleration of the early diastolic flow across the tricuspid valve was decreased after short-term caloric restriction, similar to the mean deceleration of the early diastolic flow across the mitral valve in the LV[2]. Even though the differences of the other diastolic function parameters after short-term caloric restriction did not reach statistical significance, a trend was observed of a decreased ratio of the peak filling rates of the early filling phase to atrial contraction, indicating a change in relaxation of the right ventricle. Furthermore, RV volumes were decreased after short-term caloric restriction compared to baseline. After indexing for body surface area, RV EDVI was significantly lower. Decreased RV volumes and impaired RV function have also been implicated as components of the diabetic cardiomyopathy phenotype[11].

We performed multivariate linear regression analyses to assess the relationship between the change in myocardial TG content and RV diastolic dysfunction. However, we did not

find any correlations. Nonetheless, myocardial TG accumulation may be a marker of many hormonal, metabolic, and biophysical changes within the myocardium that occur during a VLCD, and this complex interplay may be of influence on myocardial diastolic function.

Plasma CETP levels decreased by 14%. This is in full accordance with previous findings of a prolonged caloric restriction which resulted in a marked decrease in hepatic TG content and plasma CETP levels in obese type 2 diabetic patients[36]. CETP is a hydrophobic plasma glycoprotein that is involved in the exchange of cholesteryl esters and TG between HDL and apoB-containing lipoproteins (e.g., VLDL and LDL), resulting in a net transfer of cholesteryl esters from HDL to apoB-containing lipoproteins[37]. Liver macrophages largely contribute to hepatic CETP expression, and attenuation of hepatic steatosis, accompanied by attenuation of liver inflammation, as reflected by reduced macrophage content, by the anti-dyslipidemic drug niacin decreased hepatic CETP expression and the plasma CETP level[22]. To our knowledge, this study is the first to report a decrease in plasma CETP level already after three days of caloric restriction, suggesting that hepatic inflammation (i.e. macrophage content) is reduced.

Effects after high-fat high-energy diet

We created a pathophysiological model of increased plasma NEFA levels via a short-term HFHE diet and hypothesized that RV function would be decreased as a result of hepatic inflammation. Remarkably, RV diastolic function was altered after short-term high-fat diet whereas LV function was previously found to remain similar in the same study group[3]. This discrepancy might be caused by the observed increase of hepatic TG content after short-term high-fat diet leading to reduced compliance of the hepatic parenchyma. Hypertrophied hepatocytes might cause hepatic vein compression and subsequently decrease vein phasicity[38]. The hepatic veins drain blood from the hepatic sinusoids toward the inferior vena cava. As a result of abnormal flow in the hepatic veins, blood flow in the inferior vena cava may also be anomalous. It has been recognized that the hepatic vein doppler waveform alters from triphasic to biphasic or monophasic in patients with non-alcoholic fatty liver disease (NAFLD)[38, 39]. The early passive filling of the right atrium and ventricle may be disturbed, causing a decreased E/A. Unfortunately, we did not perform duplex doppler ultrasonography to investigate the waveforms of the hepatic veins.

Alternatively, taken together the rise in plasma CETP levels with our previous finding that short-term high-fat diet increases the expression of macrophage genes in muscle biopsies (MR Boon, MSc, and PCN Rensen, PhD, unpublished data, 2012), it is possible that short-term high-fat diet results in macrophage activation and recruitment into tissues including liver, muscle and possibly also the heart. Activated macrophages that adhere to intercellular adhesion molecule-1 (ICAM-1) expressed on cardiac myocytes contribute to cardiac myocyte contractile dysfunction[23]. Furthermore, macrophages and macrophage-derived mediators have been implicated in myocardial dysfunction in a number of myocardial inflammatory

states[23], including ischemic and non-ischemic cardiomyopathy[40]. A recent animal study showed that several inflammatory cytokines were upregulated accompanied by macrophage infiltration in lipotoxic cardiomyopathy, and that macrophages contribute to adverse cardiac remodeling in response to lipid overload[41]. It may be hypothesized that RV diastolic dysfunction is an early manifestation of myocardial macrophage infiltration after short-term high-fat diet.

Short-term high-fat diet induced a more than 2-fold increase in hepatic TG content in these subjects, whereas it did not influence myocardial TG content[3]. It has now been recognized that a combined hyperglycemia and hyperinsulinemia induce short-term myocardial TG accumulation and alterations in LV function in normal subjects, indicating that postprandial and/or chronic hyperglycemia and hyperinsulinemia might be involved in myocardial steatosis in metabolic diseases[42]. Healthy subjects showed hyperinsulinemia but no hyperglycemia in response to high-fat diet[3]. This could explain the absent myocardial steatosis and possibly the absence of LV dysfunction[3].

Limitations

Some potential limitations should be addressed. First, our study sample is small and the study may be underpowered to perform adequate correlative statistical analyses. Therefore, further studies with larger population should be performed. Second, we did not measure flow of the hepatic vein and inferior vena cava that could support the hypothesis that hepatic steatosis may result in anomalous flow in the hepatic vein and the inferior vena cava leading to disturbed filling of the RV. We measured hepatic TG content and plasma CETP levels as markers for hepatic inflammation. However, further studies need to be initiated combining duplex doppler ultrasonography of the hepatic vein and inferior vena cava and assessment of RV function.

In conclusion, RV function is impaired after short-term caloric restriction in healthy men. Furthermore, RV function is also impaired after short-term high-fat diet. Whereas the response of the right ventricle to short-term caloric restriction seems analogous to the left ventricle, it shows a differential response to short-term high-fat diet as compared to the left ventricle. RV dysfunction is accompanied by increased hepatic TG content and plasma CETP levels in short-term high-fat diet, suggesting that systemic inflammation reflecting local macrophage infiltration in the heart may be involved in RV dysfunction.

REFERENCES

1. Lamb HJ, Smit JW, van der Meer RW, Hammer S, Doornbos J, de Roos A, Romijn JA. Metabolic MRI of myocardial and hepatic triglyceride content in response to nutritional interventions. *Curr Opin Clin Nutr Metab Care* 2008;11:573-579.
2. van der Meer RW, Hammer S, Smit JW, Frölich M, Bax JJ, Diamant M, Rijzewijk LJ, de Roos A, Romijn JA, Lamb HJ. Short-term caloric restriction induces accumulation of myocardial triglycerides and decreases left ventricular diastolic function in healthy subjects. *Diabetes* 2007;56:2849-2853.
3. van der Meer RW, Hammer S, Lamb HJ, Frölich M, Diamant M, Rijzewijk LJ, de Roos A, Romijn JA, Smit JW. Effects of short-term high-fat, high-energy diet on hepatic and myocardial triglyceride content in healthy men. *J Clin Endocrinol Metab* 2008;93:2702-2708.
4. Hammer S, van der Meer RW, Lamb HJ, Schär M, de Roos A, Smit JW, Romijn JA. Progressive caloric restriction induces dose-dependent changes in myocardial triglyceride content and diastolic function in healthy men. *J Clin Endocrinol Metab* 2008;93:497-503.
5. Ghio S, Gavazzi A, Campana C, Inserra C, Klersy C, Sebastiani R, Arbustini E, Recusani F, Tavazzi L. Independent and additive prognostic value of right ventricular systolic function and pulmonary artery pressure in patients with chronic heart failure. *J Am Coll Cardiol* 2001;37:183-188.
6. Meluzin J, Spinarova L, Dusek L, Toman J, Hude P, Krejci J. Prognostic importance of the right ventricular function assessed by Doppler tissue imaging. *Eur J Echocardiogr* 2003;4:262-271.
7. Aziz EF, Kukin M, Javed F, Musat D, Nader A, Pratap B, Shah A, Enciso JS, Chaudhry FA, Herzog E. Right ventricular dysfunction is a strong predictor of developing atrial fibrillation in acutely decompensated heart failure patients, ACAP-HF data analysis. *J Card Fail* 2010;16:827-834.
8. Mertens LL, Friedberg MK. Imaging the right ventricle--current state of the art. *Nat Rev Cardiol* 2010;7:551-563.
9. Warnes CA. Adult congenital heart disease importance of the right ventricle. *J Am Coll Cardiol* 2009;54:1903-1910.
10. van den Brom CE, Bosmans JW, Vlasblom R, Handoko LM, Huisman MC, Lubberink M, Molthoff CF, Lammertsma AA, Ouwens MD, Diamant M, Boer C. Diabetic cardiomyopathy in Zucker diabetic fatty rats: the forgotten right ventricle. *Cardiovasc Diabetol* 2010;9:25.
11. Widya RL, van der Meer RW, Smit JW, Rijzewijk LJ, Diamant M, Bax JJ, de Roos A, Lamb HJ. Right ventricular involvement in diabetic cardiomyopathy. *Diabetes Care* 2013;36:457-462.
12. Hirsch J, Goldrick RB. Serial studies on the metabolism of human adipose tissue. I. Lipogenesis and free fatty acid uptake and release in small aspirated samples of subcutaneous fat. *J Clin Invest* 1964;43:1776-1792.
13. Schaffer JE. Lipotoxicity: when tissues overeat. *Curr Opin Lipidol* 2003;14:281-287.
14. Unger RH. Lipotoxic diseases. *Annu Rev Med* 2002;53:319-336.
15. Christoffersen C, Bollano E, Lindegaard ML, Bartels ED, Goetze JP, Andersen CB, Nielsen LB. Cardiac lipid accumulation associated with diastolic dysfunction in obese mice. *Endocrinology* 2003;144:3483-3490.
16. Ouwens DM, Boer C, Fodor M, de Galan P, Heine RJ, Maassen JA, Diamant M. Cardiac dysfunction induced by high-fat diet is associated with altered myocardial insulin signalling in rats. *Diabetologia* 2005;48:1229-1237.
17. Zhou YT, Grayburn P, Karim A, Shimabukuro M, Higa M, Baetens D, Orci L, Unger RH. Lipotoxic heart disease in obese rats: implications for human obesity. *Proc Natl Acad Sci U S A* 2000;97:1784-1789.
18. Balschi JA, Hai JO, Wolkowicz PE, Straeter-Knowlen I, Evanochko WT, Caulfield JB, Bradley E, Ku DD, Pohost GM. 1H NMR measurement of triacylglycerol accumulation in

the post-ischemic canine heart after transient increase of plasma lipids. *J Mol Cell Cardiol* 1997;29:471-480.

19. Unger RH, Orci L. Lipoapoptosis: its mechanism and its diseases. *Biochim Biophys Acta* 2002;1585:202-212.
20. Perseghin G, Lattuada G, De Cobelli F, Esposito A, Belloni E, Ntali G, Ragogna F, Canu T, Scifo P, Del Maschio A, Luzi L. Increased mediastinal fat and impaired left ventricular energy metabolism in young men with newly found fatty liver. *Hepatology* 2008;47:51-58.
21. Rijzewijk LJ, Jonker JT, van der Meer RW, Lubberink M, de Jong HW, Romijn JA, Bax JJ, de Roos A, Heine RJ, Twisk JW, Windhorst AD, Lammertsma AA, Smit JW, Diamant M, Lamb HJ. Effects of hepatic triglyceride content on myocardial metabolism in type 2 diabetes. *J Am Coll Cardiol* 2010;56:225-233.
22. Li Z, Wang Y, van der Sluis RJ, van der Hoorn JW, Princen HM, van Eck M, van Berkel TJ, Rensen PC, Hoekstra M. Niacin reduces plasma CETP levels by diminishing liver macrophage content in CETP transgenic mice. *Biochem Pharmacol* 2012;84:821-829.
23. Simms MG, Walley KR. Activated macrophages decrease rat cardiac myocyte contractility: importance of ICAM-1-dependent adhesion. *Am J Physiol* 1999;277:H253-260.
24. van der Meer RW, Doornbos J, Kozerke S, Schär M, Bax JJ, Hammer S, Smit JW, Romijn JA, Diamant M, Rijzewijk LJ, de Roos A, Lamb HJ. Metabolic imaging of myocardial triglyceride content: reproducibility of 1H MR spectroscopy with respiratory navigator gating in volunteers. *Radiology* 2007;245:251-257.
25. Naressi A, Couturier C, Devos JM, Janssen M, Mangeat C, de Beer R, Graveron-Demilly D. Java-based graphical user interface for the MRUI quantitation package. *MAGMA* 2001;12:141-152.
26. Rebergen SA, van der Wall EE, Doornbos J, de Roos A. Magnetic resonance measurement of velocity and flow: technique, validation, and cardiovascular applications. *Am Heart J* 1993;126:1439-1456.
27. Pattynama PM, Lamb HJ, van der Velde EA, van der Geest RJ, van der Wall EE, de Roos A. Reproducibility of MRI-derived measurements of right ventricular volumes and myocardial mass. *Magn Reson Imaging* 1995;13:53-63.
28. Grothues F, Moon JC, Bellenger NG, Smith GS, Klein HU, Pennell DJ. Interstudy reproducibility of right ventricular volumes, function, and mass with cardiovascular magnetic resonance. *Am Heart J* 2004;147:218-223.
29. Mosteller RD. Simplified calculation of body-surface area. *N Engl J Med* 1987;317:1098.
30. Miyatake K, Okamoto M, Kinoshita N, Owa M, Nakasone I, Sakakibara H, Nimura Y. Augmentation of atrial contribution to left ventricular inflow with aging as assessed by intracardiac Doppler flowmetry. *Am J Cardiol* 1984;53:586-589.
31. Han X, Cheng H, Mancuso DJ, Gross RW. Caloric restriction results in phospholipid depletion, membrane remodeling, and triacylglycerol accumulation in murine myocardium. *Biochemistry* 2004;43:15584-15594.
32. Huang JM, Xian H, Bacaner M. Long-chain fatty acids activate calcium channels in ventricular myocytes. *Proc Natl Acad Sci U S A* 1992;89:6452-6456.
33. Zile MR, Brutsaert DL. New concepts in diastolic dysfunction and diastolic heart failure: Part II: causal mechanisms and treatment. *Circulation* 2002;105:1503-1508.
34. Ferrannini E, Santoro D, Bonadonna R, Natali A, Parodi O, Camici PG. Metabolic and hemodynamic effects of insulin on human hearts. *Am J Physiol* 1993;264:E308-315.
35. Korvald C, Elvenes OP, Myrmel T. Myocardial substrate metabolism influences left ventricular energetics in vivo. *Am J Physiol Heart Circ Physiol* 2000;278:H1345-1351.
36. Wang Y, Snel M, Jonker JT, Hammer S, Lamb HJ, de Roos A, Meinders AE, Pijl H, Romijn JA, Smit JW, Jazet IM, Rensen PC. Prolonged caloric restriction in obese patients with type 2 diabetes mellitus decreases plasma CETP and increases apolipoprotein AI levels without

improving the cholesterol efflux properties of HDL. *Diabetes Care* 2011;34:2576-2580.

37. Hesler CB, Swenson TL, Tall AR. Purification and characterization of a human plasma cholesteryl ester transfer protein. *J Biol Chem* 1987;262:2275-2282.
38. Solhjoo E, Mansour-Ghanaei F, Moulaei-Langorudi R, Joukar F. Comparison of portal vein doppler indices and hepatic vein doppler waveform in patients with nonalcoholic fatty liver disease with healthy control. *Hepat Mon* 2011;11:740-744.
39. Oguzkurt L, Yildirim T, Torun D, Tercan F, Kizilkilic O, Niron EA. Hepatic vein Doppler waveform in patients with diffuse fatty infiltration of the liver. *Eur J Radiol* 2005;54:253-257.
40. Cappuzzello C, Di Vito L, Melchionna R, Melillo G, Silvestri L, Cesareo E, Crea F, Liuzzo G, Facchiano A, Capogrossi MC, Napolitano M. Increase of plasma IL-9 and decrease of plasma IL-5, IL-7, and IFN-gamma in patients with chronic heart failure. *J Transl Med* 2011;9:28.
41. Schilling JD, Machkovech HM, Kim AH, Schwedwener R, Schaffer JE. Macrophages modulate cardiac function in lipotoxic cardiomyopathy. *Am J Physiol Heart Circ Physiol* 2012;303:H1366-1373.
42. Winhofer Y, Krssak M, Jankovic D, Anderwald CH, Reiter G, Hofer A, Trattnig S, Luger A, Krebs M. Short-term hyperinsulinemia and hyperglycemia increase myocardial lipid content in normal subjects. *Diabetes* 2012;61:1210-1216.

Chapter 6

Exercise and type 2 diabetes mellitus: changes in tissue-specific fat distribution and cardiac function

Jacqueline T. Jonker
Pieter de Mol
Suzanna T. de Vries
Ralph L. Widya
Sebastiaan Hammer
Linda D. van Schinkel
Rutger W. van der Meer
Rijk O.B. Gans
Andrew G. Webb
Hermien E. Kan
Eelco J.P. de Koning
Henk J.G. Bilo
Hildo J. Lamb

Radiology 2013;269(2):434-442

ABSTRACT

Background

Ectopic fat accumulation in type 2 diabetes mellitus is associated with insulin resistance and increased risk for cardiovascular disease. The purpose of this study was to prospectively assess the effects of an exercise intervention on organ-specific fat accumulation and cardiac function in type 2 diabetes mellitus.

Methods

Written informed consent was obtained from all participants, and the study protocol was approved by the medical ethics committee. The study followed 12 patients with type 2 diabetes mellitus (seven men; mean age, 46 years ± 2 [standard error]) before and after 6 months of moderate-intensity exercise, followed by a high-altitude trekking expedition with exercise of long duration. Abdominal, epicardial, and paracardial fat volume were measured by using magnetic resonance (MR) imaging. Cardiac function was quantified with cardiac MR, and images were analyzed by a researcher who was supervised by a senior researcher (4 and 21 years of respective experience in cardiac MR). Hepatic, myocardial, and intramyocellular triglyceride (TG) content relative to water were measured with proton MR spectroscopy at 1.5 and 7 Tesla. Two-tailed paired *t* tests were used for statistical analysis.

Results

Exercise reduced visceral abdominal fat volume from 348 mL ± 57 to 219 mL ± 33 ($P < 0.01$), and subcutaneous abdominal fat volume remained unchanged ($P = 0.9$). Exercise decreased hepatic TG content from 6.8% ± 2.3 to 4.6% ± 1.6 ($P < 0.01$) and paracardial fat volume from 4.6 mL ± 0.9 to 3.7 mL ± 0.8 ($P = 0.02$). Exercise did not change epicardial fat volume ($P = 0.9$), myocardial TG content ($P = 0.9$), intramyocellular lipid content ($P = 0.3$), or cardiac function ($P = 0.5$).

Conclusions

A 6-month exercise intervention in type 2 diabetes mellitus decreased hepatic TG content and visceral abdominal and paracardial fat volume, which are associated with increased cardiovascular risk, but cardiac function was unaffected. Tissue-specific exercise-induced changes in body fat distribution in type 2 diabetes mellitus were demonstrated in this study.

INTRODUCTION

In patients with type 2 diabetes mellitus, both aerobic and resistance exercise have been shown to improve metabolic control and reduce cardiovascular risk. Therefore, it is recommended[1] that patients with type 2 diabetes mellitus perform moderate-intensity exercise for a minimum of 150 minutes per week.

Metabolic pathways involved in the pathogenesis of insulin resistance and cardiovascular diseases are complex. Insulin resistance is associated with increased lipolysis from the adipose tissue. The increased flux of fatty acids can be taken up by different organs, including in the liver, in the heart, and in muscle[2]. The accumulation of triglycerides (TGs) in tissues, other than adipose tissue, is called ectopic fat accumulation. Ectopic fat accumulation in the muscle and liver are involved in pathophysiologic insulin resistance[3-5].

Pericardial fat is the fat around the heart that can be divided in the epicardial and paracardial fat layer. Hepatic steatosis, myocardial TG accumulation, and pericardial fat have been associated with cardiovascular complications[2, 6, 7]. Furthermore, myocardial TG accumulation has been associated with a decrease in diastolic cardiac function[8, 9].

Therefore, strategies to limit ectopic fat accumulation are rational approaches to improve glucose homeostasis and potentially reduce cardiovascular risk. Most intervention studies have focused on visceral and subcutaneous fat; however, to our knowledge, little is known about the effect of exercise alone without diet on ectopic fat accumulation in type 2 diabetes mellitus patients.

Several studies have shown an association between epicardial fat and visceral fat volume[10, 11]. If this association holds a causal relationship, we expect that an exercise-induced decrease in visceral abdominal fat will be accompanied by a decrease in epicardial fat volume.

The purpose of our study was to prospectively assess the effects of an exercise intervention on organ-specific fat accumulation and cardiac function in type 2 diabetes mellitus.

METHODS

Patients and study design

Written informed consent was obtained from all participants, and the study protocol was approved by our medical ethics committee. Twelve patients (seven men, five women; patient age, 46 years ± 2 [standard error]) with type 2 diabetes mellitus were included. Patients were recruited by advertisements to take part in the Atlas Diabetes Challenge, a trekking expedition to Mount Toubkal in Morocco, organized by the Bas van de Goor Foundation, for which exercise training was required. At inclusion (90 days before start of training; **Figure 1**), all patients underwent screening that consisted of physical examination, electrocardiogra-

phy (ECG), echocardiography, maximal exertion cycle ergometer testing, and blood analysis. Exclusion criteria were patients older than 70 years, diabetic complications (i.e., retinopathy, neuropathy, or nephropathy), hypertension (systolic blood pressure > 165 mmHg and/or diastolic blood pressure > 95 mmHg), body mass index greater than 35 kg/m^2, smoking, known cardiac disease (i.e., abnormal ECG, cardiomyopathy, or coronary or valvular disease), use of drugs, or any contraindication for magnetic resonance (MR) imaging.

Patients underwent a 6-month individualized training program followed by a 12-day trekking expedition to Mount Toubkal (elevation, 4167 m) in Morocco. Trekking consisted of moderate-intensity exercise (walks of approximately 4-7 hours daily), of which 4 days were spent above 3000-m elevation. Patients received a written training program 6 months prior to the expedition and were advised to perform two endurance and two resistance training sessions for a total 3.5-6 hours per week.

The aims of the program were to achieve a normal estimated workload capacity and to improve general physical fitness. Patients trained themselves without supervision, but they kept in contact with the expedition physicians. Patients recorded their food intake and energy expenditure for 1 week per month during the 6-month training program and continuously during the expedition by using a web-based dietary program and a physical activity monitor (SenseWear Pro 3 Armband; BodyMedia, Pittsburgh, Pa)[12]. At inclusion and after the training period, the maximum workload capacity was determined with a maximal exertion cycle ergometer test. Maximum oxygen uptake (oxygen uptake maximum) was calculated[13]. Patients underwent MR examinations on two occasions: at 7 days before the start of training and 200 days after the start of training (**Figure 1**). At least 4 hours after the last meal, MR measurements were obtained, blood was drawn, and anthropometric measurements (i.e., body weight and blood pressure) were obtained.

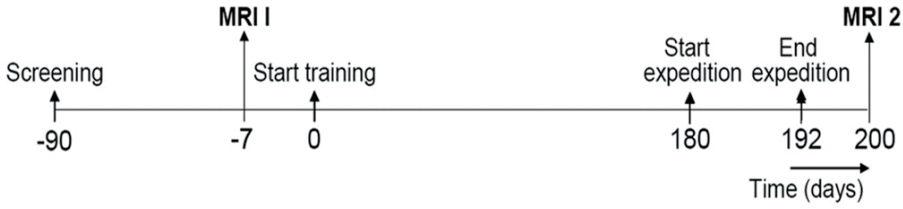

Figure 1. Timeline of the study. Screening was performed 90 days before the start of the training program. The training program consisted of a 6-month individualized training program, followed by a 12-day trekking expedition to Mount Toubkal in Morocco. An MR examination was performed approximately 1 week before the start of the training and at least 1 week after the trekking expedition.

Subcutaneous and visceral abdominal fat

A 1.5 Tesla MR imager (Gyroscan ACS-NT 15; Philips Medical Systems, Best, the Netherlands) was used for all MR imaging. Patients were examined in a supine position. Abdominal fat was imaged by using a turbo spin-echo imaging sequence[8]. Three 10-mm-thick transverse sections were imaged at the fifth lumbar vertebrae during breath holds (**Figure 2**). Imaging parameters were as follows: repetition time ms/echo time ms, 168/11; flip angle, 90°. Contours were drawn around the visceral and subcutaneous abdominal fat deposits by using software (MASS; Medis Medical Imaging Systems, Leiden, the Netherlands). The area of each section was multiplied by the section thickness to estimate the volume, and the volumes of all three sections were summed.

All MR imaging and MR spectroscopy acquisition at 1.5 T was performed by J.T.J., R.W.v.d.M., and S.H. (4, 8, and 8 years of respective experience in MR imaging and MR spectroscopy), and postprocessing was performed by J.T.J., who was supervised by H.J.L. (21 years of experience in MR imaging and MR spectroscopy).

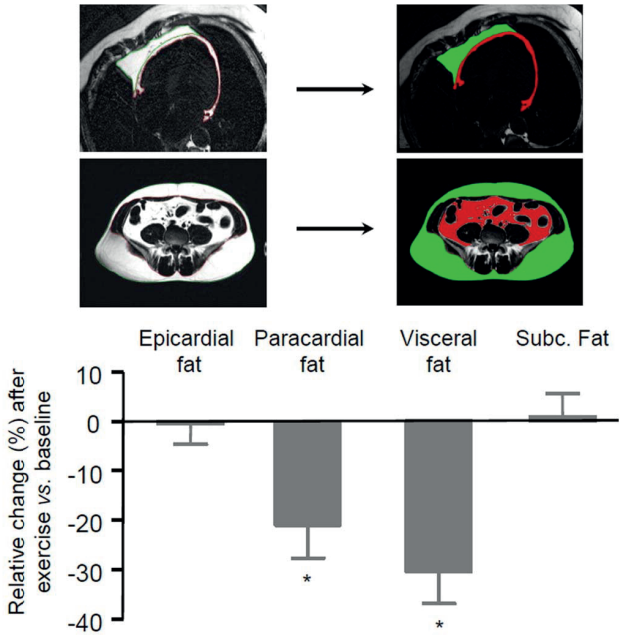

Figure 2. Top: Quantification of (upper figures) epicardial (red) and paracardial fat (green) volume and (lower figures) visceral (red) and subcutaneous (green) abdominal fat. For the abdominal fat, only one transverse section is shown; three sections were imaged. The area of fat of each individual section was multiplied by the section thickness to estimate the volume, and the volumes of all three sections were summed. Bottom: Box and whisker plot of relative changes in epicardial and paracardial (11 patients) and visceral and subcutaneous (*Subc.*) abdominal fat volume (12 patients) after 6 months of exercise compared with before start of training (12 patients; seven men, five women; mean age, 46 years ± 2). * = $P < 0.05$ change after exercise compared with baseline.

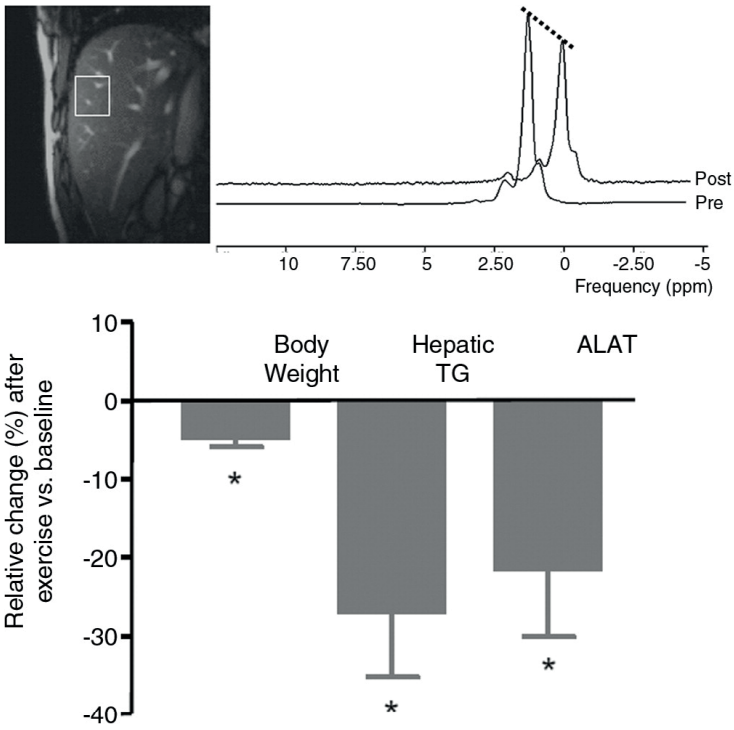

Figure 3. Top: Graph of placement of voxel for quantification of hepatic TG content and two representative proton MR spectra before and after exercise in one patient. A water-suppressed spectrum for TG signal resonances and a spectrum without water suppression as internal standard were obtained. Box in the image represents the voxel placed in the liver to assess the MR spectra. Imaging parameters were 3000/26. Bottom: Box and whisker plot shows relative changes in body weight, hepatic TG content, and alanine aminotransferase (*ALAT*) after 6 months of exercise compared with baseline (12 patients; seven men, five women; mean age, 46 years ± 2). * = $P < 0.05$ change after exercise compared with baseline.

Epicardial and paracardial fat quantification

The heart was examined by using gated ECG breath holds with a multi-shot turbo spin-echo sequence in a four-chamber view orientation (**Figure 2**). Water was suppressed by using spectral inversion recovery. Imaging parameters were ≥ 1000/8.6; flip angle, 90°; section thickness, 4 mm; 251 × 256 matrix. Contours were drawn around the epicardial and paracardial fat that surrounded the ventricles and atria by using software (MASS; Medis Medical Imaging Systems). The number of pixels was converted to square centimeters and multiplied by the section thickness to obtain volume.

Proton MR spectroscopy of myocardial and hepatic TG content

1.5 Tesla hydrogen-proton MR spectroscopy (Gyroscan ACS-NT 15; Philips Medical Systems, Best, the Netherlands) was used to quantify myocardial and hepatic TG content (**Figures**

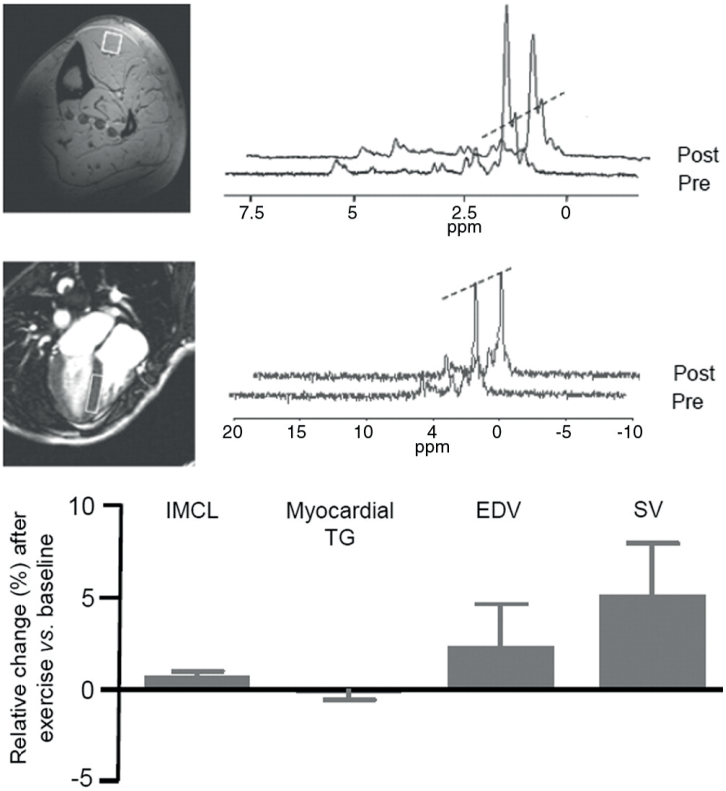

Figure 4. Top: Image of voxel placement for quantification of IMCLs in left anterior tibialis muscle and myocardial TG content in the cardiac septum. The box in the top image represents the placement of the voxel for myocardial assessment of MR spectra. Graph represents two representative proton MR spectra for IMCLs and myocardial TG content before and after exercise in one patient. Dotted line compares both spectral peaks; they are similar before and after training. For the myocardial TG content, a water-suppressed spectrum for TG signal resonances and a spectrum without water suppression for the internal standard were obtained. Myocardial TG content imaging parameters were 3000/26. IMCL imaging parameters were 2000/22. Bottom: Box and whisker plot of relative changes in IMCLs, myocardial TG content, end-diastolic volume (*EDV*), and stroke volume (*SV*) after 6 months of exercise compared with baseline (12 patients; seven men, five women; mean age, 46 years ± 2). No statistically significant changes were observed.

3 and 4)[8, 14]. Myocardial and hepatic hydrogen-proton single-voxel MR spectroscopic data were acquired by using a point-resolved spectroscopy sequence. One voxel was placed in the liver and myocardial interventricular septum. ECG triggering and respiratory pencil-beam navigators were used during acquisition[14]. A water-suppressed spectrum for TG signal resonances and a spectrum without water suppression (for internal standard) were obtained. Repetition time (ms) and echo time (ms) were ≥ 3000 and 26. For the water-suppressed spectrum, 1024 data points were obtained and averaged over 128 acquisitions, with a 1000-Hz spectral width. For the nonsuppressed spectrum, repetition time was 10000

ms and only four signal averages were acquired. MR user interface software (jMRUI version 2.2; MRUI, Leuven, Belgium), with prior knowledge files, was used to fit the spectra as previously described[15]. The TG content was calculated as (amplitude of TG signal / amplitude of water signal) × 100.

Proton MR spectroscopy of intramyocellular lipid content

Localized hydrogen-proton MR spectroscopy was performed in the left tibialis anterior muscle with a 7 Tesla whole-body imaging system (Philips Achieva; Philips Healthcare, Best, the Netherlands) to ensure optimal separation of intramyocellular lipid (IMCL) and extramyocellular lipid signals by using a stimulated echo acquisition mode sequence with variable pulse power and optimized relaxation delays water suppression with the following parameters: 2000/22; mixing time, 28 ms; voxel size, 10 × 10 × 10 mm. Unsuppressed water spectra were recorded with the same parameters. The voxel was placed in the muscle on transverse and sagittal T1-weighted images of the lower leg by avoiding vascular structures, tendon plates, and visible fat (**Figure 4**). Software (jMRUI version 2.2; MRUI) was used for postprocessing. Signals were fitted for creatine, trimethylammonium, lipids at 2.4 ppm, and six resonances for IMCL and extramyocellular lipid (around 2.2 ppm, 2 ppm, 1.45 ppm, 1.3 ppm, 1.1 ppm, and 0.8 ppm). The average separation between CH_2 of IMCL and extramyocellular lipid was 0.22 ppm ± 0.03. All values were corrected for T2 relaxation times (IMCL, 80 ms; water, 30 ms). Ratios of the CH_2 resonance of IMCL at 1.3 ppm were calculated relative to the water peak. Acquisition and postprocessing of the spectra at 7 Tesla were performed by R.L.W., H.E.K., and A.G.W. (4, 12, and 12 years of experience, respectively, in spectroscopy).

Left ventricular cardiac function

The heart was imaged from apex to base during breath holds in short-axis view with a sensitivity-encoded balanced steady-state free precession sequence. Imaging parameters were 3.4/1.7; flip angle, 35°; field of view, 400 mm^2; section thickness, 10 mm with a 0-mm gap; 256 × 256 matrix. To assess systolic function, epicardial and endocardial contours were manually drawn with software (MASS; Medis Medical Systems)[9, 16]. Left ventricular (LV) end-diastolic and end-systolic volume, ejection fraction, cardiac output, and LV mass were determined as measures of systolic function. For assessment of LV diastolic function, transmitral flow was measured by using ECG-gated gradient-echo sequence with a velocity sensitivity of 100 cm/s. Imaging parameters were 14/4.8; flip angle, 20°; field of view, 350 mm^2; section thickness, 8 mm; 256 × 256 matrix. Analytic software (FLOW; Medis Medical Systems) was used to create velocity versus time curves and to assess the peak velocity of the early diastole and atrial contraction. The peak deceleration gradient of early diastole, the early diastole-atrial contraction peak ratio, and LV filling pressures were determined[17].

Assays

Serum C-peptide was measured with an automated immunoluminometric assay on an analyzer (Immulite 2500; Siemens Diagnostics, Breda, the Netherlands). Glycated hemoglobin values were measured with a semiautomated high-performance liquid chromatography machine (Primus Ultra 2; Ordia, Leiden, the Netherlands). Serum aspartate aminotransferase, alanine aminotransferase, γ-glutamyltransferase, cholesterol, and TGs were measured by using a chemistry analyzer (Modular P800; Roche Diagnostics, Mannheim, Germany).

Statistical analysis

All statistical analyses were performed by using statistical software (SPSS 17.0; SPSS, Chicago, Ill). Nonnormally distributed data were log transformed and checked for normality after transformation. We used two-tailed paired *t* tests to compare the two study conditions. A two-tailed *P* value of 0.05 or less indicated statistical significance. Data are mean values ± standard error.

RESULTS

Clinical and biochemical characteristics

Table 1 shows the baseline characteristics. Mean energy expenditure increased from 2965 kCal/day ± 111 at day 0 to 3439 kCal/day ± 152 at day 192 ($P < 0.01$). Maximum oxygen uptake increased from 33.0 mL/kg/min ± 2.2 at beginning of training to 36.1 mL/kg/min ± 2.3 at 180 days after start of training ($P < 0.01$) (**Figure 1**). Exercise intensity did not differ significantly during the study period ($P = 0.96$); however, mean daily exercise duration increased substantially during the trekking expedition compared with the training period (138 min/day ± 43 vs. 291 min/day ± 63; $P < 0.001$). At the start of training, seven patients used metformin, three patients used a sulfonyl ureum derivate, three patients used insulin, and one patient used a dipeptidyl peptidase IV inhibitor. During the training period and before the expedition, one patient stopped using the sulfonyl ureum derivate. Self-reported caloric intake did not change during the exercise period ($P = 0.22$), nor did the composition of the diet over the exercise period. Body mass index decreased from 28.7 kg/m^2 ± 1.2 at the start of training to 27.3 kg/m^2 ± 1.1 at 200 days after the start of training ($P < 0.001$). No significant changes in plasma γ-glutamyltransferase ($P = 0.8$), aspartate aminotransferase ($P = 0.2$), glycated hemoglobin ($P = 0.5$), or C-peptide levels ($P = 0.8$) occurred (**Table 1**). Cholesterol ($P = 0.3$), high-density lipoprotein (HDL; $P = 0.4$), and TG concentrations ($P = 0.8$) did not change during the training period, but there was a decrease in the cholesterol-to-HDL ratio (3.9 ± 0.4 at the start of training to 3.3 ± 0.3 at 200 days after the start of training ($P = 0.01$) (**Table 1**). There was a significant decrease in alanine aminotransferase from 32.8 U/L ± 2.5 at the start of training to 25.6 U/L ± 3.1 at 200 days after the start of training ($P = 0.04$).

Table 1. Clinical and biochemical characteristics before and after 6 months of exercise in 12 patients with type 2 diabetes mellitus

Parameter	Baseline (start of training)	After exercise (200 days after start of training)
Weight (kg)	88.0 ± 3.9	83.7 ± 3.4*
Body mass index (kg/m^2)	28.7 ± 1.2	27.3 ± 1.1*
GGT (U/L)	35.1 ± 7.1	34.1 ± 5.5
ASAT (U/L)	29.8 ± 2.9	24.8 ± 4.0
ALAT (U/L)	32.8 ± 2.5	25.6 ± 3.1*
Glucose (mmol/L)	7.5 ± 1.0	7.0 ± 0.7
HbA_{1c} (%)	6.7 ± 0.3	6.5 ± 0.3
C-peptide (nmol/L)	0.8 ± 0.1	0.8 ± 0.2
Cholesterol (mmol/L)	4.8 ± 0.3	4.6 ± 0.3
HDL (mmol/L)	1.5 ± 0.2	1.5 ± 0.1
Cholesterol/HDL ratio	3.9 ± 0.4	3.3 ± 0.3*
LDL (mmol/L)	2.8 ± 0.3	2.7 ± 0.3
TGs (mmol/L)	1.5 ± 0.2	1.5 ± 0.2

Patient cohort was seven men, five women; age, 46 years ± 2; diabetes duration, 6.1 years ± 1.4; height, 1.75 m ± 0.02. Data are mean ± standard error. ALAT = alanine aminotransferase, ASAT = aspartate aminotransferase, GGT = γ-glutamyltransferase, HbA_{1c} = glycated hemoglobin, HDL = high-density lipoprotein.
* $P < 0.05$ after exercise compared with baseline.

Table 2. Fat compartments at baseline and after 6 months of exercise in 12 patients with type 2 diabetes mellitus

Fat compartments	Baseline (start of training)	After exercise (200 days after start of training)
Visceral abdominal fat (mL)	348 ± 57	219 ± 33*
Subcutaneous abdominal fat (mL)	699 ± 71	704 ± 74
Ratio visceral/subcutaneous fat	0.53 ± 0.11	0.34 ± 0.06*
Epicardial fat (mL)	4.7 ± 0.4	4.7 ± 0.4
Paracardial fat (mL)	4.6 ± 0.9	3.7 ± 0.8*
Hepatic TG content (%)	6.8 ± 2.3	4.6 ± 1.6*
Myocardial TG content (%)	0.61 ± 0.13	0.60 ± 0.13
IMCL/H_2O (%)	0.58 ± 0.12	0.68 ± 0.11

Data are mean ± standard error. IMCL/H_2O = ratio of IMCL and water in left tibialis anterior muscle.
* $P < 0.05$ after exercise compared with baseline.

Fat compartments

Visceral abdominal fat volume significantly decreased from 348 mL ± 57 at the start of training to 219 mL ± 33 at 200 days after the start of training ($P < 0.01$) (**Table 2**). Subcutaneous abdominal fat volume (**Table 2**) remained unchanged in terms of statistical significance ($P = 0.9$). Accordingly, the ratio between visceral and subcutaneous fat decreased significantly

Table 3. Hemodynamics and cardiac function at baseline and after 6 months of exercise in 12 patients with type 2 diabetes mellitus

Parameter	Baseline (start of training)	After exercise (200 days after start of training)
Hemodynamics		
Systolic blood pressure (mmHg)	142 ± 7	142 ± 7
Diastolic blood pressure (mmHg)	87 ± 4	83 ± 4
Heart rate (per minute)	71 ± 2	68 ± 2
Cardiac dimensions and function		
LV mass (g)	103 ± 8	107 ± 9
LV mass index (g/m^2)	50 ± 3	53 ± 4
LV end-diastolic volume (mL)	176 ± 9	179 ± 9
LV end-systolic volume (mL)	77 ± 4	76 ± 4
LV stroke volume (mL)	99 ± 5	103 ± 5
Ejection fraction (%)	56 ± 1	58 ± 1
Cardiac index (L/min/m^2)	3.1 ± 0.1	3.1 ± 0.1
E/A peak flow	1.45 ± 0.16	1.31 ± 0.11
E deceleration peak (mL/s^2 x 10^{-3})	3.9 ± 4.3	3.9 ± 3.4
E/Ea	10.8 ± 0.64	11.4 ± 0.71

Data are mean ± standard error. A = diastolic atrial contraction, E = early diastolic filling phase, E/Ea = estimate of LV filling pressure.

from 0.53 ± 0.11 at the start of training to 0.34 ± 0.06 at 200 days after the start of training ($P < 0.01$). Due to motion artifacts, the epicardial and paracardial fat of one patient could not be measured. Exercise reduced the paracardial fat volume from 4.6 mL ± 0.9 to 3.7 mL ± 0.8 in 11 patients ($P = 0.02$), and the hepatic TG content was reduced from 6.8% ± 2.3 at baseline to 4.6% ± 1.6 after the expedition ($P < 0.01$). Exercise did not affect myocardial TG content ($P = 0.9$), IMCL ($P = 0.3$), or epicardial fat volume ($P = 0.9$, **Table 2**).

No significant correlation was found between the decrease in weight and the decrease in visceral abdominal fat ($P = 0.5$), paracardial fat ($P = 0.3$), or hepatic TG content ($P = 0.9$).

The relative changes in the previously mentioned fat compartments are depicted in **Figures 2, 3, and 4**.

Myocardial function

Systolic and diastolic blood pressure, heart rate, LV mass, and diastolic function (early diastole- atrial contraction peak flow and early diastole deceleration peak) remained unchanged (**Table 3**). Ejection fraction (56% ± 1 at the start of training to 58% ± 1 at 200 days after the start of training; $P = .06$), cardiac output, and cardiac index did not change.

DISCUSSION

Our study took place in a real-life setting and was composed of a 6-month training period of moderate-intensity exercise followed by a trekking expedition with prolonged moderate-intensity exercise. This caused a greater than 20% decrease in visceral fat, hepatic TG content, and paracardial fat in patients with type 2 diabetes mellitus, but we did not observe changes in subcutaneous abdominal fat, myocardial or intramyocellular TG content, epicardial fat volume, or cardiac function.

Epicardial and paracardial fat

Because epicardial fat and visceral abdominal fat were cross-sectionally correlated[10, 11], we hypothesized that both fat compartments would be similarly affected by exercise.

Interestingly, our 6-month exercise program decreased visceral abdominal fat and paracardial fat but did not change epicardial fat volume in patients with type 2 diabetes mellitus. Recent studies[18, 19] have shown that paracardial fat volume is a better predictor of cardiovascular risk than epicardial fat, and therefore a decrease in paracardial fat might indicate a decreased cardiovascular risk. Kim et al[20] found a significant reduction in epicardial fat in obese men after a 12-week exercise program, and the change in epicardial fat correlated with the change in visceral fat. One study[21] in pigs showed that the epicardial fat around the coronary arteries and the epicardial fat around the myocardium respond differently with respect to the expression of inflammatory genes.

Therefore, epicardial fat may show regional differences in its response to exercise. Interestingly, Sicari et al[18] found a cross-sectional correlation between visceral and paracardial fat but not epicardial fat volumes. Apparently, exercise in patients with type 2 diabetes mellitus has a disparate effect on visceral and epicardial adipose tissue, which resulted in a decrease in visceral and paracardial fat without a change in epicardial fat in our study.

Hepatic TG content

At baseline, patients had a mean hepatic TG content of 6.8%. Hepatic steatosis is defined as TG content greater than 5.6% measured with hydrogen-proton MR spectroscopy[22]. We found that exercise decreased hepatic TG content by 26% in patients with type 2 diabetes mellitus, thereby reducing their hepatic TG content to normal values. This decrease was accompanied by a decrease in alanine aminotransferase. Previous studies reported on the effects of exercise on hepatic TG content, but only in patients without diabetes[23].

To our knowledge, the exact mechanism behind the exercise-induced reduction in hepatic TG content is not clear. Although patients in our study lost some weight, we found no significant correlation between changes in body weight and changes in hepatic TG content. The decrease in hepatic TG content may be due to a diminished flow of free fatty acids from

the visceral adipose tissue, in accordance with the portal hypothesis[24]. However, reduction in hepatic TG content has also been described without a reduction in visceral fat[25].

Our results indicated that the liver is not a passive bystander that adapts to changes in fatty acid metabolism. Rector et al[26] showed that sudden cessation of daily physical activity in hyperphagic or obese rats resulted in stimulation of biochemical pathways known to initiate hepatic steatosis, including decreased hepatic mitochondrial oxidative capacity, increased hepatic expression of de novo lipogenesis proteins, and increased levels of hepatic malonyl-coenzyme A.

IMCLs and myocardial TG content

Data regarding the effects of exercise on IMCL content in insulin-resistant patients are inconsistent. A 16-week moderate-intensity exercise program in obese insulin-resistant patients increased IMCL[27]; however, two studies of 10-12 weeks of exercise in overweight men and patients with type 2 diabetes mellitus found no change in IMCL[28, 29]. We found no effect of a 6-month exercise program on IMCL.

To our knowledge, only two studies have examined the effects of exercise on myocardial TG content. Twelve weeks of exercise decreased myocardial TG content in healthy obese patients[30], but it did not decrease myocardial TG content in patients with type 2 diabetes mellitus[31]. Our study confirms and extends the latter result.

Previously, an association was found between myocardial TG content and diastolic cardiac function[8, 32]. In our study, exercise did not change myocardial TG content, and we found no change in systolic or diastolic function. Similarly, 1 year of training in patients with type 2 diabetes mellitus[33] and 12 weeks of training in patients who were overweight[30] showed no significant changes in myocardial function; however, in the latter study, ejection fraction increased by 2%.

The major limitation of our study is the small number of patients. Patients acted as their own control. Despite this small patient number, our data show statistically significant changes in fat distribution with exercise. Secondly, diet could have varied between patients; we did not control for this. Finally, there were interindividual differences in the exercise duration and intensity during the training and trekking expedition.

Though exercise intensity did not differ during the study, mean exercise duration increased substantially during the trekking expedition compared with the training period. Furthermore, factors related to altitude, such as hypoxia, may have influenced the results. Many studies that examine the dynamics of ectopic fat accumulation focus on the effects of diet or combined diet and exercise on weight loss in relation to changes in imaging parameters. In our study, patients did lose some weight without specifically attempting to diet. Therefore, we assume that their weight loss was achieved only by training.

In conclusion, a 6-month exercise training regimen, without changes in diet, decreased hepatic TG content and visceral abdominal and paracardial fat volume in patients with type

2 diabetes mellitus. These fat compartments are all associated with increased cardiovascular risk. Subcutaneous fat, epicardial fat, and intramyocellular and myocardial TG content did not change. Therefore, our study demonstrated tissue-specific exercise-induced changes in body fat distribution in patients with type 2 diabetes mellitus.

REFERENCES

1. Colberg SR, Sigal RJ, Fernhall B, Regensteiner JG, Blissmer BJ, Rubin RR, Chasan-Taber L, Albright AL, Braun B. Exercise and type 2 diabetes: the American College of Sports Medicine and the American Diabetes Association: joint position statement executive summary. *Diabetes Care* 2010;33:2692-2696.
2. McGavock JM, Victor RG, Unger RH, Szczepaniak LS. Adiposity of the heart, revisited. *Ann Intern Med* 2006;144:517-524.
3. Krssak M, Falk PK, Dresner A, DiPietro L, Vogel SM, Rothman DL, Roden M, Shulman GI. Intramyocellular lipid concentrations are correlated with insulin sensitivity in humans: a 1H NMR spectroscopy study. *Diabetologia* 1999;42:113-116.
4. Perseghin G, Scifo P, De Cobelli F, Pagliato E, Battezzati A, Arcelloni C, Vanzulli A, Testolin G, Pozza G, Del Maschio A, Luzi L. Intramyocellular triglyceride content is a determinant of in vivo insulin resistance in humans: a 1H-13C nuclear magnetic resonance spectroscopy assessment in offspring of type 2 diabetic parents. *Diabetes* 1999;48:1600-1606.
5. Samuel VT, Liu ZX, Qu X, Elder BD, Bilz S, Befroy D, Romanelli AJ, Shulman GI. Mechanism of hepatic insulin resistance in non-alcoholic fatty liver disease. *J Biol Chem* 2004;279:32345-32353.
6. Greif M, Becker A, von Ziegler F, Lebherz C, Lehrke M, Broedl UC, Tittus J, Parhofer K, Becker C, Reiser M, Knez A, Leber AW. Pericardial adipose tissue determined by dual source CT is a risk factor for coronary atherosclerosis. *Arterioscler Thromb Vasc Biol* 2009;29:781-786.
7. Wong VW, Wong GL, Yip GW, Lo AO, Limquiaco J, Chu WC, Chim AM, Yu CM, Yu J, Chan FK, Sung JJ, Chan HL. Coronary artery disease and cardiovascular outcomes in patients with non-alcoholic fatty liver disease. *Gut* 2011;60:1721-1727.
8. Hammer S, van der Meer RW, Lamb HJ, de Boer HH, Bax JJ, de Roos A, Romijn JA, Smit JW. Short-term flexibility of myocardial triglycerides and diastolic function in patients with type 2 diabetes mellitus. *Am J Physiol Endocrinol Metab* 2008;295:E714-718.
9. van der Meer RW, Hammer S, Smit JW, Frölich M, Bax JJ, Diamant M, Rijzewijk LJ, de Roos A, Romijn JA, Lamb HJ. Short-term caloric restriction induces accumulation of myocardial triglycerides and decreases left ventricular diastolic function in healthy subjects. *Diabetes* 2007;56:2849-2853.
10. Iacobellis G, Ribaudo MC, Assael F, Vecci E, Tiberti C, Zappaterreno A, Di Mario U, Leonetti F. Echocardiographic epicardial adipose tissue is related to anthropometric and clinical parameters of metabolic syndrome: a new indicator of cardiovascular risk. *J Clin Endocrinol Metab* 2003;88:5163-5168.
11. Ahn SG, Lim HS, Joe DY, Kang SJ, Choi BJ, Choi SY, Yoon MH, Hwang GS, Tahk SJ, Shin JH. Relationship of epicardial adipose tissue by echocardiography to coronary artery disease. *Heart* 2008;94:e7.
12. Berntsen S, Hageberg R, Aandstad A, Mowinckel P, Anderssen SA, Carlsen KH, Andersen LB. Validity of physical activity monitors in adults participating in free-living activities. *Br J Sports Med* 2010;44:657-664.
13. Storer TW, Davis JA, Caiozzo VJ. Accurate prediction of VO2max in cycle ergometry. *Med Sci Sports Exerc* 1990;22:704-712.
14. van der Meer RW, Doornbos J, Kozerke S, Schär M, Bax JJ, Hammer S, Smit JW, Romijn JA, Diamant M, Rijzewijk LJ, de Roos A, Lamb HJ. Metabolic imaging of myocardial triglyceride content: reproducibility of 1H MR spectroscopy with respiratory navigator gating in volunteers. *Radiology* 2007;245:251-257.
15. Vanhamme L, van den Boogaart A, van Huffel S. Improved method for accurate and efficient quantification of MRS data with use of prior knowledge. *J Magn Reson* 1997;129:35-43.
16. Pattynama PM, Lamb HJ, van der Velde EA, van der Wall EE, de Roos A. Left ventricular measurements with cine and spin-echo

MR imaging: a study of reproducibility with variance component analysis. *Radiology* 1993;187:261-268.

17. Paelinck BP, de Roos A, Bax JJ, Bosmans JM, van der Geest RJ, Dhondt D, Parizel PM, Vrints CJ, Lamb HJ. Feasibility of tissue magnetic resonance imaging: a pilot study in comparison with tissue Doppler imaging and invasive measurement. *J Am Coll Cardiol* 2005;45:1109-1116.
18. Sicari R, Sironi AM, Petz R, Frassi F, Chubuchny V, De Marchi D, Positano V, Lombardi M, Picano E, Gastaldelli A. Pericardial rather than epicardial fat is a cardiometabolic risk marker: an MRI vs echo study. *J Am Soc Echocardiogr* 2011;24:1156-1162.
19. Thanassoulis G, Massaro JM, Hoffmann U, Mahabadi AA, Vasan RS, O'Donnell CJ, Fox CS. Prevalence, distribution, and risk factor correlates of high pericardial and intrathoracic fat depots in the Framingham heart study. *Circ Cardiovasc Imaging* 2010;3:559-566.
20. Kim MK, Tomita T, Kim MJ, Sasai H, Maeda S, Tanaka K. Aerobic exercise training reduces epicardial fat in obese men. *J Appl Physiol* 2009;106:5-11.
21. Company JM, Booth FW, Laughlin MH, Arce-Esquivel AA, Sacks HS, Bahouth SW, Fain JN. Epicardial fat gene expression after aerobic exercise training in pigs with coronary atherosclerosis: relationship to visceral and subcutaneous fat. *J Appl Physiol (1985)* 2010;109:1904-1912.
22. Szczepaniak LS, Nurenberg P, Leonard D, Browning JD, Reingold JS, Grundy S, Hobbs HH, Dobbins RL. Magnetic resonance spectroscopy to measure hepatic triglyceride content: prevalence of hepatic steatosis in the general population. *Am J Physiol Endocrinol Metab* 2005;288:E462-468.
23. Johnson NA, Sachinwalla T, Walton DW, Smith K, Armstrong A, Thompson MW, George J. Aerobic exercise training reduces hepatic and visceral lipids in obese individuals without weight loss. *Hepatology* 2009;50:1105-1112.
24. O'Leary VB, Marchetti CM, Krishnan RK, Stetzer BP, Gonzalez F, Kirwan JP. Exercise-induced reversal of insulin resistance in obese elderly is associated with reduced visceral fat. *J Appl Physiol* 2006;100:1584-1589.
25. Magkos F. Exercise and fat accumulation in the human liver. *Curr Opin Lipidol* 2010;21:507-517.
26. Rector RS, Uptergrove GM, Morris EM, Borengasser SJ, Laughlin MH, Booth FW, Thyfault JP, Ibdah JA. Daily exercise vs. caloric restriction for prevention of nonalcoholic fatty liver disease in the OLETF rat model. *Am J Physiol Gastrointest Liver Physiol* 2011;300:G874-883.
27. Dube JJ, Amati F, Stefanovic-Racic M, Toledo FG, Sauers SE, Goodpaster BH. Exercise-induced alterations in intramyocellular lipids and insulin resistance: the athlete's paradox revisited. *Am J Physiol Endocrinol Metab* 2008;294:E882-888.
28. Gan SK, Kriketos AD, Ellis BA, Thompson CH, Kraegen EW, Chisholm DJ. Changes in aerobic capacity and visceral fat but not myocyte lipid levels predict increased insulin action after exercise in overweight and obese men. *Diabetes Care* 2003;26:1706-1713.
29. Meex RC, Schrauwen-Hinderling VB, Moonen-Kornips E, Schaart G, Mensink M, Phielix E, van de Weijer T, Sels JP, Schrauwen P, Hesselink MK. Restoration of muscle mitochondrial function and metabolic flexibility in type 2 diabetes by exercise training is paralleled by increased myocellular fat storage and improved insulin sensitivity. *Diabetes* 2010;59:572-579.
30. Schrauwen-Hinderling VB, Hesselink MK, Meex R, van der Made S, Schär M, Lamb HJ, Wildberger JE, Glatz J, Snoep G, Kooi ME, Schrauwen P. Improved ejection fraction after exercise training in obesity is accompanied by reduced cardiac lipid content. *J Clin Endocrinol Metab* 2010;95:1932-1938.
31. Schrauwen-Hinderling VB, Meex RC, Hesselink MK, van de Weijer T, Leiner T, Schär M, Lamb HJ, Wildberger JE, Glatz JF, Schrauwen P, Kooi ME. Cardiac lipid content is unresponsive to a physical activity training intervention in type

2 diabetic patients, despite improved ejection fraction. *Cardiovasc Diabetol* 2011;10:47.

32. Hammer S, Snel M, Lamb HJ, Jazet IM, van der Meer RW, Pijl H, Meinders EA, Romijn JA, de Roos A, Smit JW. Prolonged caloric restriction in obese patients with type 2 diabetes mellitus decreases myocardial triglyceride content and improves myocardial function. *J Am Coll Cardiol* 2008;52:1006-1012.

33. Hordern MD, Coombes JS, Cooney LM, Jeffriess L, Prins JB, Marwick TH. Effects of exercise intervention on myocardial function in type 2 diabetes. *Heart* 2009;95:1343-1349.

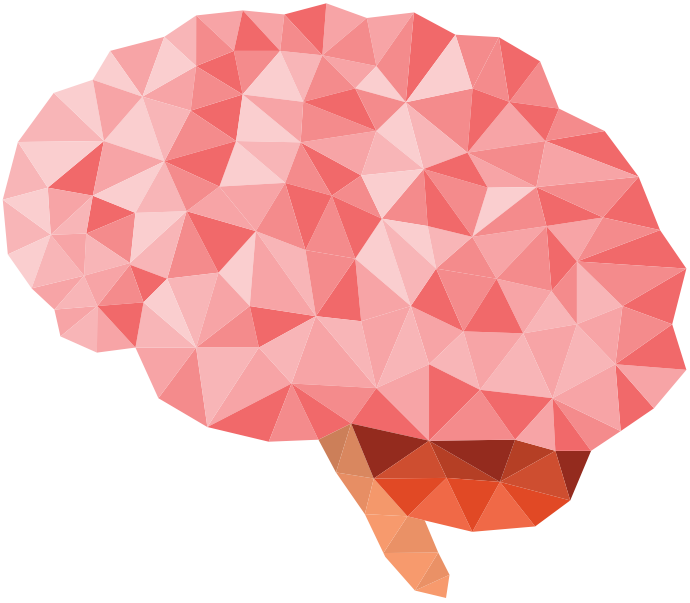

PART 2

BRAIN

Chapter 7

Short-term caloric restriction normalizes hypothalamic neuronal responsiveness to glucose ingestion in patients with type 2 diabetes

Ralph L. Widya
Wouter M. Teeuwisse
Marit Paulides
Hildo J. Lamb
Johannes W.A. Smit
Albert de Roos
Mark A. van Buchem
Hanno Pijl
Jeroen van der Grond

Diabetes 2012;61(12):3255-3259

ABSTRACT

Background

The hypothalamus is critically involved in the regulation of feeding. Previous studies have shown that glucose ingestion inhibits hypothalamic neuronal activity. However, this was not observed in patients with type 2 diabetes. Restoring energy balance by reducing caloric intake and losing weight are important therapeutic strategies in patients with type 2 diabetes. We hypothesized that caloric restriction would have beneficial effects on the hypothalamic neuronal response to glucose ingestion.

Methods

Functional magnetic resonance imaging was performed in 10 male type 2 diabetic patients before and after a 4-day very low-calorie diet (VLCD) at a 3.0 Tesla scanner using a blood oxygen level-dependent technique for measuring neuronal activity in the hypothalamus in response to an oral glucose load. Hypothalamic signals were normalized to baseline value, and differences between the pre- and postdiet condition were tested using paired *t* tests.

Results

Pre-VLCD scans showed no response of the hypothalamus to glucose intake (i.e., no signal decrease after glucose intake was observed). Post-VLCD scans showed a prolonged signal decrease after glucose ingestion.

Conclusions

The results of the current study demonstrate that short-term caloric restriction readily normalizes hypothalamic responsiveness to glucose ingestion in patients with type 2 diabetes.

INTRODUCTION

The hypothalamus plays a key role in the regulation of feeding. It contains glucose-sensitive neurons that are stimulated by falling blood glucose levels and implicated in hypoglycemia-induced feeding[1]. Moreover, various hypothalamic neuronal circuits are involved in the control of glucose metabolism[2].

Blood oxygen level-dependent (BOLD) functional magnetic resonance imaging (fMRI) has been widely applied in spatiotemporal mapping of the human brain function and measuring neuronal activity. MRI contrast in BOLD measurements is based on the fact that the BOLD signal arises from local field inhomogeneities, caused by magnetic susceptibility differences between deoxyhemoglobin levels in the blood in capillaries and venous vessels and the surrounding tissue[3]. This phenomenon enables the possibility to determine local parts in the brain that are activated by an external trigger. The main advantage of BOLD fMRI is its noninvasive nature and local sensitivity combined with a good spatial resolution. Its main disadvantage refers to the nature of the BOLD signal: it is only an indirect measure of neural activity. Nevertheless, over the years, BOLD fMRI has shown to be a sensitive marker of brain activation. In this respect, it was shown that healthy lean volunteers demonstrated a significant dose-dependent decrease of the BOLD signal in the hypothalamus after glucose ingestion[4].

Type 2 diabetes is a disease of impaired glucose homeostasis and insulin action, with energy imbalance and anomalous fuel flux as metabolic hallmarks. It has been shown that the hypothalamic neuronal activity is altered in patients with type 2 diabetes, demonstrated by the absence of a BOLD signal decrease after glucose ingestion[5]. This finding may suggest that the hypothalamus in patients with type 2 diabetes inappropriately perceives and/or processes signals in response to a nutrient load, reflecting an abnormal perception of the current metabolic status.

Restoration of the energy balance by reduction of the caloric intake and subsequent weight loss are important therapeutic strategies in type 2 diabetes. In the current study, we hypothesized that caloric restriction normalizes the hypothalamic response to a nutrient load. Therefore, the purpose of the current study was to determine the effect of a very low-calorie diet (VLCD) on hypothalamic neuronal activity after glucose ingestion measured by BOLD fMRI.

METHODS

Subjects

We recruited 10 Caucasian men diagnosed with type 2 diabetes according to World Health Organization criteria. At intake, mean age was 56.8 ± 3.9 years, weight 89.6 ± 6.9 kg, and BMI 27.9 ± 1.6 kg/m^2. Diabetes duration was 3.7 ± 1.8 years, and HbA_{1c} was 5.9 ± 0.6%. Subjects' type 2 diabetes treatment consisted of metformin and/or a diet.

Main exclusion criteria were treatment with insulin or sulfonylurea derivatives, being on a weight-reducing diet already, weight changes of > 3 kg in the last 3 months, any type of chronic disease, smoking, and contraindications for MRI. The study protocol was approved by the local institutional review board, and written informed consent was obtained from every subject.

Design

Functional MRI was performed before and following a VLCD of 4 days. The VLCD comprised three liquid food shakes per day, containing a total of 450 kcal (Modifast Intensive; Nutrition & Santé Benelux n.v., Brussels, Belgium). The subjects were advised to drink at least 1.5 L of water per day.

To assure a craving status, subjects were asked to fast from 10 p.m. the night preceding each scan the next early morning. During fasting, no food or drinks were allowed, except water. Fasting glucose and insulin levels were determined to calculate insulin sensitivity according to the homeostasis model assessment parameter of insulin resistance (HOMA-IR), which is the product of the fasting serum insulin level (mU/L) and the plasma glucose level (mmol/L) divided by 22.5 [6].

Data acquisition

MRI was performed at our institution using a 3.0 Tesla Achieva clinical scanner (Philips Healthcare, Best, the Netherlands). The protocol comprised a scout view for planning two single-slice, midsagittal scans: a T1-weighted Turbo Spin Echo sequence for imaging anatomical structures (repetition time 550 ms, echo time 10 ms, field of view 208 × 208 mm, voxel size = 0.52 × 0.52 × 14 mm, scan time 1.15 min) and a T2*-weighted, gradient echo echo-planar imaging sequence that renders BOLD contrast, which is related to neuronal activity (repetition time 120 ms, echo time 30 ms, flip angle 30°, field of view 208 × 208 mm, voxel size = 0.81 × 0.90 × 14 mm, scan time 38.10 min, 900 time points). During this sequence, 300 mL water containing 75 g of glucose (standard glucose tolerance test solution) was ingested through a tube after 8.5 min. Scanning was continued after complete ingestion of the glucose solution. Slice thickness of 14 mm was chosen to encompass the hypothalamus in the left to right direction, the single-slice technique for sufficient signal-to-noise ratio.

Functional MRI data analysis

Each of the 900 modulus images was registered to the image that was acquired halfway the scan by means of Multimodality Image Registration using Information Theory by maximization of mutual information[7]. The resulting registration matrix was then applied to the real and imaginary images that were calculated from the original modulus and phase images. To reduce phase artifacts caused by swallowing or head motion, complex data were averaged for each set of four subsequent volumes, and finally modulus images were recalculated,

rendering 225 images that were corrected for movement and phase errors. The T1 scan was also registered to the functional scan, using the same algorithm and reference image.

The hypothalamus was segmented manually, using the anatomical image as an aid to delineate anatomical borders. Subdivision of the hypothalamus into four regions of interest (ROIs) was performed according to Matsuda et al[8]. As a reference, an ROI was drawn in gray matter, superior of the genu of the corpus callosum. For each ROI, the mean signal for each time point was established, and its baseline signal was calculated (i.e., the signal averaged over all measurements up to 0.5 min before drinking of the glucose solution started). Subsequently, measurements were then normalized to the baseline value, yielding the signal change relative to baseline. To correct for scanner drift, the signal in the reference ROI was subtracted from that in the hypothalamus ROIs.

Statistical analysis

For each time point, normalized hypothalamic signal was averaged for all subjects, and data were pooled in 2-min time slots. Subsequently, differences between pre- and post-diet condition were tested by a paired *t* test for each time slot after baseline (i.e., for all 15 time slots from the moment drinking was started). Because we performed 15 *t* tests, a Bonferroni-corrected threshold of $P < 0.0033$ (= 0.05/15) was applied to correct for multiple comparisons. This method is comparable to differential regression analysis[9].

Data are expressed as mean ± SD for demographic and biochemical characteristics and as mean percentage ± SEM for BOLD signal change.

RESULTS

The VLCD was generally well tolerated and induced a mean body weight loss of 3.0 ± 1.4 kg. Consequently, weight and BMI decreased to 86.6 ± 6.7 kg ($P < 0.001$) and 26.9 ± 1.5 kg/m^2 ($P < 0.001$), respectively, after the VLCD. HOMA-IR decreased from 2.3 ± 1.1 to 1.1 ± 0.7 ($P = 0.007$) (**Table 1**).

Table 1. Patient characteristics

	pre-VLCD	post-VLCD	*P* value
Age (years)	56.8 ± 3.9	NA	NA
Weight (kg)	89.6 ± 6.9	86.6 ± 6.7	< 0.001*
BMI (kg/m^2)	27.8 ± 1.6	26.9 ± 1.5	< 0.001*
Duration of diabetes (years)	3.7 ± 1.8	NA	NA
HbA_{1c} (%)	5.9 ± 0.6	NA	NA
HOMA-IR	2.3 ± 1.1	1.1 ± 0.7	0.007*

Patient characteristics before and after the 4-day VLCD. Values are mean ± SD. NA = not applicable.
* $P < 0.05$.

Table 2. Biochemical characteristics

	Pre-VLCD		Post-VLCD		*P* value pre-VLCD vs. post-VLCD	
	After 10-h fast	After oral glucose	After 10-h fast	After oral glucose	After 10-h fast	After oral glucose
Insulin (mU/L)	8.8 ± 4.4	25.3 ± 7.8	4.8 ± 3.2	19.2 ± 8.8	0.013*	0.096
Glucose (mmol/L)	6.4 ± 1.3	9.5 ± 2.2	5.3 ± 1.0	8.2 ± 2.0	0.010*	0.009*
Triglycerides (mmol/L)	2.5 ± 2.8	2.3 ± 2.4	1.6 ± 0.9	1.5 ± 0.8	0.214	0.159
Total cholesterol (mmol/L)	4.2 ± 0.9	4.1 ± 0.7	4.2 ± 1.0	4.0 ± 1.1	0.820	0.757
HDL cholesterol (mmol/L)	1.1 ± 0.3	1.1 ± 0.3	1.1 ± 0.2	1.0 ± 0.2	0.208	0.058
Total cholesterol / HDL ratio	4.1 ± 1.3	3.9 ± 1.2	4.2 ± 1.5	4.2 ± 1.4	0.599	0.189

Biochemical characteristics before and after the 4-day VLCD. Values are mean ± SD. Measurements after 10-h fast were performed preceding the MRI scan. Blood serum levels after oral glucose were acquired following the MRI scan ~30 minutes after glucose ingestion.
* $P < 0.05$.

After the VLCD, fasting serum insulin decreased from 8.8 ± 4.4 to 4.8 ± 3.2 mU/L ($P = 0.013$) and fasting plasma glucose decreased from 6.4 ± 1.3 to 5.3 ± 1.0 mmol/L ($P = 0.010$). Triglycerides, total cholesterol, HDL cholesterol, and the total cholesterol/HDL ratio did not change (**Table 2**). Glucose drinking duration was 3.26 ± 1.20 and 3.00 ± 0.53 min for the first and second visit, respectively ($P = 0.387$).

Figure 1 shows which anatomical landmarks were used for drawing ROIs and division of the hypothalamus into four subregions. **Figure 2** shows the percentage signal change from baseline value averaged for all subjects in the total hypothalamus and its quadrants for measurements before and after the VLCD. In all graphs, a signal drop was observed that was associated with movement of the head during drinking. Pre-VLCD scans showed no response of the hypothalamus to glucose intake (i.e., no signal decrease after glucose intake was observed). Post-VLCD scans showed a prolonged signal decrease after glucose ingestion. This effect was observed in all quadrants, but was most pronounced in the lower quadrants. A significant prolonged decrease in BOLD signal of 2 to 3% after glucose administration between pre- and post-VLCD in the total hypothalamus was observed from $t = 8$ min onwards ($P < 0.0033$) (**Figure 2**).

Glucose concentrations were lower after the VLCD and may have resulted in the observed BOLD signal decrease. Therefore, the relation between fasting blood glucose level and the BOLD effect was tested in both the pre-VLCD as well as in the post-VLCD condition using a multivariate linear model adjusted for age. No significant correlations were found ($P = 0.36$ and $P = 0.70$, respectively). In addition, no correlation was found between the difference in fasting blood glucose levels between the pre- and post-VLCD condition with the difference in corresponding BOLD signals ($P = 0.89$).

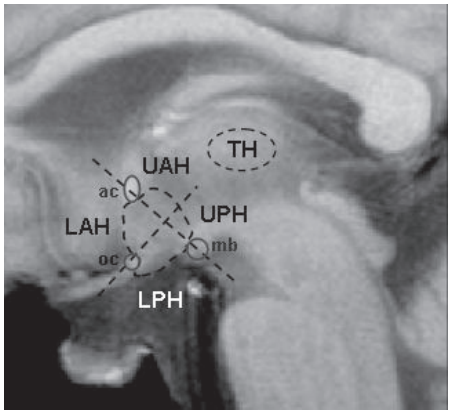

Figure 1. Anatomical landmarks used for drawing ROIs and division of the hypothalamus into subregions. ac = anterior commissure; LAH = lower anterior hypothalamus; LPH = lower posterior hypothalamus; mb = mammillary body; oc = optic chiasm; TH = thalamus; UAH = upper anterior hypothalamus; UPH = upper posterior hypothalamus.

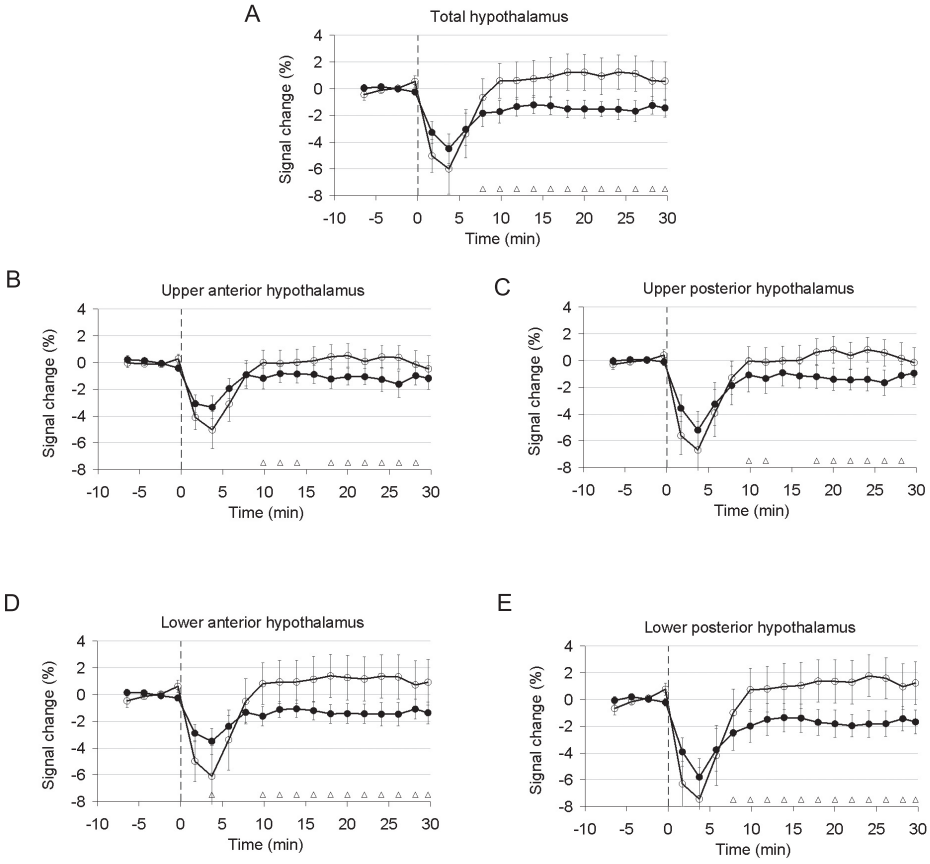

Figure 2. Relative fMRI signal in the total (*A*), upper anterior (*B*), upper posterior (*C*), lower anterior (*D*), and lower posterior (*E*) hypothalamus before and after VLCD. Signal is normalized to the preprandial signal, which is calculated as average over the first 8 min. Each circle corresponds with the average signal for 2 min in all subjects. The vertical dashed lines indicate the start of glucose ingestion. Error bars indicate ± 1 SEM. White circles = pre-VLCD; black circles = post-VLCD; white triangle = $P < 0.0033$.

DISCUSSION

We previously showed that glucose ingestion fails to inhibit hypothalamic neuronal activity in type 2 diabetic patients[5]. In this study, we demonstrate that after following a VLCD of 4 days, the hypothalamus responds to glucose ingestion with an order of magnitude similar to that in healthy subjects[4, 5]. We therefore suggest that short-term caloric restriction normalizes hypothalamic responsiveness to glucose ingestion in patients with type 2 diabetes.

The hypothalamus is critically involved in the feeding and metabolic regulatory system. Several hypothalamic nuclei, including the lateral hypothalamic area and the ventromedial hypothalamus, contain glucose-sensing neurons. These neurons communicate extensively with other appetite-regulating neuronal systems. A rise in glucose levels causes glucose-responsive neurons to increase their firing rate, whereas glucose-sensitive neurons decrease their firing rate[10, 11]. In addition, the hypothalamus contains myriad receptors responsive to neurotransmitters including dopamine, serotonin, histamine, γ-aminobutyric acid, and estrogen, which are involved in feeding behavior[11]. Furthermore, insulin and the adipocyte-derived hormone leptin signal the hypothalamus, resulting in reduced food intake[12].

Previous studies have shown a diminished hypothalamic neuronal activity after glucose ingestion in healthy subjects[4, 5, 13, 14]. High preprandial signal in the hypothalamus may be connected with a state of craving that subdues when the need for energy is met. Smeets et al[14] reported that glucose ingestion more effectively inhibited hypothalamic neuronal activity compared with intravenous glucose administration. Gastrointestinal signals and/or insulin are therefore very likely involved in the hypothalamic response to glucose intake[14]. Glucose ingestion triggers intestinal cells to release several hormones, including peptide YY, glucagon-like peptide-1, and oxyntomodulin into the circulation[15, 16]. These gut hormones signal food intake to the appetite-regulating circuits of the brain and act in the hypothalamus to induce satiety[17-19]. A functional neuroimaging study in rats showed that oxyntomodulin and glucagon-like peptide-1 inhibit neuronal activity in hypothalamic nuclei[20]. Furthermore, it has been shown that peptide YY facilitates insulin action[21].

In accordance with the findings of Vidarsdottir et al[5], glucose ingestion initially failed to reduce hypothalamic BOLD signals in our type 2 diabetic patients. Therefore, in subjects with type 2 diabetes, the hypothalamus appears to inappropriately perceive and/or process signals in response to a nutrient load. In addition, Matsuda et al[8] found attenuated hypothalamic fMRI signal inhibition in response to glucose ingestion in obese subjects with normal glucose tolerance compared with lean subjects, which was correlated with fasting plasma glucose and insulin concentration, and was independent of BMI.

Remarkably, after type 2 diabetic patients followed a 4-day VLCD, a normal BOLD signal pattern was observed after glucose ingestion (i.e., prolonged inhibition of neuronal activity). This BOLD signal pattern was comparable to those described in healthy male subjects[4, 5]. Apparently, the hypothalamus is capable to return to a normal responsive pattern following

a glucose load. It may be hypothesized that a caloric restriction recovers the sensitivity of glucose-sensitive neurons in type 2 diabetes. However, it must be noted that the magnitude of an increase in serum glucose does not increase the magnitude or duration of the decrease in hypothalamic activity[14]. Furthermore, fasting blood glucose levels were lower after the VLCD. Because no correlation was found between these glucose levels and the BOLD effect in both pre- and post-VLCD condition, it is unlikely that the lower fasting blood glucose level after the VLCD has resulted in the observed BOLD signal decrease.

More likely, insulin sensitivity may play a role. Caloric restriction has proven to be beneficial in type 2 diabetes for obtaining metabolic control[22] independent of body weight reduction[23]. Besides lowering the BMI, a 6-day VLCD improved peripheral insulin sensitivity in type 2 diabetic patients, measured by glucose disposal rate and HOMA-IR[24]. Our data also show that after a short-term VLCD, insulin sensitivity was improved, measured by HOMA-IR. Insulin signals the brain about the status of body fat stores. The arcuate nucleus, a key hypothalamic region involved in energy homeostasis, contains populations of neuropeptide Y and proopiomelanocortin neurons, which express insulin receptors. Insulin stimulates proopiomelanocortin resulting in reduced food intake and increased energy expenditure. Conversely, neuropeptide Y is inhibited by insulin, again resulting in reduced food intake[12]. Considering the afferent signaling of insulin to the arcuate nucleus, it may be possible that an improvement in insulin sensitivity after a VLCD is in part responsible for the normalization of hypothalamic responsiveness to glucose ingestion. Moreover, improved insulin sensitivity may also favor the hypothalamic response to gut hormones, because these hormones support insulin action[21].

Caloric restriction may also be a way to sensitize the hypothalamus to glucose ingestion in nondiabetic subjects. However, the intrinsic limitations of the BOLD phenomenon restrict this application. In the current study, we determined a VLCD BOLD effect up to 3% in patients with type 2 diabetes. Our current glucose-triggered BOLD response reaches levels that are comparable with healthy control subjects, also measured at a magnetic field strength of 3.0 Tesla[5]. At a field strength of 3.0 Tesla, a 3% change is about the theoretical maximal BOLD effect that can be determined using an echo time of 30 ms[25]. Although it cannot be excluded that a VLCD will have effect on the hypothalamus in nondiabetic subjects, an additional BOLD effect can hardly be measured because the normal response is already up to 3%.

We have chosen not to use water as an additional control reference because the intrinsic reference, or calibration, of our experiments is the BOLD signal before glucose administration (i.e., the BOLD signal in the first 8 min). Many experiments in both control subjects and subjects with diabetic type 2 have clearly shown that water on itself (no glucose) does not alter the BOLD response[4, 5, 8, 26]. For studying the effect of a VLCD in type 2 diabetes, the addition of water as control condition would only have very limited additional value.

Lifestyle intervention, including body weight reduction and reduced intake of total and saturated fat, can reduce the incidence of type 2 diabetes in people at risk and improve

health in type 2 diabetic patients[27, 28]. This study shows that the absence of a hypothalamic response to glucose intake in patients with type 2 diabetes can be reversed by a 4-day VLCD. As hypothalamic neuronal activity contributes to the control of postprandial metabolism, this may be one of the key factors that explain the strong metabolic improvement that can be observed in type 2 diabetic patients on caloric restriction. It must be noted that the fundamental mechanism behind the hypothalamic response to glucose ingestion is yet unclear, as is the effect of VLCD in this study, and therefore requires further research.

REFERENCES

1. Liu XH, Morris R, Spiller D, White M, Williams G. Orexin a preferentially excites glucose-sensitive neurons in the lateral hypothalamus of the rat in vitro. *Diabetes* 2001;50:2431-2437.
2. van den Hoek AM, van Heijningen C, Schröder-van der Elst JP, Ouwens DM, Havekes LM, Romijn JA, Kalsbeek A, Pijl H. Intracerebroventricular administration of neuropeptide Y induces hepatic insulin resistance via sympathetic innervation. *Diabetes* 2008;57:2304-2310.
3. Ogawa S, Lee TM, Kay AR, Tank DW. Brain magnetic resonance imaging with contrast dependent on blood oxygenation. *Proc Natl Acad Sci U S A* 1990;87:9868-9872.
4. Smeets PA, de Graaf C, Stafleu A, van Osch MJ, van der Grond J. Functional MRI of human hypothalamic responses following glucose ingestion. *Neuroimage* 2005;24:363-368.
5. Vidarsdottir S, Smeets PA, Eichelsheim DL, van Osch MJ, Viergever MA, Romijn JA, van der Grond J, Pijl H. Glucose ingestion fails to inhibit hypothalamic neuronal activity in patients with type 2 diabetes. *Diabetes* 2007;56:2547-2550.
6. Matthews DR, Hosker JP, Rudenski AS, Naylor BA, Treacher DF, Turner RC. Homeostasis model assessment: insulin resistance and beta-cell function from fasting plasma glucose and insulin concentrations in man. *Diabetologia* 1985;28:412-419.
7. Maes F, Collignon A, Vandermeulen D, Marchal G, Suetens P. Multimodality image registration by maximization of mutual information. *IEEE Trans Med Imaging* 1997;16:187-198.
8. Matsuda M, Liu Y, Mahankali S, Pu Y, Mahankali A, Wang J, DeFronzo RA, Fox PT, Gao JH. Altered hypothalamic function in response to glucose ingestion in obese humans. *Diabetes* 1999;48:1801-1806.
9. Cho ZH, Son YD, Kang CK, Han JY, Wong EK, Bai SJ. Pain dynamics observed by functional magnetic resonance imaging: differential regression analysis technique. *J Magn Reson Imaging* 2003;18:273-283.
10. Williams G, Bing C, Cai XJ, Harrold JA, King PJ, Liu XH. The hypothalamus and the control of energy homeostasis: different circuits, different purposes. *Physiol Behav* 2001;74:683-701.
11. King BM. The rise, fall, and resurrection of the ventromedial hypothalamus in the regulation of feeding behavior and body weight. *Physiol Behav* 2006;87:221-244.
12. Niswender KD, Schwartz MW. Insulin and leptin revisited: adiposity signals with overlapping physiological and intracellular signaling capabilities. *Front Neuroendocrinol* 2003;24:1-10.
13. Liu Y, Gao JH, Liu HL, Fox PT. The temporal response of the brain after eating revealed by functional MRI. *Nature* 2000;405:1058-1062.
14. Smeets PA, Vidarsdottir S, de Graaf C, Stafleu A, van Osch MJ, Viergever MA, Pijl H, van der Grond J. Oral glucose intake inhibits hypothalamic neuronal activity more effectively than glucose infusion. *Am J Physiol Endocrinol Metab* 2007;293:E754-758.
15. Kim BJ, Carlson OD, Jang HJ, Elahi D, Berry C, Egan JM. Peptide YY is secreted after oral glucose administration in a gender-specific manner. *J Clin Endocrinol Metab* 2005;90:6665-6671.
16. Meier JJ, Nauck MA, Kranz D, Holst JJ, Deacon CF, Gaeckler D, Schmidt WE, Gallwitz B. Secretion, degradation, and elimination of glucagon-like peptide 1 and gastric inhibitory polypeptide in patients with chronic renal insufficiency and healthy control subjects. *Diabetes* 2004;53:654-662.
17. Batterham RL, Cowley MA, Small CJ, Herzog H, Cohen MA, Dakin CL, Wren AM, Brynes AE, Low MJ, Ghatei MA, Cone RD, Bloom SR. Gut hormone PYY(3-36) physiologically inhibits food intake. *Nature* 2002;418:650-654.
18. Flint A, Raben A, Astrup A, Holst JJ. Glucagon-like peptide 1 promotes satiety and sup-

presses energy intake in humans. *J Clin Invest* 1998;101:515-520.

19. Cohen MA, Ellis SM, Le Roux CW, Batterham RL, Park A, Patterson M, Frost GS, Ghatei MA, Bloom SR. Oxyntomodulin suppresses appetite and reduces food intake in humans. *J Clin Endocrinol Metab* 2003;88:4696-4701.
20. Chaudhri OB, Parkinson JR, Kuo YT, Druce MR, Herlihy AH, Bell JD, Dhillo WS, Stanley SA, Ghatei MA, Bloom SR. Differential hypothalamic neuronal activation following peripheral injection of GLP-1 and oxyntomodulin in mice detected by manganese-enhanced magnetic resonance imaging. *Biochem Biophys Res Commun* 2006;350:298-306.
21. van den Hoek AM, Heijboer AC, Corssmit EP, Voshol PJ, Romijn JA, Havekes LM, Pijl H. PYY3-36 reinforces insulin action on glucose disposal in mice fed a high-fat diet. *Diabetes* 2004;53:1949-1952.
22. Henry RR, Gumbiner B. Benefits and limitations of very-low-calorie diet therapy in obese NIDDM. *Diabetes Care* 1991;14:802-823.
23. Williams KV, Mullen ML, Kelley DE, Wing RR. The effect of short periods of caloric restriction on weight loss and glycemic control in type 2 diabetes. *Diabetes Care* 1998;21:2-8.
24. Lara-Castro C, Newcomer BR, Rowell J, Wallace P, Shaughnessy SM, Munoz AJ, Shiflett AM, Rigsby DY, Lawrence JC, Bohning DE, Buchthal S, Garvey WT. Effects of short-term very low-calorie diet on intramyocellular lipid and insulin sensitivity in nondiabetic and type 2 diabetic subjects. *Metabolism* 2008;57:1-8.
25. van der Zwaag W, Francis S, Head K, Peters A, Gowland P, Morris P, Bowtell R. fMRI at 1.5, 3 and 7 T: characterising BOLD signal changes. *Neuroimage* 2009;47:1425-1434.
26. Smeets PA, de Graaf C, Stafleu A, van Osch MJ, van der Grond J. Functional magnetic resonance imaging of human hypothalamic responses to sweet taste and calories. *Am J Clin Nutr* 2005;82:1011-1016.
27. Lindström J, Ilanne-Parikka P, Peltonen M, Aunola S, Eriksson JG, Hemiö K, Hämäläinen H, Härkönen P, Keinänen-Kiukaanniemi S, Laakso M, Louheranta A, Mannelin M, Paturi M, Sundvall J, Valle TT, Uusitupa M, Tuomilehto J, on behalf of the Finnish Diabetes Prevention Study Group. Sustained reduction in the incidence of type 2 diabetes by lifestyle intervention: follow-up of the Finnish Diabetes Prevention Study. *Lancet* 2006;368:1673-1679.
28. Uusitupa M, Lindi V, Louheranta A, Salopuro T, Lindström J, Tuomilehto J, for the Finnish Diabetes Prevention Study Group. Long-term improvement in insulin sensitivity by changing lifestyles of people with impaired glucose tolerance: 4-year results from the Finnish Diabetes Prevention Study. *Diabetes* 2003;52:2532-2538.

Chapter 8

Increased amygdalar and hippocampal volumes in elderly obese individuals with or at risk of cardiovascular disease

Ralph L. Widya
Albert de Roos
Stella Trompet
Anton J.M. de Craen
Rudi G.J. Westendorp
Johannes W.A. Smit
Mark A. van Buchem
Jeroen van der Grond

for the PROSPER Study Group

American Journal of Clinical Nutrition 2011;93(6):1190-1195

ABSTRACT

Background

The basal ganglia, hippocampus, and thalamus are involved in the regulation of human feeding behavior. Recent studies have shown that obesity [body mass index (BMI; in kg/m^2) > 30] is associated with loss of gray and white matter. It is unknown whether the subcortical brain structures that are actually involved in feeding behavior also show volume changes in obesity. Therefore, the purpose of this study was to evaluate the volumes of the basal ganglia, hippocampus, and thalamus in obesity.

Methods

Three-dimensional T1-weighted magnetic resonance imaging scans of the brain were analyzed by using automatic segmentation to measure volumes of the nucleus accumbens, globus pallidus, amygdala, putamen, caudate nucleus, thalamus, and hippocampus in 471 subjects (mean age: 74.4 y; 56% men).

Results

Obese subjects had larger left ($P = 0.013$) and right ($P = 0.003$) amygdalar volumes and a larger left hippocampal volume ($P = 0.040$) than did normal-weight subjects (BMI < 25). None of the other subcortical structures differed in size between these groups. After correction for age, sex, smoking, hypertension, and pravastatin use, BMI was associated with left ($\beta = 0.175$, $P = 0.001$) and right ($\beta = 0.157$, $P = 0.001$) amygdalar volumes and with left hippocampal volume ($\beta = 0.121$, $P = 0.016$).

Conclusions

This study showed that the amygdala and hippocampus are enlarged in obesity. In consideration of the function of these structures, this finding may indicate that hedonic memories could be of major importance in the regulation of feeding. Because of the cross-sectional design, cause and effect could not be discriminated in this study.

INTRODUCTION

Obesity is a major public health issue strongly associated with chronic diseases, including diabetes mellitus and cardiovascular disease[1, 2]. It is well recognized that many brain structures are functionally involved in the regulation of food intake, including internal and external sensory inputs[3]. Regulation of food intake is controlled by multiple cognitive factors, including memorial representations of foods and their environmental context, and emotional and rewarding properties of such representations and their hedonic effects[3]. These factors are regulated by signaling molecules through the corticolimbic brain systems, in which the basal ganglia have an important role[4].

In addition to homeostatic regulation of food intake driven by inputs of the basal ganglia, thalamus, and hippocampus, generic morphometric changes of the brain have been described as well. There is growing evidence that an increased body mass index (BMI) is independently associated with whole-brain atrophy[5, 6]. Other studies have shown an evident correlation between obesity and loss of cortical gray matter[7-10]. On the other hand, cortical gray and white matter volume loss has also been described in patients with a very low BMI, as in anorexia nervosa[11-15]. Mechanisms behind these relations have not yet been clarified.

To our knowledge, the relation between obesity and the anatomy of subcortical structures that play a role in human food regulation have not been investigated previously. In the present study we aimed to investigate whether the basal ganglia, hippocampus, and thalamus are different between obese subjects and overweight and normal-weight subjects.

METHODS

Subjects

All subjects were derived from the magnetic resonance imaging (MRI) substudy of the PROspective Study of Pravastatin in the Elderly at Risk (PROSPER). PROSPER was a double-blind, randomized, placebo-controlled trial aimed at assessing the effect of therapy with 40 mg pravastatin on vascular events in 5804 men and women from Scotland, Ireland, and the Netherlands aged 70-82 y with vascular disease or at risk of vascular disease[16]. The PROSPER study was initiated in 1997. In the Netherlands, all consenting subjects were enrolled beginning in May 1998. The inclusion criteria for this study were as follows: men or women aged 70-82 y; total cholesterol of 4.0-9.0 mmol/L; stroke, transient ischemic attack, myocardial infarction, arterial surgery, or amputation for vascular disease > 6 mo before study entry; or one or more of the following risk factors for vascular disease: current smoking, hypertension, current drug treatment, known diabetes mellitus, or fasting blood glucose > 7 mmol/L. The institutional ethics review boards of all centers approved the protocol, and all participants gave written informed consent. The protocol was consistent with the Declaration of Hel-

sinki. All subjects had a Mini-Mental State Examination score of ≥ 24. Effects of dementia and/or Alzheimer disease on the volumes of the basal ganglia were hereby automatically eliminated[16, 17]. Weight and height data for all participants were collected. The results were compared between subjects on the basis of BMI (in kg/m^2) groups: normal-weight subjects (BMI < 25), overweight subjects (BMI = 25-30), and obese subjects (BMI > 30).

Magnetic resonance acquisition

Of the 1100 Dutch participants in PROSPER, 494 subjects underwent a high-resolution three-dimensional (3D) T1-weighted (T1-w) MRI. All imaging was performed on an MR system operating at a field strength of 1.5 Tesla (Philips Medical Systems, Best, Netherlands). Three-dimensional T1-w scans were obtained by using the following parameters: repetition time = 30 ms, echo time = 4.6 ms, flip angle = 30°, slice thickness = 1.5 mm, 120 slices, no interslice gap, field of view = 220 × 220 mm, matrix = 256 × 256, and in-plane resolution = 1.12 × 1.12 mm.

MRI processing

Segmentation of the various subcortical structures was performed on the original data set (n = 494) and on the same data set of which the left and right hemispheres were mirrored in the lateral plane. This approach was chosen to overcome potential systematic lateralization bias in preferential volume determinations by the algorithm FIRST (FMRIB's Integrated Registration and Segmentation Tool). To calculate the individual left and right volumes of the separate basal ganglia, the original volume and the corresponding mirrored volume of that particular intracranial structure were averaged.

FIRST was applied to estimate the volumes of left and right structures separately in 7 subcortical regions: nucleus accumbens, globus pallidus, amygdala, putamen, caudate nucleus, thalamus, and hippocampus. FIRST is part of FSL (FMRIB's Software Library) and performs both registration and segmentation of the mentioned subcortical regions[18, 19]. During registration, the input data (3D T1 images) are transformed to Montreal Neurological Institute (MNI) 152 standard space. For intrasubject comparison studies, the algorithm uses 12 df to transform the image (i.e., 3 translations, 3 rotations, 3 scalings, and 3 skews). After registration, a subcortical mask was applied to locate the different subcortical structures, followed by segmentation based on voxel intensities. Absolute volumes of subcortical structures were calculated, taking into account the transformations made in the first stage. The software was set to archive all single-structure segmentations. Border correction was used to increase the accuracy of the volumetric measurements[20]. Border-corrected segmentations were archived as well. Volumetric data were obtained from the archived segmentations and normalized to MNI space. Incorrect segmentation of individual structures (volume greater or less than the mean group volume ± 3 × SD, usually with the value of "0") was excluded for analysis based on Tukey's rule[21].

The single time point measurement technique SIENAX was performed to obtain estimates of gray and white matter volumes as well as brain volume. SIENAX starts by extracting brain and skull images from the single whole-head input data. The brain image is then affine-registered to MNI 152 space (by using the skull image to determine the registration scaling), done primarily to obtain the volumetric scaling factor to be used as normalization for head size. Next, tissue-type segmentation with partial volume estimation is carried out to calculate total volume of brain tissue (including separate estimates of volumes of gray matter, white matter, peripheral gray matter, and ventricular cerebrospinal fluid)[19]. Atrophy was defined as intracranial volume: parenchymal volume / intracranial volume × 100%. All volumetric data were normalized to standard space, thereby correcting for interindividual differences in brain size. All MRI scans were reviewed by M.A.v.B. (> 15 y of neuroradiologic experience) for incidental findings.

Statistical analysis

Statistical analysis was performed by using SPSS for Windows (version 16.0.2; SPSS, Chicago, Ill). All descriptive data were expressed as means ± SDs or *n* (%). To compare group data, a one-factor analysis of variance was used, followed by a Scheffe's post hoc test to correct for multiple comparisons. For categorical variables, the chi-square test or Fisher's exact test was used. The association between basal ganglia volumes and BMI was determined by using a multiple linear regression analysis, with age, sex, smoking, hypertension, and pravastatin use as covariates. β regression coefficients and *P* values are reported. *P* values < 0.05 were considered significant.

RESULTS

Three-dimensional T1-w MRI of the brain was performed in 494 subjects. Except for age-related changes, none of our subjects had unexpected findings on MRI. After exclusion of cases with poor segmentation, 471 subjects (mean age: 74.4 y; 56% men) remained for volume calculation. The BMI of our sample population was 26.8 ± 3.6, with a minimum of 15.8 and a maximum of 43.5. The distribution of all BMIs is shown in **Figure 1**. On the basis of BMI, 140 subjects were classified as normal-weight (BMI = 23.2 ± 1.6), 256 subjects as overweight (BMI = 27.0 ± 1.4), and 75 subjects as obese (BMI = 32.8 ± 2.9). Demographic profiles for each group are shown in **Table 1**.

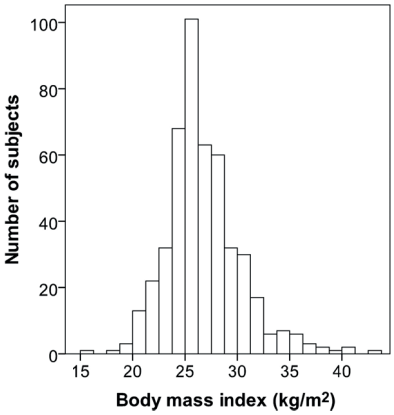

Figure 1. BMI distribution for all subjects.

Table 1. Demographics and group characteristics

Variable	Normal-weight	Overweight	Obese	*P* value		
	(*n* = 140)	(*n* = 256)	(*n* = 75)	Normal-weight vs. overweight	Overweight vs. obese	Normal-weight vs. obese
Male sex [*n* (%)]†	82 (59)	152 (59)	29 (39)	0.961	0.002*	0.008*
Age (y)	74.8 ± 3.3	74.3 ± 3.1	73.8 ± 3.0	0.277	0.469	0.071
Weight (kg)	67.7 ± 8.4	78.7 ± 8.2	92.6 ± 11.5	0.000*	0.000*	0.000*
Height (cm)	170.7 ± 7.9	170.5 ± 8.4	167.9 ± 9.3	0.978	0.062	0.068
BMI (kg/m^2)	23.2 ± 1.6	27.0 ± 1.4	32.8 ± 2.9	0.000*	0.000*	0.000*
MMSE score (points)	28.4 ± 1.3	28.4 ± 1.4	28.1 ± 1.6	0.993	0.288	0.397
History of vascular disease [*n* (%)]†	60 (43)	109 (43)	29 (39)	0.958	0.637	0.653
History of MI [*n* (%)]†	7 (5)	34 (13)	13 (17)	0.083	0.486	0.079
History of stroke/TIA [*n* (%)]†	30 (21)	30 (12)	13 (17)	0.121	0.281	0.592
Current smokers [*n* (%)]†	37 (26)	47 (18)	10 (13)	0.080	0.401	0.042*
Hypertension [*n* (%)]†	77 (55)	159 (62)	58 (77)	0.203	0.021*	0.002*
DM [*n* (%)]†	14 (10)	50 (20)	17 (23)	0.047*	0.666	0.020*
Insulin use [*n* (%)]‡	1 (1)	6 (2)	3 (4)	0.429	0.428	0.123
Fasting glucose (mmol/L)	5.4 ± 1.1	5.9 ± 1.7	6.0 ± 1.8	0.003*	0.883	0.013*
Systolic BP (mmHg)	155.6 ± 21.9	158.8 ± 21.9	158.2 ± 18.2	0.375	0.982	0.694
Diastolic BP (mmHg)	84.7 ± 10.6	86.3 ± 10.7	87.7 ± 10.9	0.327	0.634	0.143
Total cholesterol (mmol/L)	5.8 ± 0.9	5.7 ± 0.8	5.7 ± 0.8	0.832	0.968	0.793
LDL cholesterol (mmol/L)	3.9 ± 0.7	3.9 ± 0.7	3.9 ± 0.7	0.880	0.997	0.957
HDL cholesterol (mmol/L)	1.3 ± 0.4	1.2 ± 0.3	1.2 ± 0.3	0.000*	0.509	0.000*
Triglycerides (mmol/L)	1.3 ± 0.5	1.6 ± 0.7	1.6 ± 0.6	0.000*	0.845	0.003*

MMSE = Mini-Mental State Examination, MI = myocardial infarction, TIA = transient ischemic attack, DM = diabetes mellitus, BP = blood pressure. Data were compared by one-factor ANOVA with Scheffe's post hoc analysis.
* $P < 0.05$.
† Chi-square test.
‡ Fisher's exact test.

Obese subjects had larger left ($P = 0.013$) and right ($P = 0.003$) amygdalar volumes and a larger left hippocampal volume ($P = 0.040$) than did normal-weight subjects. None of the other basal ganglia or the thalamus differed significantly in size between groups (**Table 2**).

Multiple linear regression analysis examined the association between BMI and the basal ganglia, thalamus, and hippocampus, the left and right sides of which were assessed separately. After correction for age, sex, smoking, hypertension, and pravastatin use, a significant association was observed between BMI and normalized left ($\beta = 0.175$, $P = 0.001$) and right ($\beta = 0.157$, $P = 0.001$) amygdalar volumes, and normalized left hippocampal volume ($\beta = 0.121$, $P = 0.016$) (**Figure 2**). This indicates that a high BMI is associated with large volumes

Table 2. Magnetic resonance imaging characteristics of normal-weight, overweight, and obese subjects

	Normal-weight		Overweight		Obese		*P* value		
	n	**Volume**	***n***	**Volume**	***n***	**Volume**	**Normal-weight vs. overweight**	**Overweight vs. obese**	**Normal-weight vs. obese**
		cm^3		cm^3		cm^3			
L nuc acc	86	0.58 ± 0.16	156	0.60 ± 0.16	45	0.61 ± 0.18	0.728	0.879	0.577
R nuc acc	68	0.54 ± 0.16	164	0.54 ± 0.16	38	0.51 ± 0.16	1.000	0.779	0.814
L glob pal	117	1.96 ± 0.46	214	1.95 ± 0.40	65	1.97 ± 0.43	0.978	0.939	0.986
R glob pal	119	1.97 ± 0.45	213	1.95 ± 0.34	64	1.99 ± 0.41	0.864	0.733	0.948
L amyg	126	1.95 ± 0.36	226	2.02 ± 0.33	66	2.10 ± 0.33	0.144	0.253	0.013*
R amyg	130	1.93 ± 0.32	224	2.01 ± 0.33	68	2.10 ± 0.35	0.151	0.097	0.003*
L putam	120	5.16 ± 0.61	226	5.18 ± 0.61	69	5.17 ± 0.75	0.952	0.996	0.988
R putam	123	5.34 ± 0.61	220	5.33 ± 0.61	67	5.18 ± 0.61	1.000	0.184	0.235
L caud nuc	126	3.57 ± 0.50	222	3.58 ± 0.51	69	3.51 ± 0.53	0.966	0.611	0.772
R caud nuc	127	4.05 ± 0.57	225	3.98 ± 0.63	68	3.84 ± 0.63	0.560	0.277	0.077
L thal	129	8.01 ± 0.65	224	8.09 ± 0.64	69	8.09 ± 0.74	0.481	0.998	0.707
R thal	128	8.04 ± 0.66	224	8.13 ± 0.68	69	8.13 ± 0.74	0.506	0.998	0.656
L hipp	124	4.52 ± 0.68	223	4.63 ± 0.58	64	4.77 ± 0.70	0.309	0.301	0.040*
R hipp	124	4.60 ± 0.63	219	4.66 ± 0.59	64	4.77 ± 0.57	0.600	0.476	0.177
Gray matter	143	$5.93 \pm 0.50 \times 10^2$	252	$5.91 \pm 0.41 \times 10^2$	76	$5.93 \pm 0.44 \times 10^2$	0.953	0.923	0.990
White matter	143	$7.71 \pm 0.41 \times 10^2$	252	$7.66 \pm 0.36 \times 10^2$	76	$7.66 \pm 0.41 \times 10^2$	0.495	0.999	0.665
Gray + white	143	$13.64 \pm 0.71 \times 10^2$	252	$13.57 \pm 0.62 \times 10^2$	76	$13.60 \pm 0.69 \times 10^2$	0.667	0.970	0.911

Values are means ± SDs unless otherwise indicated. L = left, R = right, nuc acc = nucleus accumbens, glob pal = globus pallidus, amyg = amygdala, putam = putamen, caud nuc = caudate nucleus, thal = thalamus, hipp = hippocampus, Gray matter = volume of normalized gray matter, White matter = volume of normalized white matter, Gray + white = total volume of white and gray matter. Data were compared by one-factor ANOVA with Scheffe's post hoc analysis.

* $P < 0.05$.

of amygdala and left hippocampus. BMI showed no association with other basal ganglia or thalamus volumes (**Table 3**).

The subjects included in this study might have had one or more risk factors for vascular disease, namely current smoking, hypertension, current drug treatment, known diabetes mellitus, or fasting blood glucose > 7 mmol/L. We found no association between volumes of basal ganglia and any of these cardiovascular disease risk factors.

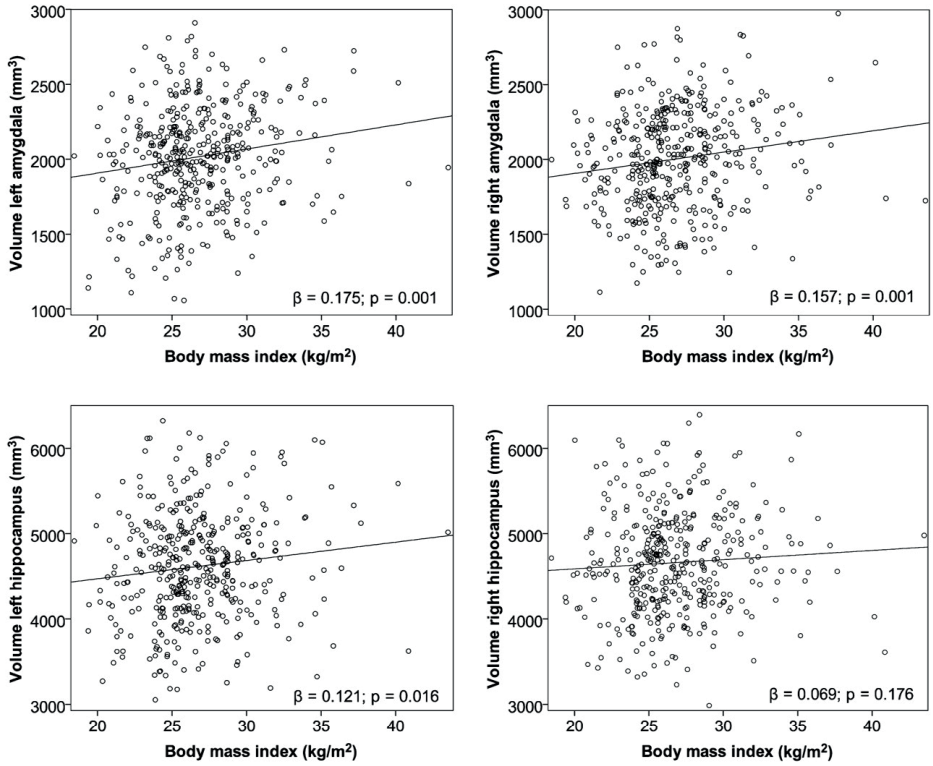

Figure 2. Bivariate relations between amygdalar and hippocampal volumes and BMI. Reported β and *P* values were obtained by multiple linear regression analysis with correction for age, sex, smoking, hypertension, and pravastatin use.

DISCUSSION

The main findings of this study were enlargements of the amygdala and hippocampus in the obese subjects. In addition, an association of amygdalar and hippocampal enlargement with BMI corrected for age, sex, smoking, hypertension, and pravastatin use was observed. Both brain structures play a crucial role in the process of feeding behavior. Interestingly, none of the other investigated brain structures showed a significant association with BMI.

Table 3. Association between BMI and volumes of subcortical structures

	Crude		Adjusted	
	β	*P* value	β	*P* value
L nuc acc	0.036	0.543	0.044	0.455
R nuc acc	-0.012	0.843	0.002	0.968
L glob pal	0.023	0.650	0.021	0.683
R glob pal	0.021	0.679	0.020	0.707
L amyg	0.164	0.001*	0.175	0.001*
R amyg	0.151	0.002*	0.157	0.001*
L putam	-0.011	0.818	0.020	0.667
R putam	-0.068	0.171	-0.050	0.300
L caud nuc	-0.050	0.308	-0.027	0.577
R caud nuc	-0.079	0.109	-0.045	0.353
L thal	0.022	0.658	0.056	0.229
R thal	0.037	0.446	0.064	0.180
L hipp	0.118	0.016*	0.121	0.016*
R hipp	0.063	0.202	0.069	0.176
Gray matter	0.005	0.921	-0.054	0.202
White matter	-0.060	0.190	-0.057	0.226
Gray + white	-0.032	0.485	-0.070	0.119

Results are from a multiple linear regression analysis. L = left, R = right, nuc acc = nucleus accumbens, glob pal = globus pallidus, amyg = amygdala, putam = putamen, caud nuc = caudate nucleus, thal = thalamus, hipp = hippocampus, Gray matter = volume of normalized gray matter, White matter = volume of normalized white matter, Gray + white = total volume of white and gray matter.

* Significant β values before and after adjustment for age, sex, smoking, hypertension, and pravastatin use.

The amygdala plays an important role in the coordination of appetitive behavior. It is part of a complex neural system that is responsible for the evaluation of food. The electrophysiological responses on taste and picture-odor contingencies in the amygdala suggest a sensory function[22, 23]. Furthermore, rat studies suggest that the amygdala is critical to learning representations of specific experiences with food and using them to guide appetitive behavior[24]. Enlargement of the amygdala with respect to BMI has not been described before. It is known that enlargement can occur in patients with depression[25, 26], psychosis[27], autism[28], and bipolar disorder[29, 30]. A slight enlargement of the hippocampus has also been reported in bipolar disorder[30].

Although we found that volume changes were more pronounced in the right hemisphere of the amygdala and in the left hemisphere of the hippocampus, we believe that these differences are statistically not convincing enough to speculate on lateralization.

A possible explanation for amygdalar enlargement is higher glucose metabolism and cerebral blood flow[31]. However, a direct relation with amygdalar enlargement remains unclear, because cerebral blood flow and metabolism might be affected by multiple physi-

ologic events, e.g., dynamic changes in neurotransmitter-neuroreceptor function[26]. Other proposed mechanisms of amygdalar enlargement are an increase in size or number of neurons or glial cells, increased connective tissue, and increased intercellular fluid[31]. Rat studies have shown that chronic stress induces dendritic remodeling of the hippocampus and amygdala, which leads to atrophy and hypertrophy, respectively[32]. Hypermetabolism of the amygdala may also result from an increased afferent glutamatergic transmission between and within amygdala nuclei[33]. Glutamatergic transmission is part of the endocannabinoid system, which is related to obesity when dysregulated[34]. On the basis of this principle, pharmacologic agents, particularly cannabinoid receptor antagonists, are currently used as antiobesity drugs[35].

The amygdala and hippocampus relate memory to pleasure, respectively, by establishing the reward value of food and food-related stimuli or situations and by consolidating pleasure memories. On the basis of the previously described mechanisms, we assume that our findings are in part explained by an increased activity and possibly an elevated metabolism in the amygdala and hippocampus. Statements about the order of events (excessive feeding leading to or resulting from enlargement) are limited because this study was cross-sectional. However, it is just as likely that the described changes are the effect of enjoying food on hedonic centers, rather than hedonic center changes leading to eating more food.

Studies have shown that smoking history is associated with brain atrophy[36-39]. Therefore, we adjusted for smoking in the linear regression analysis. Hypertension has also been recognized as a risk factor for brain atrophy[40, 41], and moreover, hippocampal atrophy[42]. Hence, we used hypertension as a covariate in the linear regression analysis.

We realize that in an explorative study, significant results may occur by coincidence. In the current study, we performed a one-factor analysis of variance with subsequent Scheffe's post hoc analysis, correcting for multiple comparisons between groups (Table 2). We did not correct a priori for the number of structures (Tables 2 and 3). Because the amygdala is associated with BMI (Tables 2 and 3) in both hemispheres, we believe that our data are not driven by coincidence. Still, it must be emphasized that significant findings that are just below the threshold value ($P = 0.05$) should, in general, be treated with care.

No association was found between volumes of basal ganglia and cardiovascular disease risk factors. Because only cross-sectional data were available, no statements can be made about the influence of the duration of cardiovascular disease risk factors. For the same reason, cause and effect cannot be distinguished.

The obese group consisted of more women than men. Estrogen use has been shown to increase hippocampal volume relative to estrogen nonuse and findings in males[43]. Estrogen therapy was not investigated in this study. Therefore, sex or estrogen therapy could have been confounders in the relation between BMI and hippocampal volume.

We used the algorithm FIRST to estimate volumes. Existing and upcoming evidence indicate that different segmentation tools show structural differences between them. Com-

parison of data assessed with different segmentation techniques is therefore discouraged. A final limitation of this study was that it was performed in elderly individuals. Therefore, our results cannot be generalized to the population aged < 70 y.

In conclusion, this explorative study showed that the amygdala and hippocampus, which are very important structures in regulating feeding behavior, are enlarged in obesity. Furthermore, an association between BMI and enlargement was seen. The finding that these anatomic changes only occurred in the amygdala and hippocampus, and not in other brain structures that play a role in feeding behavior, suggests that cognitive aspects may be a major issue in the regulation of feeding. To our knowledge, this is the first study to have explored the relation between obesity and the basal ganglia specifically. Additional studies are required to examine the mechanisms behind enlargement of the amygdala and hippocampus in obesity.

REFERENCES

1. Flegal KM, Carroll MD, Ogden CL, Curtin LR. Prevalence and trends in obesity among US adults, 1999-2008. *JAMA* 2010;303:235-241.
2. Flegal KM, Graubard BI, Williamson DF, Gail MH. Sources of differences in estimates of obesity-associated deaths from first National Health and Nutrition Examination Survey (NHANES I) hazard ratios. *Am J Clin Nutr* 2010;91:519-527.
3. Berthoud HR. Interactions between the "cognitive" and "metabolic" brain in the control of food intake. *Physiol Behav* 2007;91:486-498.
4. Adan RA, Vanderschuren LJ, la Fleur SE. Anti-obesity drugs and neural circuits of feeding. *Trends Pharmacol Sci* 2008;29:208-217.
5. Ward MA, Carlsson CM, Trivedi MA, Sager MA, Johnson SC. The effect of body mass index on global brain volume in middle-aged adults: a cross sectional study. *BMC Neurol* 2005;5:23.
6. Gunstad J, Paul RH, Cohen RA, Tate DF, Spitznagel MB, Grieve S, Gordon E. Relationship between body mass index and brain volume in healthy adults. *Int J Neurosci* 2008;118:1582-1593.
7. Pannacciulli N, Del Parigi A, Chen K, Le DS, Reiman EM, Tataranni PA. Brain abnormalities in human obesity: a voxel-based morphometric study. *Neuroimage* 2006;31:1419-1425.
8. Taki Y, Kinomura S, Sato K, Inoue K, Goto R, Okada K, Uchida S, Kawashima R, Fukuda H. Relationship between body mass index and gray matter volume in 1,428 healthy individuals. *Obesity (Silver Spring)* 2008;16:119-124.
9. Walther K, Birdsill AC, Glisky EL, Ryan L. Structural brain differences and cognitive functioning related to body mass index in older females. *Hum Brain Mapp* 2010;31:1052-1064.
10. Raji CA, Ho AJ, Parikshak NN, Becker JT, Lopez OL, Kuller LH, Hua X, Leow AD, Toga AW, Thompson PM. Brain structure and obesity. *Hum Brain Mapp* 2010;31:353-364.
11. Katzman DK, Lambe EK, Mikulis DJ, Ridgley JN, Goldbloom DS, Zipursky RB. Cerebral gray matter and white matter volume deficits in adolescent girls with anorexia nervosa. *J Pediatr* 1996;129:794-803.
12. Frank GK, Bailer UF, Henry S, Wagner A, Kaye WH. Neuroimaging studies in eating disorders. *CNS Spectr* 2004;9:539-548.
13. Wagner A, Greer P, Bailer UF, Frank GK, Henry SE, Putnam K, Meltzer CC, Ziolko SK, Hoge J, McConaha C, Kaye WH. Normal brain tissue volumes after long-term recovery in anorexia and bulimia nervosa. *Biol Psychiatry* 2006;59:291-293.
14. Muhlau M, Gaser C, Ilg R, Conrad B, Leibl C, Cebulla MH, Backmund H, Gerlinghoff M, Lommer P, Schnebel A, Wohlschlager AM, Zimmer C, Nunnemann S. Gray matter decrease of the anterior cingulate cortex in anorexia nervosa. *Am J Psychiatry* 2007;164:1850-1857.
15. Castro-Fornieles J, Bargallo N, Lazaro L, Andres S, Falcon C, Plana MT, Junque C. A cross-sectional and follow-up voxel-based morphometric MRI study in adolescent anorexia nervosa. *J Psychiatr Res* 2009;43:331-340.
16. Shepherd J, Blauw GJ, Murphy MB, Bollen EL, Buckley BM, Cobbe SM, Ford I, Gaw A, Hyland M, Jukema JW, Kamper AM, Macfarlane PW, Meinders AE, Norrie J, Packard CJ, Perry IJ, Stott DJ, Sweeney BJ, Twomey C, Westendorp RG, on behalf of the PROSPER study group. Pravastatin in elderly individuals at risk of vascular disease (PROSPER): a randomised controlled trial. *Lancet* 2002;360:1623-1630.
17. Folstein MF, Folstein SE, McHugh PR. "Mini-mental state". A practical method for grading the cognitive state of patients for the clinician. *J Psychiatr Res* 1975;12:189-198.
18. de Jong LW, van der Hiele K, Veer IM, Houwing JJ, Westendorp RG, Bollen EL, de Bruin PW, Middelkoop HA, van Buchem MA, van der Grond J. Strongly reduced volumes of putamen and thalamus in Alzheimer's disease: an MRI study. *Brain* 2008;131:3277-3285.
19. Smith SM, Jenkinson M, Woolrich MW, Beckmann CF, Behrens TE, Johansen-Berg H,

Bannister PR, De Luca M, Drobnjak I, Flitney DE, Niazy RK, Saunders J, Vickers J, Zhang Y, De Stefano N, Brady JM, Matthews PM. Advances in functional and structural MR image analysis and implementation as FSL. *Neuroimage* 2004;23(Suppl 1):S208-219.

20. Patenaude B. Bayesian shape and appearance models. Technical report TR07BP1. FMRIB Center, University of Oxford. 2007. Published 2007.
21. Tukey JW. Exploratory data analysis. Reading, MA: Addison-Wesley Publishing Co., 1977.
22. Rolls ET, Critchley HD, Browning AS, Hernadi I, Lenard L. Responses to the sensory properties of fat of neurons in the primate orbitofrontal cortex. *J Neurosci* 1999;19:1532-1540.
23. Gottfried JA, O'Doherty J, Dolan RJ. Encoding predictive reward value in human amygdala and orbitofrontal cortex. *Science* 2003;301:1104-1107.
24. Hatfield T, Han JS, Conley M, Gallagher M, Holland P. Neurotoxic lesions of basolateral, but not central, amygdala interfere with Pavlovian second-order conditioning and reinforcer devaluation effects. *J Neurosci* 1996;16:5256-5265.
25. Tebartz van Elst L, Woermann F, Lemieux L, Trimble MR. Increased amygdala volumes in female and depressed humans. A quantitative magnetic resonance imaging study. *Neurosci Lett* 2000;281:103-106.
26. Frodl T, Meisenzahl EM, Zetzsche T, Born C, Jäger M, Groll C, Bottlender R, Leinsinger G, Möller HJ. Larger amygdala volumes in first depressive episode as compared to recurrent major depression and healthy control subjects. *Biol Psychiatry* 2003;53:338-344.
27. Velakoulis D, Wood SJ, Wong MT, McGorry PD, Yung A, Phillips L, Smith D, Brewer W, Proffitt T, Desmond P, Pantelis C. Hippocampal and amygdala volumes according to psychosis stage and diagnosis: a magnetic resonance imaging study of chronic schizophrenia, first-episode psychosis, and ultra-high-risk individuals. *Arch Gen Psychiatry* 2006;63:139-149.
28. Mosconi MW, Cody-Hazlett H, Poe MD, Gerig G, Gimpel-Smith R, Piven J. Longitudinal study of amygdala volume and joint attention in 2- to 4-year-old children with autism. *Arch Gen Psychiatry* 2009;66:509-516.
29. Altshuler LL, Bartzokis G, Grieder T, Curran J, Mintz J. Amygdala enlargement in bipolar disorder and hippocampal reduction in schizophrenia: an MRI study demonstrating neuroanatomic specificity. *Arch Gen Psychiatry* 1998;55:663-664.
30. Strakowski SM, DelBello MP, Sax KW, Zimmerman ME, Shear PK, Hawkins JM, Larson ER. Brain magnetic resonance imaging of structural abnormalities in bipolar disorder. *Arch Gen Psychiatry* 1999;56:254-260.
31. Altshuler LL, Bartzokis G, Grieder T, Curran J, Jimenez T, Leight K, Wilkins J, Gerner R, Mintz J. An MRI study of temporal lobe structures in men with bipolar disorder or schizophrenia. *Biol Psychiatry* 2000;48:147-162.
32. Vyas A, Mitra R, Shankaranarayana Rao BS, Chattarji S. Chronic stress induces contrasting patterns of dendritic remodeling in hippocampal and amygdaloid neurons. *J Neurosci* 2002;22:6810-6818.
33. Drevets WC, Price JL, Bardgett ME, Reich T, Todd RD, Raichle ME. Glucose metabolism in the amygdala in depression: relationship to diagnostic subtype and plasma cortisol levels. *Pharmacol Biochem Behav* 2002;71:431-447.
34. Mouslech Z, Valla V. Endocannabinoid system: An overview of its potential in current medical practice. *Neuro Endocrinol Lett* 2009;30:153-179.
35. Rodriguez de Fonseca F, Del Arco I, Bermudez-Silva FJ, Bilbao A, Cippitelli A, Navarro M. The endocannabinoid system: physiology and pharmacology. *Alcohol Alcohol* 2005;40:2-14.
36. Swan GE, Lessov-Schlaggar CN. The effects of tobacco smoke and nicotine on cognition and the brain. *Neuropsychol Rev* 2007;17:259-273.
37. Swan GE, Decarli C, Miller BL, Reed T, Wolf PA, Carmelli D. Biobehavioral characteristics of

nondemented older adults with subclinical brain atrophy. *Neurology* 2000;54:2108-2114.

38. Longstreth WT, Jr., Diehr P, Manolio TA, Beauchamp NJ, Jungreis CA, Lefkowitz D, for the Cardiovascular Health Study Collaborative Research Group. Cluster analysis and patterns of findings on cranial magnetic resonance imaging of the elderly: the Cardiovascular Health Study. *Arch Neurol* 2001;58:635-640.
39. Brody AL, Mandelkern MA, Jarvik ME, Lee GS, Smith EC, Huang JC, Bota RG, Bartzokis G, London ED. Differences between smokers and nonsmokers in regional gray matter volumes and densities. *Biol Psychiatry* 2004;55:77-84.
40. Gianaros PJ, Greer PJ, Ryan CM, Jennings JR. Higher blood pressure predicts lower regional grey matter volume: Consequences on short-term information processing. *Neuroimage* 2006;31:754-765.
41. Wiseman RM, Saxby BK, Burton EJ, Barber R, Ford GA, O'Brien JT. Hippocampal atrophy, whole brain volume, and white matter lesions in older hypertensive subjects. *Neurology* 2004;63:1892-1897.
42. Korf ES, White LR, Scheltens P, Launer LJ. Midlife blood pressure and the risk of hippocampal atrophy: the Honolulu Asia Aging Study. *Hypertension* 2004;44:29-34.
43. Lord C, Buss C, Lupien SJ, Pruessner JC. Hippocampal volumes are larger in postmenopausal women using estrogen therapy compared to past users, never users and men: a possible window of opportunity effect. *Neurobiol Aging* 2008;29:95-101.

Chapter 9

Visceral adipose tissue is associated with microstructural brain tissue damage

Ralph L. Widya
Lucia J.M. Kroft
Irmhild Altmann-Schneider
Annette A. van den Berg-Huysmans
Noortje van der Bijl
Albert de Roos
Hildo J. Lamb
Mark A. van Buchem
P. Eline Slagboom
Diana van Heemst
Jeroen van der Grond

on behalf of the Leiden Longevity Study Group

Obesity 2015;23(5):1092-1096

ABSTRACT

Background

Obesity has been associated with microstructural brain tissue damage. Different fat compartments demonstrate different metabolic and endocrine behaviors. The aim was to investigate the individual associations between abdominal visceral adipose tissue (VAT) and subcutaneous adipose tissue (SAT) and microstructural integrity in the brain.

Methods

This study comprised 243 subjects aged 65.4 ± 6.7 years. The associations between abdominal VAT and SAT, assessed by CT, and magnetization transfer imaging markers of brain microstructure for gray and white matter were analyzed and adjusted for confounding factors.

Results

VAT was associated with normalized magnetization transfer ratio (MTR) peak height in gray (β −0.216) and white matter (β −0.240) (both $P < 0.01$) after adjustment for confounding factors. After adjustment for sex, age, and descent, SAT was associated with normalized MTR peak height in gray and white matter, but not after additional correction for BMI, hypertension, current smoking, statin use, and type 2 diabetes (respectively, β −0.055 and β 0.035, both $P > 0.05$). Stepwise linear regression analysis showed that only VAT was associated with normalized MTR peak height in gray and white matter (both $P < 0.001$).

Conclusions

Our data indicate that increased abdominal VAT rather than SAT is associated with microstructural brain tissue damage in elderly individuals.

INTRODUCTION

Obesity has been linked to brain atrophy, and many studies have suggested that body mass index (BMI) is associated with brain damage and cognitive decline[1-4]. The distribution of body fat is crucial to understanding the adverse effects of obesity. Excess fat is stored subcutaneously, as well as at ectopic sites, such as the visceral fat depot. Visceral adipose tissue (VAT), as opposed to subcutaneous adipose tissue (SAT), is considered to play a key role in the atherogenic effects of obesity[5] and is associated with incident cardiovascular disease and cancer[6]. VAT is increasingly appreciated as an endocrine organ which produces cytokines, such as interleukin-6 and tumor necrosis factor alpha, which induce hepatic production of the acute phase protein C-reactive protein[7, 8]. Production of these cytokines and systemic low-grade inflammation are considered as important mechanisms for the adverse effects of obesity on the vessel wall. It can be hypothesized that inflammation also induces subtle microstructural brain changes, which by themselves may lead to cognitive decline[9, 10]. Magnetization transfer imaging (MTI) is an MRI technique that is more sensitive to subtle microstructural changes in the brain than conventional techniques[11-13]. Although the association between high BMI and brain damage is apparent, the individual contributions of VAT and SAT are unknown. Accordingly, the aim of the present study was to investigate the individual associations between abdominal VAT and SAT and the integrity of the microstructure in the brain.

METHODS

Subjects

This study comprises subjects from the Leiden Longevity Study, which is described extensively elsewhere[14]. In summary, in the Leiden Longevity Study subjects genetically enriched for familial longevity are compared with their partners to determine genetic factors contributing to longevity. Inclusion criteria for the study as a whole were: [1] men must be aged ≥ 89 years and women ≥ 91 years; [2] subjects must have at least one living brother or one living sister who fulfilled the first criterion and was willing to participate; [3] the sib pairs have an identical mother and father; [4] the parents of the sibship are Dutch and Caucasian. The Leiden Longevity Study cohort included 421 Dutch Caucasian families consisting of 943 long-lived siblings with 1671 of their offspring and 745 of the partners thereof. The offspring carries on average 50% of the genetic propensity of their long-lived parent and were shown to have a lower mortality (standardized mortality ratio 0.65) compared with their birth cohort[14]. Their partners, with who most have shared the same environment for decades were included as matched controls. There was no selection on demographic or health characteristics[14, 15].

Participants for the current study were recruited from the offspring of the long-lived siblings and their partners. The subjects were pooled for analysis. After exclusion of subjects with contraindications for MRI, the current study included 243 nondemented subjects (127 offspring and 116 controls) who underwent MTI of the brain and abdominal CT on the same day.

This study was approved by the Medical Ethical Committee of the Leiden University Medical Center and was conducted in accordance with the Declaration of Helsinki. Written informed consent was obtained from all participants.

Abdominal adipose tissue measurement

Measures of abdominal adiposity were assessed by nonenhanced CT (Toshiba Aquilion ONE, Toshiba Medical Systems, Otawara, Japan). The examinations were performed between September 2009 and December 2010. A single-slice 8.0 mm acquisition was planned at the L4/L5 vertebra level. Tube voltage was 120 kV, tube current 310 mA, rotation time 0.5 s. Imaging was performed during breath hold after expiration. Analysis of visceral fat and subcutaneous fat was performed with dedicated fat measurement software available at the CT scanner console. The single slice image was selected within the software program. An automated tool was used for recognizing fat, using predefined thresholds for adipose tissue ranging from −150 to −30 HU. Visceral fat was defined as fat enclosed by the peritoneal cavity. Abdominal subcutaneous fat was defined as fat outside the peritoneal cavity.

MRI acquisition

Imaging was performed on an MR system operating at a field strength of 3 Tesla (Philips Medical Systems, Best, the Netherlands). MTI was part of a more extended protocol described previously[16], which included T1-w, T2-w, FLAIR, and DTI MRI scans. MTI was performed with the following parameters: TR = 100 ms, TE = 11 ms, FA = 9°, FOV = 224 × 180 × 144 mm, matrix size 224 × 169, and 20 slices with a 7 mm thickness, no slice gap.

MRI processing

Magnetization transfer ratio (MTR) was investigated for gray and white matter separately. Nonsaturated and saturated MTI images were co-registered to the three-dimensional T1-weighted images and subsequently processed with FSL tools[17, 18]. For creation of individual brain masks for cortical gray and white matter, three-dimensional T1-weighted images were skull stripped[19] and subsequently segmented[20] into cortical gray and white matter. For all analyses basal ganglia, hippocampus, and amygdala were excluded from data analysis. Individual MTR maps were calculated voxel by voxel following the equation MTR = (M0 − M1) / M0. Mean MTR and normalized MTR peak height were determined[11] after masking the MTR maps with the respective brain masks. For correction for possible partial volume effects, 1 voxel eroded gray and white matters masks were applied.

Statistical analysis

All descriptive data were presented as mean ± standard deviation or as percentage. Offspring and partners were pooled. Multivariate linear regression and stepwise backward regression analyses were performed to investigate the associations between VAT and SAT and MTI markers of brain microstructure. First, analyses were adjusted for sex, age, and descent (being partner or offspring of long lived siblings) (Model 1). Second, analyses were additionally adjusted for BMI, hypertension, current smoking, statin use, and type 2 diabetes (Model 2). Regression coefficients, 95% confidence intervals (CI), *P* values, and R^2 values are reported. $P < 0.05$ was considered statistically significant. Statistical analyses were performed using IBM SPSS Statistics for Windows, version 20.0 (IBM Corp., Armonk, NY).

RESULTS

This analysis comprised 243 subjects. Subject characteristics are shown in **Table 1**. Mean age was 65.4 ± 6.7 years and mean BMI 26.3 ± 3.8 kg/m^2. The gray matter and white matter MTI parameters (mean MTR and normalized MTR peak height) of the entire group are summarized in **Table 2**. BMI was associated with normalized MTR peak height in both gray matter (standardized β: −0.217, $P < 0.001$) and white matter (standardized β: −0.208, $P < 0.001$) after adjustment for sex, age, and descent. BMI was associated neither with mean MTR in gray matter ($P = 0.957$) nor in white matter ($P = 0.315$).

Table 1. Subject characteristics

Men, *n* (%)	112 (46)
Age (years)	65.4 ± 6.7
BMI (kg/m^2)	26.3 ± 3.8
VAT (cm^2)	128.9 ± 61.7
SAT (cm^2)	236.1 ± 91.7
Systolic blood pressure (mmHg)	138.9 ± 19.6
Diastolic blood pressure (mmHg)	83.3 ± 9.4
Hypertension, *n* (%)	55 (23)
Current smokers, *n* (%)	27 (11)
Type 2 diabetes, *n* (%)	16 (7)
Statin use, *n* (%)	19 (8)
History of stroke	5 (2)
History of myocardial infarction	3 (1)
Total cholesterol (mmol/L)	5.6 ± 1.2
HDL cholesterol (mmol/L)	1.5 ± 0.4

Values are means ± standard deviation or *n* (%).
BMI = body mass index, VAT = visceral adipose tissue, SAT = subcutaneous adipose tissue, HDL = high-density lipoprotein.

Table 2. Magnetization transfer imaging parameters

	Normalized MTR peak height (pixel count x 10^3)	Coefficient of variation
Gray matter	76 ± 11	0.14
White matter	117 ± 23	0.20
	Mean MTR (value x 10^3)	**Coefficient of variation**
Gray matter	335 ± 9	0.03
White matter	394 ± 9	0.02

MTR = magnetization transfer ratio.

Table 3 shows the associations between VAT and MTI parameters in gray and white matter. VAT was associated with normalized MTR peak height in both gray matter ($P < 0.001$) and white matter ($P < 0.001$) after adjustment for sex, age, and descent. After additional adjustment for BMI, hypertension, current smoking, statin use, and type 2 diabetes, the associations remained for gray matter ($P = 0.003$) and white matter ($P < 0.001$). An increase of VAT with 1 cm^2 reduced normalized MTR peak height in the gray matter with 46.1 (95% CI −85.4, −6.7), which roughly corresponds to an overall decrease in normalized MTR peak height of 0.1%. In the white matter, 1 cm^2 increase in VAT resulted in a MTR peak height decrease of 103.6 (95% CI −190.2, −17.1), which also roughly corresponds to a 0.1% overall decrease. No significant associations between VAT and mean MTR in the gray and white matter were found.

Table 4 shows the associations between SAT and MTI parameters in gray and white matter. SAT was associated with normalized MTR peak height in both the gray matter ($P < 0.001$) and white matter ($P = 0.001$) after adjustment for sex, age, and descent. However, after additional

Table 3. Associations between visceral adipose tissue and magnetization transfer imaging parameters

	Standardized β	*P*	R^2
Normalized MTR peak height - gray matter			
Model 1	-0.361	< 0.001	0.283
Model 2	-0.216	0.003	0.262
Normalized MTR peak height - white matter			
Model 1	-0.396	< 0.001	0.305
Model 2	-0.240	< 0.001	0.287
Mean MTR - gray matter			
Model 1	0.006	0.923	0.169
Model 2	0.058	0.475	0.171
Mean MTR - white matter			
Model 1	0.033	0.611	0.106
Model 2	0.076	0.110	0.255

Model 1: Adjusted for sex, age and descent. Model 2: Adjusted for sex, age, descent, BMI, hypertension, current smoking, statin use, and type 2 diabetes.
β = regression coefficient, R^2 = proportion of explained variance; MTR = magnetization transfer ratio.

adjustment for BMI, hypertension, current smoking, statin use, and type 2 diabetes, the associations for both gray matter ($P = 0.284$) and white matter ($P = 0.938$) were abolished. No significant associations between SAT and mean MTR in the gray and white matter were found.

When analyzing both VAT and SAT in a stepwise backward regression model adjusted for sex, age, and descent, only VAT remained associated with normalized MTR peak height in gray and white matter (both $P < 0.001$). Additional adjustment for BMI, hypertension, current smoking, statin use, and type 2 diabetes did not alter these findings.

Table 4. Associations between subcutaneous adipose tissue and magnetization transfer imaging parameters

	Standardized β	*P*	R^2
Normalized MTR peak height - gray matter			
Model 1	-0.274	< 0.001	0.233
Model 2	-0.055	0.284	0.235
Normalized MTR peak height - white matter			
Model 1	-0.217	0.001	0.207
Model 2	0.035	0.938	0.233
Mean MTR - gray matter			
Model 1	-0.003	0.965	0.168
Model 2	0.052	0.501	0.171
Mean MTR - white matter			
Model 1	0.052	0.434	0.108
Model 2	-0.024	0.580	0.106

Model 1: Adjusted for sex, age and descent. Model 2: Adjusted for sex, age, descent, BMI, hypertension, current smoking, statin use, and type 2 diabetes.
β = regression coefficient, R^2 = proportion of explained variance; MTR = magnetization transfer ratio.

DISCUSSION

In the current study, we observed lower integrity of the microstructure in the brain with increasing VAT, as well as SAT. When entered in one regression model, VAT appeared to have a much stronger association with microstructural brain tissue damage than SAT.

It has been shown that obesity is related to neurodegenerative, vascular, and metabolic processes that affect brain structures underlying cognitive decline and dementia, with increasing evidence of a greater role of visceral rather than subcutaneous adiposity[8, 21]. It has also been shown that visceral rather than subcutaneous fat, expressed as a percentage of total fat, was significantly correlated with the volume of white matter lesions in subjects with acute ischemic stroke. In that particular study, study population was small ($n = 25$), consisted mostly of men, and adjustments for potential confounders were not performed[22]. A more recent study reported a link between having more than 100 cm^2 visceral fat and the presence of white matter lesions and silent lacunar infarctions in subjects free of symptomatic cerebrovascular

disease, suggesting a role of visceral fat on the development of cerebral small vessel disease. This association was found to be independent of age ≥ 60 years, waist circumference, BMI ≥ 25 kg/m^2, and hypertension[23]. In a large cohort study, it was found that VAT and total brain volume were associated; however, VAT was not associated with markers of vascular brain injury such as volume of white matter lesions and brain infarcts[8]. In the latter study no associations between VAT or SAT and temporal horn volume, a surrogate measure for hippocampal volume, was found. In a study with healthy nondemented elderly subjects it was demonstrated that VAT was significantly associated with verbal memory and low hippocampal volume after accounting for SAT, indicating an adverse effect of VAT on cognitive performance[24]. In general, these studies demonstrate associations between VAT and brain damage.

The current study shows that VAT is strongly associated with MTI parameters reflecting discrete brain lesions that may not be detected by conventional imaging. MTI has the potential to quantify the pathologic changes in central nervous system disorders in the normal appearing white and gray matter on conventional MRI sequences[11, 13, 25]. MTI offers a way of examining tissue structure and structural components, normally not resolvable with conventional MRI[12]. This allows for examination of structural integrity in a different and possibly more sensitive manner than volumetric changes alone. MTI contrast is based on magnetization transfer between protons, which are bound to macromolecules and therefore restricted in motion, and protons in water, which can move freely[26]. The MTR, representing the percentage of variation in the MR signal between the saturated and unsaturated acquisitions, is an effective and simple MTI measure to use as a clinical application. Within the brain, myelin water contributes disproportionately to the MTR, which therefore has been suggested to be a relatively specific quantitative measure of myelin integrity[27-29]. MTR histogram analysis is a technique which displays MTR values of the segmented brain. MTR histograms of normal brains are characterized by the presence of a single, sharp peak, indicating that most normal brain voxels have approximately the same MTR values[30]. In general mean MTR and histogram peak height are reported both. It should be realized that both measures reflect different processes and may show different sensitivity to demonstrate brain changes. In most cases histogram peak height is a more sensitive marker than mean MTR[31-33]. On the other hand it has also been reported that both measures demonstrate a comparable sensitivity[34]. Therefore, although both measures are related, they may demonstrate a different sensitivity in detecting structural changes in the brain.

Widespread MTI changes are associated with cognition. Previously, patients with Alzheimer disease, and mild cognitive impairment were shown to have lower mean MTR and normalized MTR peak height in gray and white matter compared to controls[35]. In the current study, VAT was associated with normalized MTR peak height in gray and white matter, however not with mean MTR. It may be hypothesized that subtle brain changes in the state of overweight and obesity might not yet be detected by the mean MTR parameter. Unfortunately, we did not measure cognition in this study.

The pathophysiological pathways linking obesity and structural brain changes are not completely understood, but systemic low-grade inflammation associated with inflamed and expanded VAT has been a proposed mechanism. Compared to SAT, VAT was stronger associated with systemic biomarkers including C-reactive protein, interleukin-6, monocyte chemoattractant protein-1, and isoprostanes reflecting inflammation and oxidative stress[7]. Excess visceral fat accumulation has been associated with various atherogenic and diabetogenic abnormalities[36], and weight loss decreased VAT[37], carotid intima-media thickness[38], arterial stiffness[39], and improves inflammatory profile[38]. Altogether, there is growing evidence that VAT has a unique metabolic and endocrine function with deleterious effects on multiple organs, which may also include the brain.

Strengths of this study are the availability of combined data of abdominal adipose tissue distribution and microstructural brain tissue damage in a large cohort. A few limitations should be addressed. The study population is an elderly population, consisting of offspring of long-lived siblings and their partners. The cross-sectional nature of our study limits to differentiate cause and effect. It can be hypothesized that the observed relationship between VAT and microstructural brain tissue damage is merely a result of the potential confounding factor ageing. In this study, we attempted to correct for age in the multivariate linear regression analysis. However, because the age range is relatively small, we cannot completely exclude that age in part affects our results. Furthermore, part of our study population is offspring of long-lived persons and therefore may be different than the general population, which could limit the generalizability of our results. Because of the cross-sectional design of the study, it could be postulated that microscopic brain tissue damage may lead to obesity. However, it has been shown that obese nondiabetic adolescents with metabolic syndrome have lower cognitive performance compared to adolescents without metabolic syndrome. Moreover, smaller hippocampal volumes and reductions of white matter microstructural integrity were found[40]. It is not very likely that these brain impairments were pre-existing. Thus the observations in this early stage of life strengthen the hypothesis that obesity leads to reductions in cognitive function and structural brain changes, and not vice versa.

Further research in a general population with a wider age range is necessary to study whether the relationship between visceral adiposity and microstructural brain tissue damage is merely a result of ageing, or exists independently of age. Furthermore, cognition tests could be of additional value for evaluating the clinical consequences of these findings.

In conclusion, this study indicates that increasing VAT rather than SAT is associated with microstructural brain tissue damage in elderly individuals. This association cannot be accounted for by BMI, which is an easily obtainable clinical measure of obesity but does not discriminate different fat compartments. Awareness of differences in the underlying mechanisms between body fat patterns and brain damage may offer more focused individual advice or treatment than considering BMI only.

REFERENCES

1. Raji CA, Ho AJ, Parikshak NN, Becker JT, Lopez OL, Kuller LH, Hua X, Leow AD, Toga AW, Thompson PM. Brain structure and obesity. *Hum Brain Mapp* 2010;31:353-364.
2. Taki Y, Kinomura S, Sato K, Inoue K, Goto R, Okada K, Uchida S, Kawashima R, Fukuda H. Relationship between body mass index and gray matter volume in 1,428 healthy individuals. *Obesity (Silver Spring)* 2008;16:119-124.
3. Sala M, de Roos A, van den Berg A, Altmann-Schneider I, Slagboom PE, Westendorp RG, van Buchem MA, de Craen AJ, van der Grond J. Microstructural brain tissue damage in metabolic syndrome. *Diabetes Care* 2014;37:493-500.
4. Sluimer JD, van der Flier WM, Karas GB, Fox NC, Scheltens P, Barkhof F, Vrenken H. Whole-brain atrophy rate and cognitive decline: longitudinal MR study of memory clinic patients. *Radiology* 2008;248:590-598.
5. Mathieu P, Lemieux I, Despres JP. Obesity, inflammation, and cardiovascular risk. *Clin Pharmacol Ther* 2010;87:407-416.
6. Britton KA, Massaro JM, Murabito JM, Kreger BE, Hoffmann U, Fox CS. Body fat distribution, incident cardiovascular disease, cancer, and all-cause mortality. *J Am Coll Cardiol* 2013;62:921-925.
7. Pou KM, Massaro JM, Hoffmann U, Vasan RS, Maurovich-Horvat P, Larson MG, Keaney JF, Jr., Meigs JB, Lipinska I, Kathiresan S, Murabito JM, O'Donnell CJ, Benjamin EJ, Fox CS. Visceral and subcutaneous adipose tissue volumes are cross-sectionally related to markers of inflammation and oxidative stress: the Framingham Heart Study. *Circulation* 2007;116:1234-1241.
8. Debette S, Beiser A, Hoffmann U, Decarli C, O'Donnell CJ, Massaro JM, Au R, Himali JJ, Wolf PA, Fox CS, Seshadri S. Visceral fat is associated with lower brain volume in healthy middle-aged adults. *Ann Neurol* 2010;68:136-144.
9. Inglese M, Ge Y. Quantitative MRI: hidden age-related changes in brain tissue. *Top Magn Reson Imaging* 2004;15:355-363.
10. Seiler S, Cavalieri M, Schmidt R. Vascular cognitive impairment - an ill-defined concept with the need to define its vascular component. *J Neurol Sci* 2012;322:11-16.
11. van Buchem MA, McGowan JC, Grossman RI. Magnetization transfer histogram methodology: its clinical and neuropsychological correlates. *Neurology* 1999;53:S23-28.
12. Henkelman RM, Stanisz GJ, Graham SJ. Magnetization transfer in MRI: a review. *NMR Biomed* 2001;14:57-64.
13. Filippi M, Rocca MA. Magnetization transfer magnetic resonance imaging of the brain, spinal cord, and optic nerve. *Neurotherapeutics* 2007;4:401-413.
14. Schoenmaker M, de Craen AJ, de Meijer PH, Beekman M, Blauw GJ, Slagboom PE, Westendorp RG. Evidence of genetic enrichment for exceptional survival using a family approach: the Leiden Longevity Study. *Eur J Hum Genet* 2006;14:79-84.
15. Westendorp RG, van Heemst D, Rozing MP, Frölich M, Mooijaart SP, Blauw GJ, Beekman M, Heijmans BT, de Craen AJ, Slagboom PE, for the Leiden Longevity Study Group. Nonagenarian siblings and their offspring display lower risk of mortality and morbidity than sporadic nonagenarians: The Leiden Longevity Study. *J Am Geriatr Soc* 2009;57:1634-1637.
16. Altmann-Schneider I, de Craen AJ, Slagboom PE, Westendorp RG, van Buchem MA, Maier AB, van der Grond J. Brain tissue volumes in familial longevity: the Leiden Longevity Study. *Aging Cell* 2012;11:933-939.
17. Smith SM, Jenkinson M, Woolrich MW, Beckmann CF, Behrens TE, Johansen-Berg H, Bannister PR, De Luca M, Drobnjak I, Flitney DE, Niazy RK, Saunders J, Vickers J, Zhang Y, De Stefano N, Brady JM, Matthews PM. Advances in functional and structural MR image analysis and implementation as FSL. *Neuroimage* 2004;23(Suppl 1):S208-219.
18. Woolrich MW, Jbabdi S, Patenaude B, Chappell M, Makni S, Behrens T, Beckmann C,

Jenkinson M, Smith SM. Bayesian analysis of neuroimaging data in FSL. *Neuroimage* 2009;45:S173-186.

19. Smith SM. Fast robust automated brain extraction. *Hum Brain Mapp* 2002;17:143-155.
20. Zhang Y, Brady M, Smith S. Segmentation of brain MR images through a hidden Markov random field model and the expectation-maximization algorithm. *IEEE Trans Med Imaging* 2001;20:45-57.
21. Jagust W, Harvey D, Mungas D, Haan M. Central obesity and the aging brain. *Arch Neurol* 2005;62:1545-1548.
22. Karcher HS, Holzwarth R, Mueller HP, Ludolph AC, Huber R, Kassubek J, Pinkhardt EH. Body fat distribution as a risk factor for cerebrovascular disease: an MRI-based body fat quantification study. *Cerebrovasc Dis* 2013;35:341-348.
23. Yamashiro K, Tanaka R, Tanaka Y, Miyamoto N, Shimada Y, Ueno Y, Urabe T, Hattori N. Visceral fat accumulation is associated with cerebral small vessel disease. *Eur J Neurol* 2014;21:667-673.
24. Isaac V, Sim S, Zheng H, Zagorodnov V, Tai ES, Chee M. Adverse associations between visceral adiposity, brain structure, and cognitive performance in healthy elderly. *Front Aging Neurosci* 2011;3:12.
25. Dehmeshki J, Chard DT, Leary SM, Watt HC, Silver NC, Tofts PS, Thompson AJ, Miller DH. The normal appearing grey matter in primary progressive multiple sclerosis: a magnetisation transfer imaging study. *J Neurol* 2003;250:67-74.
26. Grossman RI, Gomori JM, Ramer KN, Lexa FJ, Schnall MD. Magnetization transfer: theory and clinical applications in neuroradiology. *Radiographics* 1994;14:279-290.
27. Wozniak JR, Lim KO. Advances in white matter imaging: a review of in vivo magnetic resonance methodologies and their applicability to the study of development and aging. *Neurosci Biobehav Rev* 2006;30:762-774.
28. Holland PR, Bastin ME, Jansen MA, Merrifield GD, Coltman RB, Scott F, Nowers H, Khallout K, Marshall I, Wardlaw JM, Deary IJ, McCulloch J, Horsburgh K. MRI is a sensitive marker of subtle white matter pathology in hypoperfused mice. *Neurobiol Aging* 2011;32:2325-2326.
29. Song SK, Sun SW, Ramsbottom MJ, Chang C, Russell J, Cross AH. Dysmyelination revealed through MRI as increased radial (but unchanged axial) diffusion of water. *Neuroimage* 2002;17:1429-1436.
30. Bosma GP, Rood MJ, Zwinderman AH, Huizinga TW, van Buchem MA. Evidence of central nervous system damage in patients with neuropsychiatric systemic lupus erythematosus, demonstrated by magnetization transfer imaging. *Arthritis Rheum* 2000;43:48-54.
31. Ropele S, Enzinger C, Sollinger M, Langkammer C, Wallner-Blazek M, Schmidt R, Fazekas F. The impact of sex and vascular risk factors on brain tissue changes with aging: magnetization transfer imaging results of the Austrian stroke prevention study. *AJNR Am J Neuroradiol* 2010;31:1297-1301.
32. van den Bogaard SJ, Dumas EM, Milles J, Reilmann R, Stout JC, Craufurd D, van Buchem MA, van der Grond J, Roos RA. Magnetization transfer imaging in premanifest and manifest Huntington disease. *AJNR Am J Neuroradiol* 2012;33:884-889.
33. Benedetti B, Charil A, Rovaris M, Judica E, Valsasina P, Sormani MP, Filippi M. Influence of aging on brain gray and white matter changes assessed by conventional, MT, and DT MRI. *Neurology* 2006;66:535-539.
34. Ropele S, Schmidt R, Enzinger C, Windisch M, Martinez NP, Fazekas F. Longitudinal magnetization transfer imaging in mild to severe Alzheimer disease. *AJNR Am J Neuroradiol* 2012;33:570-575.
35. van Es AC, van der Flier WM, Admiraal-Behloul F, Olofsen H, Bollen EL, Middelkoop HA, Weverling-Rijnsburger AW, van der Grond J, Westendorp RG, van Buchem MA. Lobar distribution of changes in gray matter and white matter in memory clinic patients: detected using magnetization transfer imaging. *AJNR Am J Neuroradiol* 2007;28:1938-1942.

36. Després JP, Lemieux I. Abdominal obesity and metabolic syndrome. *Nature* 2006;444:881-887.
37. Wajchenberg BL. Subcutaneous and visceral adipose tissue: their relation to the metabolic syndrome. *Endocr Rev* 2000;21:697-738.
38. Masquio DC, de Piano A, Sanches PL, Corgosinho FC, Campos RM, Carnier J, da Silva PL, Caranti DA, Tock L, Oyama LM, Oller do Nascimento CM, de Mello MT, Tufik S, Damaso AR. The effect of weight loss magnitude on pro-/anti-inflammatory adipokines and carotid intima-media thickness in obese adolescents engaged in interdisciplinary weight loss therapy. *Clin Endocrinol (Oxf)* 2013;79:55-64.
39. Cooper JN, Buchanich JM, Youk A, Brooks MM, Barinas-Mitchell E, Conroy MB, Sutton-Tyrrell K. Reductions in arterial stiffness with weight loss in overweight and obese young adults: potential mechanisms. *Atherosclerosis* 2012;223:485-490.
40. Yau PL, Castro MG, Tagani A, Tsui WH, Convit A. Obesity and metabolic syndrome and functional and structural brain impairments in adolescence. *Pediatrics* 2012;130:e856-864.

Chapter 10

Summary

Nederlandse samenvatting

This thesis describes cardiovascular and cerebral features in people with obesity and type 2 diabetes.

Chapter 1 provides a general introduction about the burden of obesity and type 2 diabetes in relation to cardiovascular disease, brain activity, and structural brain changes. Several imaging techniques used in this thesis are briefly discussed.

CARDIOVASCULAR SYSTEM

Chapter 2 describes the associations between hepatic triglyceride content and left ventricular diastolic heart function. Many studies have shown a relationship between nonalcoholic fatty liver disease and cardiovascular disease. This study was designed to further investigate the relationship between fatty liver and cardiovascular disease while taking several potential confounding factors into account. In 714 participants aged 45-65 years who underwent magnetic resonance spectroscopy and imaging to assess hepatic triglyceride content and left ventricular diastolic heart function (ratio of peak filling rates of the early filling phase and atrial contraction), the association between hepatic triglyceride content and decreased left ventricular diastolic function was largely explained by confounding factors, including the metabolic syndrome. Only in persons with obesity could an association independent of the metabolic syndrome and abdominal visceral adiposity be demonstrated significantly. Therefore, fatty liver itself could, at least in obesity, pose a risk of myocardial dysfunction above and beyond known cardiovascular risk factors that are clustered within the metabolic syndrome. Future studies with larger sample sizes should reveal to what extent associations between hepatic triglyceride content and diastolic function exist and differ in normal-weight, overweight, and obese persons.

Chapter 3 evaluates the associations between hepatic triglyceride content and central arterial stiffness and subclinical atherosclerosis. In a large population-based cohort of 1899 individuals aged 45-65 years, magnetic resonance spectroscopy, magnetic resonance imaging, and ultrasound were used to assess hepatic triglyceride content, aortic pulse wave velocity, and carotid intima-media thickness, respectively. After adjustments for several possible confounding factors, including all individual components of the metabolic syndrome and visceral adiposity, hepatic triglyceride content was associated with aortic pulse wave velocity, and more in particular with the pulse wave velocity of the abdominal aortic segment. In addition, hepatic triglyceride content was associated with carotid intima-media thickness after adjustments for several cardiometabolic risk factors, including all individual components of the metabolic syndrome. These results suggest a unique contribution of fatty liver to subclinical vascular impairment. Prospective follow-up research is required to study the effect of hepatic steatosis on incident cardiovascular events.

Chapter 4 focuses on the right ventricle in type 2 diabetes. Subclinical left ventricular dysfunction in the absence of significant coronary artery disease and hypertension in type 2 diabetes is called diabetic cardiomyopathy. However, the right ventricle is largely overlooked in studies on diabetic cardiomyopathy. Right ventricular involvement in diabetic cardiomyopathy might be of importance because the right ventricle has a substantial contribution to overall myocardial contractility. The study described in this chapter was conducted to compare magnetic resonance-derived right ventricular dimensions and function between 78 male type 2 diabetic patients and 28 male healthy subjects. Main findings were right ventricular remodeling and impaired systolic and diastolic functions in men with uncomplicated type 2 diabetes, in a similar manner as changes in left ventricular dimensions and functions. These results suggest that right ventricular impairment might be a component of the diabetic cardiomyopathy phenotype and that both ventricles are influenced by the metabolic abnormalities characterizing diabetes.

Chapter 5 reports on the effects of two nutritional interventions on right ventricular function in lean healthy men. Unlike the effects on left ventricular function, little is known about possible changes of the right ventricle. The study investigated the effects of increased plasma nonesterified fatty acid levels in two different conditions: the first was a physiological model created by a short-term caloric restriction; the second was a pathophysiological model created by a short-term high-fat diet. Fifteen healthy men underwent magnetic resonance scanning at three different occasions. Before every visit, subjects were instructed to follow different dietary regimes: a 3-day normal diet, a 3-day very low-calorie diet, and a 3-day high-fat high-energy diet. The sequence of the nutritional interventions was randomly assigned. Right ventricular diastolic function was impaired after a short-term very low-calorie diet. The concomitant decrease of left ventricular diastolic function, increase of plasma nonesterified fatty acid levels and increase of myocardial triglyceride content suggest that myocardial lipotoxicity may be of importance in decreased right ventricular diastolic function after short-term caloric restriction. A short-term high-fat high-energy diet also induced decreased right ventricular diastolic function, whereas left ventricular diastolic function remained similar. These results were accompanied by increased hepatic triglyceride content and plasma cholesteryl ester transfer protein levels, suggesting that systemic inflammation reflecting local macrophage infiltration in the heart may be involved in right ventricular dysfunction. An alternative hypothesis includes anomalous blood flow in the inferior vena cava caused by reduced compliance of the hepatic parenchyma in fatty liver. Further studies need to be initiated combining assessment of right ventricular function and blood flow in the hepatic veins and inferior vena cava in patients with fatty liver.

Chapter 6 evaluates the effects of an exercise intervention on ectopic fat compartments in 12 patients with type 2 diabetes. All patients underwent a 6-month individualized training program followed by a 12-day trekking expedition to Mount Toubkal in Morocco. Patients underwent MR examinations on two occasions: at 7 days before the start of training

and 200 days after the start of training. Self-reported caloric intake did not change during the exercise period, nor did the composition of the diet over the exercise period. Mean weight loss was 5% (88.0 ± 3.9 vs. 83.7 ± 3.4 kg). After the 6-month exercise intervention a greater than 20% decrease in visceral abdominal fat, hepatic triglyceride content, and paracardial fat was observed. No changes in subcutaneous abdominal fat, myocardial or intramyocellular triglyceride content, epicardial fat volume, or cardiac function were seen. This study demonstrated tissue-specific exercise-induced changes in ectopic fat compartments in patients with type 2 diabetes, and dietary interventions or substantial weight loss did not seem to be a requisite for beneficial reductions in visceral abdominal, paracardial, and hepatic fat volume. Future studies should aim to investigate the biochemical properties of these fat compartments and how they relate to cardiovascular risk.

BRAIN

Chapter 7 describes the effect of a very low calorie diet on hypothalamic neuronal activity after glucose ingestion measured by blood oxygen level-dependent (BOLD) functional magnetic resonance imaging. The hypothalamus plays a key role in the regulation of feeding, and previous studies have shown a significant dose-dependent decrease of the BOLD signal in the hypothalamus after glucose ingestion in healthy lean volunteers, and an absent BOLD signal decrease after glucose ingestion in patients with type 2 diabetes. Restoration of the energy balance by reduction of the caloric intake and subsequent weight loss are important therapeutic strategies in type 2 diabetes. Therefore the hypothesis of the study described in this chapter was that caloric restriction normalizes the hypothalamic response to a nutrient load. Ten male patients with type 2 diabetes completed a very low calorie diet of 4 days. They underwent functional magnetic resonance imaging before and after the diet. During scanning a glucose solution was ingested. Pre-diet scans showed no response of the hypothalamus to glucose intake (i.e., no signal decrease after glucose intake was observed). Post-diet scans showed a prolonged signal decrease after glucose ingestion with an order of magnitude similar to that in healthy subjects. These results show that short-term caloric restriction normalizes hypothalamic responsiveness to glucose ingestion in patients with type 2 diabetes. The fundamental mechanism behind the hypothalamic response to glucose ingestion is yet unclear, as is the effect of very low calorie diet in this study, and therefore requires further research.

Chapter 8 is an explorative cross-sectional study investigating the anatomy of subcortical structures that play a role in human food regulation. Other studies have demonstrated associations of obesity with whole-brain atrophy and loss of cortical gray matter, but it is unknown whether the subcortical brain structures that are actually involved in feeding behavior also show volume changes. In 471 elderly subjects magnetic resonance imaging of

the brain was performed. Automatic segmentation was used to measure the volumes of the basal ganglia, hippocampus, and thalamus. Obese subjects had larger left and right amygdalar volumes and a larger left hippocampal volume than did normal-weight subjects. None of the other subcortical structures differed in size between normal-weight, overweight and obese subjects. After correction for possible confounding factors, BMI was associated with left and right amygdalar volumes and with left hippocampal volume, but not with any of the other investigated brain structures. The amygdala and hippocampus relate memory to pleasure, respectively, by establishing the reward value of food and food-related stimuli or situations and by consolidating pleasure memories. The results of this study may indicate that hedonic memories could be of major importance in the regulation of feeding. However, the mechanisms behind the enlargement of the amygdala and hippocampus in obesity are speculative and therefore further study is needed to identify possible pathways.

Chapter 9 reveals that abdominal visceral and subcutaneous adipose tissue relate differently to microstructural brain tissue damage. Magnetization transfer imaging was used to measure subtle microstructural changes in the brain in 243 elderly subjects. Increased abdominal visceral adipose tissue rather than subcutaneous adipose tissue was associated with microstructural brain tissue damage. This association could not be accounted for by body mass index, which is an easily obtainable measure of obesity but does not discriminate different fat compartments. The outcome of this study strengthens the concept that visceral adipose tissue, as opposed to subcutaneous adipose tissue, plays a key role in the deleterious effects of obesity. The pathophysiological pathways linking obesity and structural brain changes are not completely understood, but systemic low-grade inflammation associated with inflamed and expanded visceral adipose tissue has been a proposed mechanism. Awareness of differences in the underlying mechanisms between body fat patterns and brain damage may offer more focused individual advice or treatment than considering body mass index only.

NEDERLANDSE SAMENVATTING

Dit proefschrift beschrijft cardiovasculaire en cerebrale kenmerken van mensen met obesitas en diabetes type 2.

Hoofdstuk 1 geeft een algemene introductie over de ongewenste gevolgen van obesitas en diabetes type 2 wat betreft hart- en vaatziekten, hersenactiviteit en structurele veranderingen in het brein. Meerdere beeldvormende technieken, zoals magnetic resonance imaging (MRI) en magnetic resonance spectroscopy (MRS), die in dit proefschrift zijn gebruikt worden kort besproken.

CARDIOVASCULAIRE SYSTEEM

Hoofdstuk 2 beschrijft de associaties tussen het triglyceridegehalte in de lever en de diastolische hartfunctie van de linker ventrikel. Veel studies hebben een relatie aangetoond tussen leververvetting en hart- en vaatziekten. Deze studie was ontworpen om de relatie tussen leververvetting en hart- en vaatziekten verder te onderzoeken, waarbij rekening werd gehouden met meerdere factoren die deze relatie zouden kunnen verstoren. Bij 714 deelnemers met een leeftijd van 45-65 jaar werden MRS en MRI verricht om respectievelijk het triglyceridengehalte in de lever en de diastolische hartfunctie van de linker ventrikel te bepalen. Het bleek dat de relatie tussen deze twee parameters voor het grootste deel werden veroorzaakt door verstorende factoren, zoals het metabool syndroom. Alleen in mensen met obesitas kon een associatie onafhankelijk van het metabool syndroom en visceraal buikvet significant worden aangetoond. Een vervette lever zou dus, in ieder geval in obesitas, een risico met zich mee kunnen dragen op dysfunctie van de hartspier bovenop de cardiovasculaire risicofactoren die in het metabool syndroom zijn geclusterd. Toekomstige studies met grotere studiepopulaties zouden moeten uitwijzen in hoeverre de associaties tussen het triglyceridegehalte in de lever en diastolische hartfunctie bestaat en verschilt tussen mensen met een normaal gewicht, overgewicht en obesitas.

Hoofdstuk 3 evalueert de associaties tussen het triglyceridegehalte in de lever, de stijfheid van de aorta en subklinische atherosclerose. In een groot cohort gebaseerd op de algemene bevolking van 1.899 mensen met een leeftijd van 45-65 jaar werden MRS, MRI en echo verricht om respectievelijk het triglyceridegehalte in de lever, de pulse wave velocity (maat voor stijfheid) van de aorta, en de wanddikte van de halsslagader te meten. Na correcties voor meerdere mogelijke verstorende factoren, inclusief alle individuele componenten van het metabool syndroom en visceraal buikvet, was het triglyceridegehalte in de lever geassocieerd met de pulse wave velocity van de aorta, en meer specifiek met de pulse wave velocity van de aorta in de buik. Tevens was het triglyceridegehalte in de lever geassocieerd met de wanddikte van de halsslagader na correcties voor meerdere cardiale en metabole

risicofactoren, inclusief alle individuele componenten van het metabool syndroom. Deze resultaten suggereren een unieke bijdrage van leververvetting aan subklinische verslechtering van de vaten. Prospectief vervolgonderzoek is nodig om het effect van leververvetting op nieuwe gevallen van hart- en vaatziekten te bestuderen.

Hoofdstuk 4 richt zich op de rechter ventrikel in diabetes type 2. Subklinische dysfunctie van de linker ventrikel in afwezigheid van significante kransslagadervernauwing en hoge bloeddruk in diabetes type 2 wordt ook wel diabetische cardiomyopathie genoemd. De rechter ventrikel wordt echter grotendeels over het hoofd gezien in studies gericht op diabetische cardiomyopathie. Betrokkenheid van de rechter ventrikel in diabetische cardiomyopathie zou van belang kunnen zijn omdat de rechter ventrikel een substantiële bijdrage levert aan de algehele pompfunctie van het hart. De in dit hoofdstuk beschreven studie werd uitgevoerd om de dimensies en functie van de rechter ventrikel, gemeten met MRI, te vergelijken tussen 78 mannelijke diabetes type 2 patiënten en 28 mannelijke gezonde vrijwilligers. De belangrijkste bevindingen waren veranderingen in dimensie en verslechtering van de systolische en diastolische functie van de rechter ventrikel in mannen met ongecompliceerde diabetes type 2. Deze veranderingen waren vergelijkbaar met veranderingen van de linker ventrikel. Deze resultaten suggereren dat de rechter ventrikel betrokken is bij diabetische cardiomyopathie, en dat beide ventrikels vermoedelijk worden beïnvloed door de afwijkingen in stofwisseling die karakteristiek zijn voor de ziekte diabetes.

Hoofdstuk 5 rapporteert over de effecten van twee voedingsinterventies op de rechter ventrikel in gezonde mannen. In tegenstelling tot de linker ventrikel is er weinig bekend over de mogelijke veranderingen in functie van de rechter ventrikel. Deze studie onderzocht de effecten van een verhoogde bloedspiegel van vrije vetzuren in twee verschillende omstandigheden: de eerste was een fysiologisch model gecreëerd door een kortdurend zeer laag calorisch dieet; de tweede was een pathofysiologisch model gecreëerd door een kortdurend vetrijk dieet. Vijftien gezonde mannen ondergingen een MRI op drie tijdstippen. Voorafgaand aan elk bezoek werden de deelnemers geïnstrueerd om een dieet te volgen: een 3-daags normaal dieet, een 3-daags zeer laag calorisch dieet, en een 3-dags vet- en energierijk dieet. De volgorde van de dieetinterventies werd willekeurig aangewezen. De diastolische functie van de rechter ventrikel was verslechterd na een kortdurend zeer laag calorisch dieet. De bijkomende afname van diastolische functie van de linker ventrikel, de toegenomen bloedspiegel van vrije vetzuren, en het toegenomen triglyceridegehalte in de hartspier suggereren dat 'myocardiale lipotoxiciteit' van belang kan zijn in de afname van diastolische functie van de rechter ventrikel na een kortdurende caloriebeperking. Een kortdurend vet- en energierijk dieet verlaagde ook de diastolische functie van de rechter ventrikel, terwijl de diastolische functie van de linker ventrikel hetzelfde bleef. Deze resultaten gingen gepaard met een verhoogd triglyceridegehalte in de lever en een verhoogde spiegel van het eiwit 'cholesteryl ester transfer protein'. Hiermee kan worden gesuggereerd dat systemische ontsteking, mede gekenmerkt door lokale infiltratie van macrofagen in het

hart, betrokken is bij dysfunctie van de rechter ventrikel. Een alternatieve hypothese betreft een afwijkende bloedstroom in de onderste holle ader, veroorzaakt door een verminderde compliantie van het leverweefsel bij leververvetting. Nadere studies moeten worden verricht die zowel de functie van de rechter ventrikel meten als de bloedstroom in de levervenen en onderste holle ader in patiënten met leververvetting.

Hoofdstuk 6 evalueert de effecten van een trainingsprogramma op ectopische vetdeposities in 12 patiënten met diabetes type 2. Alle patiënten ondergingen een geïndividualiseerde training van 6 maanden gevolgd door een 12-daagse expeditie naar de berg Toubkal in Marokko. De patiënten ondergingen MRI onderzoek op twee momenten: 7 dagen vóór en 200 dagen na de start van de training. Zowel de zelf-gerapporteerde calorie-inname als de inhoud van het dieet veranderde niet tijdens het trainingsprogramma. Het gemiddelde gewichtsverlies was 5% (88.0 ± 3.9 vs. 83.7 ± 3.4 kg). Na de training van 6 maanden was het viscerale buikvet, het triglyceridegehalte in de lever en het paracardiale vet met meer dan 20% gedaald. Er werden geen verschillen waargenomen in het subcutane buikvet, het triglyceridegehalte in het hart of in de beenspier, het epicardiale vetvolume of hartfunctie. Deze studie laat weefselspecifieke trainings-geïnduceerde veranderingen zien in ectopische vetdeposities in patiënten met diabetes type 2, en dieetinterventies of substantieel gewichtsverlies leken niet een voorwaarde te zijn om gunstige reducties te bewerkstelligen van visceraal buikvet, paracardiaal vet en levervet. Toekomstige studies zouden zich moeten richten op de biochemische eigenschappen van deze vetcompartimenten en op welke wijze deze relateren aan cardiovasculair risico.

HERSENEN

Hoofdstuk 7 beschrijft het effect van een zeer laag calorisch dieet op de activiteit van de hypothalamus na glucose-inname, gemeten door middel van blood oxygen level-dependent (BOLD) functionele MRI. De hypothalamus speelt een belangrijke rol in de regulering van voeding, en eerdere studies hebben aangetoond dat een significante afname van het BOLD signaal optreedt na glucose-inname bij gezonde vrijwilligers, en dat deze afname afwezig is bij patiënten met diabetes type 2. Herstel van de energiebalans door reductie van calorie-inname en het hieruit volgende gewichtsverlies zijn belangrijke therapeutische strategieën in diabetes type 2. Daarom was de hypothese van de in dit hoofdstuk beschreven studie dat een caloriebeperking de respons van de hypothalamus op een voedingsstofbelasting normaliseert. Tien mannelijke patiënten met diabetes type 2 volgden een zeer laag calorisch dieet van 4 dagen. Zij ondergingen een functionele MRI vóór en na het dieet. Tijdens de scan werd een glucoseoplossing ingeslikt. De scans vóór het dieet lieten geen respons van de hypothalamus zien (met andere woorden, er werd geen signaalafname na de glucose-inname gezien). De scans na het dieet lieten een langdurige signaalafname zien

na de glucose-inname, met een vergelijkbare orde van grootte als in gezonde vrijwilligers. Deze resultaten laten zien dat een kortdurende caloriebeperking de reactie van de hypothalamus op een glucose-inname bij patiënten met diabetes type 2 normaliseert. Zowel het fundamentele mechanisme achter deze reactie als het effect van het zeer laag calorische dieet is nog onduidelijk, en behoeft daarom meer onderzoek.

Hoofdstuk 8 is een exploratieve cross-sectionele studie over de anatomie van subcorticale structuren die een rol spelen in de regulatie van voeding in de mens. Andere studies hebben aangetoond dat obesitas is geassocieerd met hersenatrofie en verlies van grijze stof. Het is echter onbekend of de hersenstructuren die een rol spelen in voedingsgedrag ook volumeveranderingen vertonen. Bij 471 oudere mensen werd een MRI van het brein verricht. Er werd gebruik gemaakt van automatische segmentatie om de volumina van de basale kernen, hippocampus en thalamus te meten. Obese mensen hadden een groter volume van de linker en rechter amygdala en een grote volume van de linker hippocampus vergeleken met mensen met een normaal gewicht. Geen van de andere subcorticale structuren verschilde in grootte tussen mensen met een normaal gewicht, overgewicht en obesitas. Na correctie voor mogelijke verstorende factoren was BMI geassocieerd met de volumina van de linker en rechter amygdala en de linker hippocampus, echter niet met de andere onderzochte hersenstructuren. De amygdala en hippocampus relateren geheugen aan plezier door respectievelijk de beloningswaarde van voedsel en voedsel-gerelateerde stimuli of situaties vast te stellen, en plezierige herinneringen vast te houden. De resultaten van deze studie zouden erop kunnen wijzen dat hedonistische herinneringen van groot belang zijn in de regulatie van voeding. De mechanismen achter de vergroting van de amygdala en hippocampus in obesitas zijn echter speculatief en daarom is meer onderzoek nodig om mogelijke ontstaanswijzen te achterhalen.

Hoofdstuk 9 brengt aan het licht dat visceraal en subcutaan buikvet op een andere manier gerelateerd zijn aan microstructurele hersenschade. Magnetization transfer imaging werd gebruikt om subtiele microstructurele veranderingen in het brein van 243 oudere mensen te meten. Eerder een verhoogde hoeveelheid aan visceraal buikvet dan subcutaan buikvet was geassocieerd met microstructurele hersenschade. Deze associatie kon niet toegeschreven worden aan de body mass index, wat een eenvoudig te verkrijgen maat is voor obesitas maar niet de verschillende vetcompartimenten kan onderscheiden. De uitkomst van deze studie versterkt het concept dat visceraal vetweefsel, in tegenstelling tot subcutaan vetweefsel, een belangrijke rol speelt in de schadelijke effecten van obesitas. De pathofysiologische link tussen obesitas en structuurveranderingen in de hersenen zijn nog niet volledig begrepen, echter een mogelijk mechanisme betreft systemische laaggradige ontsteking gerelateerd aan ontstoken en uitgezet visceraal vetweefsel. Bewustheid van de verschillen in onderliggende mechanismen tussen lichaamsvetverdelingen en hersenschade zouden een meer gericht geïndividualiseerd advies of behandeling kunnen bieden dan enkel het in aanmerking nemen van de body mass index.

DANKWOORD

Hierbij wil ik iedereen bedanken die heeft bijgedragen aan de totstandkoming van dit proefschrift, en in het bijzonder:

Mijn begeleiders Hildo, Albert, Jan en Jeroen. Dank voor al jullie hulp, supervisie en feedback tijdens het gehele traject van mijn onderzoek. Ik heb bijzonder veel kunnen leren van jullie expertise en aanpak.

Alle co-auteurs, oud-kamergenoten van C5-52, collega's van de NEO studie (in het bijzonder Renée en Ingeborg), LKEB, Gorter Centrum, MRI-bus laboranten, Gerrit, contour-medewerkers en studie-deelnemers: dank voor ieders zeer gewaarde bijdrage aan mijn promotieonderzoek.

Familie en vrienden, bedankt voor jullie steun en belangstelling.

Lieve papa († 2012), ik weet dat je trots op mij bent. Ik hoop dat je rust hebt gevonden. Je bent mijn drijfveer om door te zetten en daarom draag ik dit werk op aan jou.

Lieve mam, dank je wel voor je goede zorgen. Weet dat ik van je hou.

Gimmie en Texas, trouwste maatjes, jullie hebben mij blijdschap gegeven op de momenten dat het het meest nodig was. En overigens ook als het niet nodig was.

Lieve Myra, ik kan je niet genoeg bedanken voor je onvoorwaardelijke liefde. Ik kan me geen beter persoon wensen om naast me te hebben.

LIST OF PUBLICATIONS

Widya RL, de Roos A, Trompet S, de Craen AJM, Westendorp RGJ, Smit JWA, van Buchem MA, van der Grond J, for the PROSPER Study Group. Increased amygdalar and hippocampal volumes in elderly obese individuals with or at risk of cardiovascular disease.
Am J Clin Nutr 2011;93(6):1190-1195

Widya RL, Teeuwisse WM, Paulides M, Lamb HJ, Smit JWA, de Roos A, van Buchem MA, Pijl H, van der Grond J. Short-term caloric restriction normalizes hypothalamic neuronal responsiveness to glucose ingestion in patients with type 2 diabetes.
Diabetes 2012;61(12):3255-3259

Widya RL, Hammer S, Boon MR, van der Meer RW, Smit JWA, de Roos A, Rensen PCN, Lamb HJ. Effects of short-term nutritional interventions on right ventricular function in healthy men.
PLOS ONE 2013;8(9):e76406

Widya RL, van der Meer RW, Smit JWA, Rijzewijk LJ, Diamant M, Bax JJ, de Roos A, Lamb HJ. Right ventricular involvement in diabetic cardiomyopathy.
Diabetes Care 2013;36(2):457-462

Widya RL, Pijl H, van der Grond J. Response to Comment on: Teeuwisse et al. Short-term caloric restriction normalizes hypothalamic neuronal responsiveness to glucose ingestion in patients with type 2 diabetes. Diabetes 2012;61:3255-3259.
Diabetes 2013;62(6):e6

Jonker JT, de Mol P, de Vries ST, **Widya RL**, Hammer S, van Schinkel LD, van der Meer RW, Gans ROB, Webb AG, Kan HE, de Koning EJP, Bilo HJG, Lamb HJ. Exercise and type 2 diabetes mellitus: changes in tissue-specific fat distribution and cardiac function.
Radiology 2013;269(2):434-442

Visser AW, Ioan-Facsinay A, de Mutsert R, **Widya RL**, Loef M, de Roos A, le Cessie S, den Heijer M, Rosendaal FR, Kloppenburg M, for the NEO Study Group. Adiposity and hand osteoarthritis: the Netherlands Epidemiology of Obesity study.
Arthritis Res Ther 2014;16(1):R19

Widya RL, Kroft LJM, Altmann-Schneider I, van den Berg-Huysmans AA, van der Bijl N, de Roos A, Lamb HJ, van Buchem MA, Slagboom PE, van Heemst D, van der Grond J, on behalf of the Leiden Longevity Study Group. Visceral adipose tissue is associated with microstructural brain tissue damage.
Obesity 2015;23(5):1092-1096

Gast KB, den Heijer M, Smit JWA, **Widya RL**, Lamb HJ, de Roos A, Jukema JW, Rosendaal FR, de Mutsert R, for the NEO Study Group. Individual contributions of visceral fat and total body fat to subclinical atherosclerosis: The NEO study.
Atherosclerosis 2015;241(2):547-554

Widya RL, de Mutsert R, den Heijer M, le Cessie S, Rosendaal FR, Jukema JW, Smit JWA, de Roos A, Lamb HJ, for the NEO Study Group. Association between hepatic triglyceride content and left ventricular diastolic function in a population-based cohort: the Netherlands Epidemiology of Obesity study.
Radiology 2016;279(2):443-450

Widya RL, de Mutsert R, Westenberg JJM, Gast KB, den Heijer M, le Cessie S, Smit JWA, Jukema JW, Rosendaal FR, de Roos A, Lamb HJ, for the NEO Study Group. Is hepatic triglyceride content associated with aortic pulse wave velocity and carotid intima-media thickness? The Netherlands Epidemiology of Obesity study.
Radiology 2017; Epub ahead of print

CURRICULUM VITAE

Ralph Lennart Widya was born on March 6 1984 in Delft, the Netherlands, and lived in Vlaardingen until the age of 18. He attended secondary school at Scholengemeenschap Spieringshoek in Schiedam, at which he passed his gymnasium exam in 2002. In that same year he started medical school at Leiden University Medical Center (LUMC). In 2005 he performed a clinical internship at the *Female cancer Foundation* in Jakarta, Tasikmalaya, and Bali, Indonesia. Alongside medical school he worked as a paramedic passenger assistant at Amsterdam Airport Schiphol. He obtained his medical degree in 2008. After traveling for two months in New Zealand he started his PhD program at the LUMC in 2009, supervised by prof. dr. H.J. Lamb, prof. dr. A. de Roos (Department of Radiology) and prof. dr. J.W.A. Smit (Department of Endocrinology) which resulted in this thesis. Ralph joined the radiology residency program at the Department of Radiology, LUMC (head: prof. dr. M.A. van Buchem) in 2013.